HPLC method optimization for the preclinical and clinical assessment of neurological disorders

Gábor Veres Pharm.D.

Ph.D. Thesis

Szeged

2017

HPLC method optimization for the preclinical and clinical assessment of neurological disorders

Ph.D. Thesis

Gábor Veres Pharm.D.

Department of Neurology
Faculty of Medicine
Albert Szent-Györgyi Clinical Center
Doctoral School of Clinical Medicine
University of Szeged

Supervisor: Dénes Zádori M.D., Ph.D.

Szeged
2017

Original publications directly related to the Ph.D. thesis:

I. **Veres G**, Molnár M, Zádori D, Szentirmai M, Szalárdy L, Török R, Fazekas E, Ilisz I, Vécsei L, Klivényi P. Central nervous system-specific alterations in the tryptophan metabolism in the 3-nitropropionic acid model of Huntington's disease. Pharmacol Biochem Behav. 2015 13: 115–24. (original paper, **IF: 2.537**)

II. **Veres G**, Fejes-Szabó A, Zádori D, Nagy-Grócz G, László AM, Bajtai A, Mándity I, Szentirmai M, Bohár Z, Laborc K, Szatmári I, Fülöp F, Vécsei L, Párdutz Á. A comparative assessment of two kynurenic acid analogs in the formalin model of trigeminal activation: a behavioral, immunohistochemical and pharmacokinetic study. J Neural Transm. 2017 124: 99-112. (original paper, **IF (2015): 2.587**)

III. Török R, Salamon A, Sümegi E, Zádori D, **Veres G**, Molnár MF, Vécsei L, Klivényi P. Effect of MPTP on mRNA expression of PGC-1α in mouse brain. Brain Res. 2017 1660: 20-26. (original paper, **IF (2015): 2.561**)

IV. **Veres G**, Szpisjak L, Bajtai A, Siska A, Klivényi P, Ilisz I, Földesi I, Vécsei L, Zádori D. The establishment of tocopherol reference intervals for Hungarian adult population using a validated HPLC method. Biomed Chromatogr. 2017 e3953: 1-8. (original paper, epub, **IF (2015): 1.729**)

Cumulative impact factor of the publications directly related to the thesis: **9.414**

Publications not directly related to the Ph.D. thesis:

Samavati R, Zádor F, Szűcs E, Tuka B, Martos D, **Veres G**, Gáspár R, Mándity I, Fülöp F, Vécsei L, Benyhe S, Borsodi A. Kynurenic acid and its analogue can alter the opioid receptor G-protein signaling after acute treatment via NMDA receptor in rat cortex and striatum. J. Neurol. Sci. 2017 http://dx.doi.org/10.1016/j.jns.2017.02.053. (original paper, ahead of print, **IF (2015): 2.126**)

Zádori D, **Veres G**, Szalárdy L, Klivényi P, Fülöp F, Toldi J, Vécsei L. Inhibitors of the kynurenine pathway as neurotherapeutics: A patent review (2012–2015). Expert Opin Ther Pat, 2016 26: 815-832. (review, **IF (2015): 4.626**)

Török R, Kónya JA, Zádori D, **Veres G**, Szalárdy L, Vécsei L, Klivényi P. mRNA expression levels of PGC-1alpha in a transgenic and a toxin model of Huntington's disease. Cell Mol Neurobiol. 2015 35: 293-301. (original paper, **IF: 2.328**)

Zádori D, **Veres G**, Szalárdy L, Klivényi P, Vécsei L. Drug-induced movement disorders. Expert Opin Drug Saf. 2015 14: 877-890. (review, **IF: 2.896**)

Fejes-Szabó A, Bohár Z, Vámos E, Nagy-Grócz G, Tar L, **Veres G**, Zádori D, Szentirmai M, Tajti J, Szatmári I, Fülöp F, Toldi J, Párdutz Á, Vécsei L. Pre-treatment with new kynurenic acid amide dose-dependently prevents the nitroglycerine-induced neuronal activation and sensitization in cervical part of trigemino-cervical complex. J Neural Transm. 2014 121: 725-738. (original paper, **IF: 2.402**)

Grozdics E, Berta L, Gyarmati B, **Veres G**, Zádori D, Szalárdy L, Vécsei L, Tulassay T, Toldi G. B7 Costimulation and intracellular indoleamine 2,3-dioxygenase expression in umbilical cord blood and adult peripheral blood. Biol Blood Marrow Transplant. 2014 20: 1659-1665. (original paper, **IF: 3.404**)

Grozdics E, Berta L, Bajnok A, **Veres G**, Ilisz I, Klivényi P, Rigo J Jr, Vécsei L, Tulassay T, Toldi G. B7 costimulation and intracellular indoleamine-2,3-dioxygenase (IDO) expression in

peripheral blood of healthy pregnant and non-pregnant women. BMC Pregnancy Childbirth. 2014 14: 306-315 (original paper, **IF: 2.190**)

Zádori D, **Veres G**, Szalárdy L, Klivényi P, Toldi J, Vécsei L. Glutamatergic dysfunctioning in Alzheimer's disease and related therapeutic targets. J Alzheimers Dis. 2014 42: S177-S187. (review, **IF: 4.151**)

Cumulative impact factor of publications not directly related to the thesis: **24.123**

Total impact factor: **33.537**

Table of contents

List of abbreviations

3-NLT – 3-nitro-L-tyrosine

3-NP – 3-nitropropionic acid

3-OHK – 3-hydroxy-L-kynurenine

αTTP – α-tocopherol transfer protein

ACN – acetonitrile

AD – Alzheimer's disease

AMPA – α-amino-3-hydroxy-5-methyl-4-isoxazolepropionic acid

AVED – ataxia with vitamin E deficiency

BBB – blood brain barrier

BHT –- butylated hydroxytoluene

CAG – cytosine-adenine-guanine

CV – coefficient of variation

DA – dopamine

DAD – diode array detector

DOPAC – 3,4-dihydroxyphenylacetic acid

FLD – fluorescent detection

GSH – glutathione

HD – Huntington's disease

HPLC – high performance liquid chromatography

Htt – huntingtin protein

HVA – homovanillic acid

ICH – International Conference on Harmonisation

IPR – isoproterenol

KA-1 – N-(2-N,N-dimethylaminoethyl)-4-oxo-1H-quinoline-2-carboxamide hydrochloride

KA-2 – N-(2-N-pyrrolidinylethyl)-4-oxo-1H-quinoline-2-carboxamide hydrochloride

KAT – kynurenine aminotransferase

KP – kynurenine pathway

KYNA – kynurenic acid

LLOQ – lower limit of quantification

LOD – limit of detection

MassSpec – mass spectrometry

mHtt – mutant Htt

MPTP – 1-methyl-4-phenyl-1,2,3,6- tetrahydropyridine

MS – multiple sclerosis

Na_2EDTA – disodium ethylenediaminetetraacetate

NMDAR – N-methyl-D-aspartate receptors

OND – other neurological diseases

PBS – phosphate-buffered saline

PCA – perchloric acid

PD – Parkinson's disease

PGC-1α – PPARγ coactivator-1 alpha

PPARγ – proliferator-activated receptor-gamma

QUIN – quinolinic acid

RCF – relative centrifugal force

RI – reference intervals

SDH – succinate dehydrogenase

SN – substantia nigra

TNC – trigeminal nucleus pars caudalis

TRP – tryptophan

Summary

The main aim of neuroscience research is the assessment of the nervous system under physiological and pathological conditions, with the purpose of acquiring knowledge about the diagnosis, prevention and treatment of neuropsychiatric disorders. A substantial portion of research is engaged in the discovery of biomarkers, not only to help to better understand of the underlying pathomechanisms, but also because they may be suitable for monitoring disease progression and the evaluation of therapeutic effects of already applied drugs. Amongst analytical methods, high performance liquid chromatography is one of the most popular options because it provides fast and robust determination of a wide range of compounds. However, these methods need substantial procedural development to be able to obtain valid, i.e., replicable, results.

Amongst neurological disorders, headache is one of the most common conditions, whereas, neurodegenerative disorders including Alzheimer's, Parkinson's (PD) and Huntington's disease (HD) affect a smaller portion of the general population.

The kynurenine pathway (KP) of tryptophan (TRP) metabolism is extensively studied, mostly because of the well-established endogenous protective properties of kynurenic acid (KYNA) against the excitotoxic and oxidative stress inducing effects of other KP metabolites, such as quinolinic acid (QUIN) and 3-hydroxy-L-kynurenine (3-OHK). It is assumed that KYNA, and some of its analogs with improved pharmacokinetic or pharmacodynamic properties, may have modifying effects on nociception. With regard to HD, there is evidence that glutamatergic excitotoxicity is involved in the development of the disease which may be influenced by endogenous substances, including certain metabolites of the KP of TRP metabolism. Based on these findings several metabolites of the KP were investigated in a well-known model of trigeminal nociception, the orofacial formalin test, and in the 3-nitropropionic acid toxin model of HD. As a result, we were able to provide some pharmacokinetic insight into the different characteristics of two KYNA analogs in the animal headache model, and we were the first to demonstrate some differences in the KP in the widely used 3-nitropropionic acid toxin model of HD. Another neurodegenerative disorder in our field of interest is PD, which is characterized by the loss of dopaminergic (DAergic)

neurons in the substantia nigra pars compacta caused by mitochondrial dysfunction, which results in energy deficit and oxidative stress. With regard to environmental factors, one of the well-established causes of this condition is the long, cumulative, low-dose exposure to mitochondrial toxins. 1-Methyl-4-phenyl-1,2,3,6-tetrahydropyridine (MPTP) is a widely used neurotoxin in various *in vivo* animal studies to investigate the pathogenesis of PD and to assess the therapeutic effect of potential neuroprotective agents. DA measurements provide a well-established way to confirm DAergic neuronal loss. Accordingly, in our study 2 MPTP treatment regimens were compared (acute and chronic low dose) by measuring their striatal DA concentrations. The results demonstrated the presence of significant neurotoxicity in the acute treatment regimens, while the chronic low dose regimen failed to evoke any significant changes in striatal DA levels. Besides QUIN and 3-OHK, there are numerous other substances that can facilitate the formation of reactive species (RS) which are responsible for most of the deleterious effects of pathological processes in the nervous system. The toxic effects of RS are decreased by a system of antioxidant machinery involving non-enzymatic mechanisms, such as vitamin E which has proven antioxidant properties. Vitamin E refers to a group of molecules including 4 tocotrienols and 4 tocopherols, as lipidsoluble antioxidants. Decreased tocopherol levels are associated with several neurological symptoms, such as cerebellar ataxia, peripheral neuropathy and myopathy, as the nervous system is particularly sensitive to oxidative damage resulting from increased energy demand and reduced antioxidant capacity. Severe tocopherol deficiency develops mainly as a result of malabsorption disorders, abetalipoproteinemia and ataxia with vitamin E deficiency (AVED). Differential diagnosis can sometimes be difficult in certain conditions accompanied by neurological symptoms (especially in AVED). Therefore the measurement of serum tocopherol levels is advised in cases of ataxia, myopathy or cognitive deficiency. To facilitate the diagnostic process, reference intervals for α-, γ-, and δ-tocopherols were determined for the adult Hungarian population.

1 Introduction

According to the Global Burden of Disease Study (Patel et al. 2016), neurological disorders such as headache disorders (migraine, tension-type headache and medication-overuse headache), Alzheimer's disease (AD) and other dementias, multiple sclerosis (MS), Parkinson's disease (PD) and epilepsy are responsible for 3 percent of the worldwide burden of disease. Despite this seemingly small percentage, dementia, epilepsy, migraine, and stroke rank in the top 50 causes of disability-adjusted life years, furthermore, dementia and PD are among the top 15 conditions with the most substantial increase in burden in the past decade.

Headache, one of the most common disorders of the nervous system, is a major health problem worldwide. The global prevalence of active headache disorders for the adult population is 46% for headache in general, 11% for migraine, 42% for tension-type headache and 3% for chronic daily headache (Stovner et al. 2007). The treatment of primary headache disorders is challenging, requiring both acute and preventive therapeutic strategies (Weatherall 2015). The efficacy of these treatments is not always satisfactory and the contraindications and side-effects often limit the options of the physician (Obermann et al. 2015, Diener et al. 2015). There is, therefore, a constant need to study and develop new molecules.

Although neurodegenerative disorders, including AD, PD, Huntington's disease (HD) and amyotrophic lateral sclerosis, affect a smaller portion of the general population, there is no proven causative therapy (Zádori et al. 2011b). Only symptomatic treatment is available, and with the exception of PD, the efficacy of these medications is quite limited with regard to symptom management (Klivényi and Vécsei 2010, Dézsi and Vécsei 2017). The complex and partially unrevealed pathomechanism of these disorders may be the underlying reason for the lack of causative therapy. Neurodegeneration can be described as progressive neuronal loss resulting in severe neuronal dysfunction. There are several identified and suspected genetic mutations and environmental factors in the background, but in most cases, despite the well delineated cellular and molecular events such as mitochondrial dysfunction and increased formation of reactive species, glutamate excitotoxicity, deposition of aggregated proteins, inflammatory response and altered gene expression, the pathogenic process is hard to influence (Jellinger 2001, Parihar et al. 2008).

The main aim of neuroscience research is the assessment of the nervous system under physiological and pathological conditions with the purpose of acquiring knowledge about the diagnosis, prevention and treatment of neuropsychiatric disorders. A substantial portion of research is engaged in the discovery of biomarkers in patients or in animal models of the assessed pathological conditions. These biomarkers may not only help in better understanding the underlying pathomechanisms of the investigated disorders with the possibility of finding novel therapeutic targets, but they may be suitable for monitoring disease progression and the evaluation of the therapeutic effects of already applied and potential novel drugs, as well.

Animal and human studies suggest that glutamate receptors are present in various parts of the trigeminal system (Tallaksen-Greene et al. 1992, Sahara et al. 1997, Quartu et al. 2002) which is the system responsible for processing most of the pain originating from the head area (Carpenter and Sutin 1983). The stimulation of the trigeminal nerve results in elevated glutamate levels in the spinal trigeminal nucleus pars caudalis (TNC, (Oshinsky and Luo 2006)). The peripheral application of glutamate to deep craniofacial tissue proved to activate and sensitize nociceptive afferents and neurons in the upper cervical cord (Lam et al. 2009a, 2009b). These findings suggest that excitatory amino acid receptors (particularly N-methyl-D-aspartate receptors (NMDAR)), which are also present in migraineurs, play an important role in pain processing and the sensitization process (Vikelis and Mitsikostas 2007).

Despite the above-mentioned data, amongst NMDAR antagonists, only ketamine was delineated as a promising therapeutic option in patients with severe or long lasting migraine aura (Afridi et al. 2013). Substances which can act on α-amino-3-hydroxy-5-methyl-4-isoxazolepropionic acid (AMPA) and kainate subtypes of ionotropic glutamate receptors are also limited, but among them, tezampanel (Alt et al. 2006) has demonstrated promising results in acute migraine therapy (Sang et al. 2004).

The kynurenine pathway (KP) of tryptophan (TRP) metabolism is extensively studied, mostly because of the well-established endogenous protective properties of kynurenic acid (KYNA) against the excitotoxic and oxidative stress inducing effects of other KP metabolites, such as quinolinic acid (QUIN) and 3-hydroxy-L-kynurenine (3-OHK) (Vécsei et al. 2013). KYNA is a non-selective antagonist of the NMDA receptor with a high affinity to its strychnine-insensitive glycine co-agonist site and also exerts weak antagonistic effects on kainate and AMPA receptors (Pereira et al. 2002, Prescott et al. 2006, Szalárdy et al. 2012b). On the basis

of this antagonism on glutamatergic neurotransmission, it is assumed that KYNA and some of its analogs with improved pharmacokinetic or pharmacodynamic properties may have a modifying effect on nociception (Näsström et al. 1992, Párdutz et al. 2012) and thus might be future candidates in headache treatment. A well-known model of trigeminal nociception is the orofacial formalin test, where a formalin solution is administered subcutaneously into the upper lip of rats, causing tissue injury, inflammation and nociception (Clavelou et al. 1995, Raboisson and Dallel 2004). By using this model, both peripheral and central components of pain processing (Chichorro et al. 2017) can be assessed in preclinical studies.

HD is an autosomal, dominantly inherited, progressive neurodegenerative disorder which results in cognitive, psychiatric and motor disturbances. HD is caused by an expansion of the cytosine-adenine-guanine (CAG) repeat in the gene coding for the *N*-terminal region of the huntingtin protein (Htt), which leads to the formation of a polyglutamine stretch. Above 39 CAGs, there is obligatory disease development (The Huntington's Disease Collaborative Research Group 1993). Although the exact mechanisms through which mutant Htt (mHtt) leads to the characteristic neuropathology are not fully understood, the potential roles of excitotoxicity and neuronal mitochondrial dysfunction are among the best-established concepts (Szalárdy et al. 2012a, Zádori et al. 2012). Accordingly, striatal glutamatergic excitotoxicity is involved in the development of HD and predominantly mediated by the overactivation of NMDARs, and most specifically through NR2B subunit-containing NMDARs at the extrasynaptic sites (Milnerwood et al. 2010). In line with this, the expression of mHtt has been shown to sensitize the NR2B subunit-containing NMDARs (Chen et al. 1999). There is evidence indicating that such excitotoxic injury is mediated, at least in part, by endogenous substances, including certain metabolites of the KP of TRP metabolism (Zádori et al. 2011b). Previous studies pointed out several alterations in the KP in tissues from HD patients and transgenic animals (Schwarcz et al. 1988, Beal et al. 1990, 1992, Pearson and Reynolds 1992, Heyes et al. 1992, Jauch et al. 1995) and these results indicated decreased KYNA concentrations relative to the levels of toxic neuroactive kynurenines (Zádori et al. 2011b). Further investigation of these changes in toxin or genetic animal models of HD may yield biomarkers with the above-mentioned properties. A decreased activity of the succinate dehydrogenase (SDH), complex II of the electron transport chain in post-mortem HD brains was one of the early findings suggestive of the role of mitochondrial dysfunction in the

development of HD (Stahl and Swanson 1974). Furthermore, mHtt has been shown to be able to bind directly to the mitochondria, altering their normal function (Choo et al. 2004). In line with the decreased SDH activity, mitochondrial II complex inhibitors, such as 3-nitropropionic acid (3-NP), have been found to be useful in the investigation of HD through their utilization in animal toxin models (Túnez et al. 2010). Accordingly, the 3-NP model is frequently applied as an easy and rapid way to study certain aspects of neurodegenerative processes in HD (Brouillet 2014).

Besides genetic predisposition, like in HD, certain environmental factors may also be responsible for the development of neurodegenerative processes. One of the main culprits in the pathomechanism of PD, which is characterized by the loss of dopaminergic (DAergic) neurons and the presence of Lewy bodies in the substantia nigra (SN) pars compacta (Forno 1996), is mitochondrial dysfunction resulting in energy deficit and oxidative stress (Bose and Beal 2016). With regard to environmental factors, one of the well-established causes of this condition is the life-long cumulative low-dose exposure to mitochondrial toxins (Harris and Blain 2004). The observation of 1-methyl-4-phenyl-1,2,3,6-tetrahydropyridine (MPTP) induced Parkinsonian symptoms yielded one of the first pieces of evidence for toxin-induced parkinsonism (Forno et al. 1993) and since then, systemic MPTP administration has been widely used in various *in vivo* animal studies to investigate the pathogenesis of PD and to assess the therapeutic effect of potential neuroprotective agents (Javitch et al. 1985).

MPTP can easily cross the blood brain barrier (BBB) and is metabolized by monoamine oxidase to 1-methyl-4-phenyl-pyridinium cation (Chiba et al. 1984), which is taken up by DAergic neurons and damages complex I in the mitochondrial electron transport chain (Nicklas et al. 1985). The most sensitive brain region to this toxin is the nigrostriatal system where neuronal loss and reduced DA levels are well-established by both histo- and biochemical methods in MPTP-treated animal models (Hallman et al. 1984). Histochemical confirmation of neuronal loss can be time consuming and is usually is only done for a few subjects not for the whole experimental group and there is already evidence that several MPTP treatment regimens cause DAerg neuronal loss associated with decreased DA concentrations in the striatum (Kurosaki et al. 2004, Jackson-Lewis and Przedborski 2007). Compared to histochemical methods, the levels of DA and its metabolites can be determined by high performance liquid chromatography (HPLC), and can be used on all of the animals in

a reasonable time. According to the above-mentioned mitochondrial dysfunction in PD, several causative and susceptibility genes were identified (Kalinderi et al. 2016), including peroxisome proliferator-activated receptor-gamma (PPARγ) coactivator-1 alpha (PGC-1α). PGC-1α is a multifunctional transcriptional coactivator of nuclear respiratory factors 1 and 2, estrogen-related receptors and PPARs amongst others, and hereby regulates mitochondrial function and biogenesis (Knutti and Kralli 2001). According to St-Pierre et al., PGC-1α-deficient mice are more sensitive to MPTP toxicity compared to the controls (St-Pierre et al. 2006). Furthermore, sub-chronic administration of the toxin can result in significantly elevated PGC-1α expression in the striatum after 24 hours that was normalized 72 hours after treatment (Swanson et al. 2013). This evidence suggests an adaptive mechanism to neurotoxicity, but neuroprotective effects of PGC-1α were also demonstrated in pioglitazone- and resveratrol-treated mice against MPTP toxicity (Breidert et al. 2002, Dehmer et al. 2004). Despite these findings, the available data are limited with regard to the alteration of tissue-specific PGC-1a expression in the brain following various MPTP administration regimens.

Besides QUIN and 3-OHK there are numerous other substances that can facilitate the formation of reactive species (RS) which are responsible for most of the deleterious effects of pathological processes in the nervous system (Szalárdy et al. 2015). The synthesis and toxic effects of RS are decreased by a complex system of antioxidant machinery, including enzymatic (e.g., superoxide dismutase, catalase and glutathione (GSH) peroxidase, (Sies 1997)) and non-enzymatic mechanisms. The latter group consists of chemical compounds, such as, among others, vitamin E, vitamin C, coenzyme Q10, β-carotene, GSH and flavonoids with proven antioxidant properties (Sies 1993). Vitamin E refers to a group of molecules including 4 tocotrienols and 4 tocopherols as lipid soluble antioxidants. Their molecular structure comprises a chromanol ring with an aliphatic side chain, unsaturated for tocotrienols and saturated for tocopherols. Depending on the number and position of methyl groups on the chromanol ring, α-, β-, γ- and δ-tocotrienols and tocopherols can be distinguished (Hacquebard and Carpentier 2005).

Severe tocopherol deficiency develops mainly as a result of malabsorption disorders, abetalipoproteinemia and ataxia with vitamin E deficiency (AVED). AVED is caused by the mutation of the TTPA gene resulting in the decreased activity of the α-tocopherol transfer protein (αTTP, (Morley et al. 2004)). Decreased tocopherol levels are associated with several

neurological symptoms, such as cerebellar ataxia, peripheral neuropathy and myopathy (Ueda et al. 2009, Muller 2010), as the nervous system is particularly sensitive to oxidative damage resulting from increased energy demand and reduced antioxidant capacity (Szalárdy et al. 2015). In addition to the above-mentioned disorders with their characteristic symptoms, some other neuropsychiatric conditions, such as AD (Lopes da Silva et al. 2014) and the exacerbation of MS (Karg et al. 1999) can also be accompanied by significantly reduced serum or plasma tocopherol levels. Differential diagnosis sometimes can be difficult in certain conditions accompanied by neurological symptoms (especially in AVED), therefore the measurement of serum tocopherol levels is advised in cases of ataxia, myopathy or cognitive deficiency (Muller 2010, Fata et al. 2014).

During the analytical procedure to determine concentrations of various compounds from biological matrices, several difficulties can emerge. With regard to the metabolites of TRP, the main problem is that there are several compounds with neuroactive properties (e.g., KYNA, 3-OHK and QUIN) and, so far, there is no simple way to determine their concentrations in a single run. In most cases, multiple runs with different methods (Gas Chromatography-Mass Spectrometry (MassSpec), HPLC-MassSpec, HPLC-UV/Fluorescent detection (FLD)) cannot be applied because of limited amounts of sample (e.g., mouse CNS samples). Another challenge is the measurement of novel KYNA analogs (Fülöp et al. 2009) which requires advanced HPLC-MassSpec method development.

With regard to animal toxin models of neurodegenerative diseases, such as the MPTP model of PD, the main limiting factors are the size of the sample and the small concentration of the measured compounds. Neuronal loss, the decisive trait of neurodegeneration, can be evaluated by specific histochemical methods, but they are time consuming. However, it has been proven that DAergic neuronal loss correlates with the measured decrease in DA concentration in the striatum (Kurosaki et al. 2004). Accordingly, the determination of the levels of DA and some of its metabolites, 3,4-dihydroxyphenylacetic acid (DOPAC) and homovanillic acid (HVA) with HPLC and electrochemical detection may be simpler than cell counting with design-based stereological methods following immunohistochemical labeling (Jackson-Lewis and Przedborski 2007). Electrochemical detectors are one of the most sensitive detector options for HPLC measurements and they are typically used for determining catecholamines, aromatic amines and phenolics. However, there are some drawbacks to these detectors

because they are sensitive to changes in temperature and pressure, and furthermore, the detector cell needs to be properly shielded from electromagnetic radiation.

Tocopherol measurements pose a different challenge to the analytical procedure. During sample preparation there is liquid-liquid extraction into n-hexane, evaporation under nitrogen flow and reconstitution in organic solvents, all of which may contribute to overall errors in measurement.

2 Aims

I., To study the possible pharmacokinetic explanation of the protective effects of two KYNA analogs (KA-1: N-(2-N,N-dimethylaminoethyl)-4-oxo-1H-quinoline-2-carboxamide hydrochloride and KA-2: N-(2-N-pyrrolidinylethyl)-4-oxo-1H-quinoline-2-carboxamide hydrochloride) in the orofacial formalin model of headache.

II., To examine the alterations in concentrations of some initial compounds in the KP of TRP metabolism following 3-NP administration as a toxin model of HD.

III., To determine the biochemical background to assess of the presence or the lack of MPTP-induced changes in tissue specific PGC1-α expression when grading nigrostriatal injury.

IV., To establish reference intervals (RI) for serum tocopherol concentrations in relation to the adult Hungarian population.

3 Materials and methods

3.1 Pharmacokinetic assessment of KYNA and KYNA amides

During the experiments, adult male Sprague-Dawley rats weighing 200-250 g were used. The animals were housed under standard laboratory conditions (in an air-conditioned, humidity-controlled and ventilated room) and were allowed free access to drinking water and regular rat chow on a 12 h−12 h dark-light cycle. The procedures used in this study were approved by the Committee of Animal Research at the University of Szeged (I-74-12/2012) and the Scientific Ethics Committee for Animal Research of the Protection of Animals Advisory Board (XXIV./352/2012.).

At set time points (15, 30, 60, 120 and 300 min) following the intraperitoneal (i.p.) injection with the KYNA amides (1 mmol/kg), the rats were deeply anesthetized with i.p. injection of chloral hydrate (0.4 g/kg, Sigma-Aldrich). Blood samples were collected from vena cava caudalis and centrifuged at 13709 relative centrifugal force (RCF) for 10 min at 4°C. The supernatants, i.e., the serum samples, were collected and centrifuged at 13709 RCF for 10 min at 4°C again and the supernatants were stored at - 80°C until use. After the collection of blood samples, the animals were transcardially perfused with 100 ml 0.1 M phosphate-buffered saline (PBS) for 5 min. The CNS samples containing the medullary segment of the TNC were then removed and stored at - 80°C until measurements. The animals in the control group underwent a similar procedure.

For the measurement of KYNA concentration, the CNS samples were cut in half, weighed and then sonicated for 1.5 min in an ice-cooled solution (250 µl) comprising perchloric acid (PCA, 2.5% w/w), 3-nitro-L-tyrosine (3-NLT, 10 or 2 µM) and distilled water in an Eppendorf tube. The content of the Eppendorf tube was centrifuged at 13709 RCF for 10 min at 4°C and the supernatant was measured. Before analysis, the serum samples were thawed and, after a brief vortex, the serum sample was 'shot' onto a precipitation solvent (containing PCA with 3-NLT as internal standard, with resulting concentrations of 2.5 w/w% and 2 µM, respectively). The samples were subsequently centrifuged at 13709 RCF for 10 min at 4°C, and the supernatants were collected for measurement.

For the analysis of KYNA amides (KA-1 and KA-2, Figure 1), the other half of the CNS samples were weighed and then sonicated in ice-cold (250 µl) distilled water for 1.5 min and centrifuged at 13709 RCF for 10 min at 4°C. From the supernatant, 100 µl was transferred to an Eppendorf tube containing 750 µl HPLC gradient grade acetonitrile and 150 µl distilled water. After a brief vortex, the samples were centrifuged at 13709 RCF for 10 min at 4°C and 900 µl of supernatant was evaporated in a vacuum centrifuge. After thawing and brief stirring with a vortex, 200 µl of serum sample was transferred to an Eppendorf tube containing 700 µl HPLC gradient grade acetonitrile (ACN) and 100 µl distilled water. After a brief vortex, the samples were centrifuged at 13709 RCF for 10 min at 4°C and 900 µl of supernatant was evaporated in a vacuum centrifuge. The resulting samples were stored at 4°C until use.

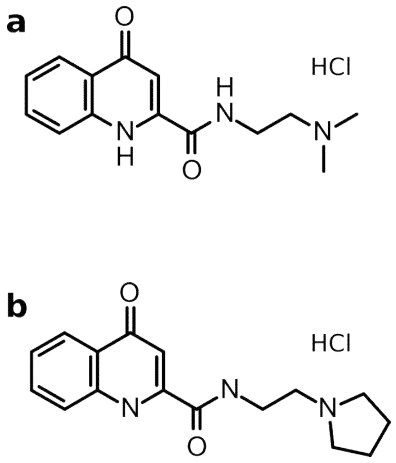

Figure 1 The chemical structure of N-(2-N,N-dimethylaminoethyl)-4-oxo-1H-quinoline-2-carboxamide hydrochloride (KA-1, a) and N-(2-N-pyrrolidinylethyl)-4-oxo-1H-quinoline-2-carboxamide hydrochloride (KA-2, b)

The KYNA concentrations of the serum and CNS samples were quantified on the basis of a slight modification of a literature method (Hervé et al. 1996). Briefly, we used an Agilent 1100 HPLC system (Agilent Technologies, Santa Clara, CA, USA) equipped with fluorescence and a UV detector; the former was applied at excitation and emission wavelengths of 344 nm and 398 nm for the determination of KYNA and the latter was set at 365 nm for the determination of the internal standard (3-NLT). Chromatographic separations were performed on an Onyx Monolithic C18 column, 100 mm x 4.6 mm I.D. (Phenomenex Inc., Torrance, CA, USA) after passage through a SecurityGuard pre-column C18, 4 x 3.0 mm I.D., 5 µm particle size (Phenomenex Inc., Torrance, CA, USA) with a mobile phase composition of 0.2 M zinc acetate/ACN = 95/5 (v/v), the pH of which was adjusted to 6.2

with acetic acid, applying isocratic elution. The flow rate was 1.5 ml/min and the injection volume was 20 µl for serum, and 50 µl for CNS samples.

For the determination of KYNA amides, a Thermo LCQFleet ion trap mass spectrometer was used equipped with an ESI ion source combined with a Dionex Ultimate3000 HPLC system. The ionization parameters were as follows: heater temperature: 500°C, sheath gas flow rate: 60, auxiliary gas flow rate: 20, spray voltage: 4 kV, capillary temperature: 400°C. Chromatographic separations were performed on a Kinetex C18 column, 100 mm x 4.6 mm, 2.6 µm particle size (Phenomenex Inc., Torrance, CA, USA) after passage through a SecurityGuard pre-column C18, 4 x 3.0 mm, 5 µm particle size (Phenomenex Inc., Torrance, CA, USA), with a mobile phase composition of 0.05% aqueous CH_3COOH/ACN = 90/10 (v/v), applying isocratic elution. The flow rate and the injection volume were 1 ml/min and 50 µl, respectively.

Calibrants were prepared at 6 different concentration levels, from 1 to 100 nM, 0.5 to 5 µM and 0.01 to 100 µM for KYNA, 3-NLT and the KYNA amides, respectively. 3 parallel injections of each solution were made under the chromatographic conditions described above. The peak area responses were plotted against the corresponding concentration, and the linear regression computations were carried out by the least square method with the freely available R software (R Development Core Team 2008). Very good linearity ($R^2 \leq 0.99$) was observed throughout the investigated concentration ranges for KYNA, 3-NLT and the KYNA amides when fluorescence, UV or MassSpec detection was applied.

The selectivity of the method was checked by comparing the chromatograms of KYNA, KYNA amides and the internal standard for a blank serum and CNS sample and those for a spiked sample. All compounds could be detected in their own selected chromatograms without any significant interference.

The limit of detection (LOD) and the lower limit of quantification (LLOQ) were determined via the signal-to-noise ratio with a threshold of 3 and 10, respectively, according to the International Conference on Harmonization guidelines (ICH 1995). The LOD and LLOQ for KYNA in the serum samples were 1 nM and 3.75 nM, respectively, while in the CNS samples they were 0.4 nM and 1 nM, respectively. The LOD and LLOQ for the samples in MS detection were 1 nM and 15 nM, respectively.

Replicate HPLC analysis showed that the coefficient of variation (CV) was ≤ 2.2% for the peak area response and ≤ 0.1% for the retention time for KYNA and the KYNA amides.

The relative recoveries were estimated by measuring spiked samples of KYNA and the KYNA amides at 2 concentrations with 3 replicates of each. No significant differences were observed for the lower and higher concentrations. The recoveries for the serum samples ranged from 103 to 108%, 81 to 94% and 79 to 80% for KYNA, KA-1 and KA-2, respectively. The recoveries for the CNS samples ranged from 82 to 92% and 78 to 84% for KYNA and KA-2, respectively. The peaks of the different compounds obtained during HPLC-MassSpec analysis are presented in Figure 2.

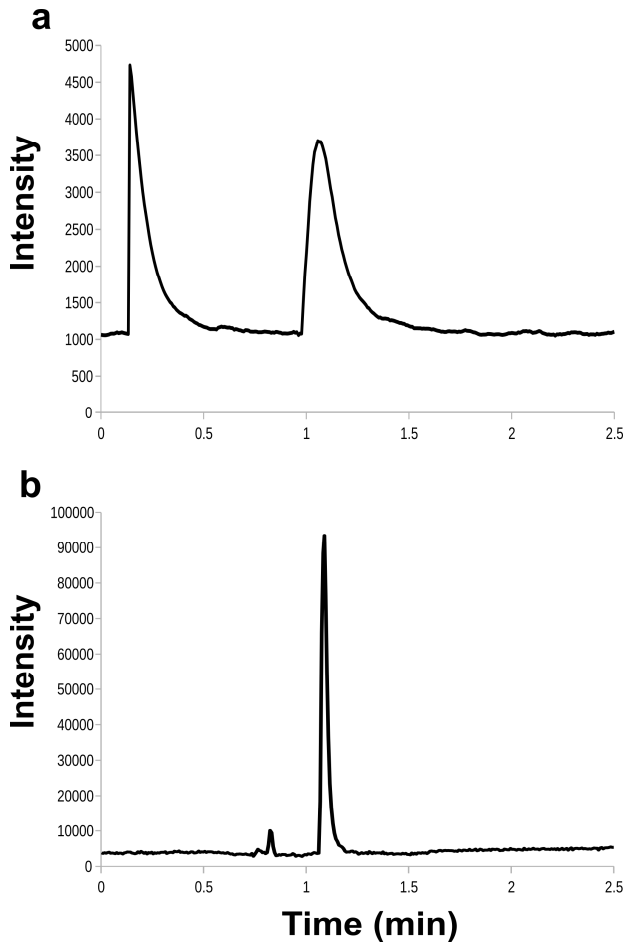

Figure 2 Chromatograms of the analyzed kynurenic acid analogs, KA-1 (N-(2-N,N-dimethylaminoethyl)-4-oxo-1H-quinoline-2-carboxamide hydrochloride; a) and KA-2 (N-(2-N-pyrrolidinylethyl)-4-oxo-1H-quinoline-2-carboxamide hydrochloride; b) obtained with mass spectrometric detection from the serum of Sprague-Dawley rats.

3.2 Measurement of TRP metabolites in a toxin model of HD

We used 30 5-month-old male C57Bl/6 mice in this study. The animals were housed in cages under standard conditions with a 12-12-h light-dark cycle and free access to food and water. The experiments were carried out in accordance with the European Communities Council Directive (86/609/EEC) and were approved by the local animal care committee as well. The animals were randomly divided into two groups (n = 16 and n = 14, respectively). In the first group, 3-NP (Sigma-Aldrich, Saint Louis, MO, USA; dissolved in PBS, pH adjusted to 7.4) was administered in a subacute dosing regimen as reported previously (Török et al. 2015), with 2 daily i.p. injections (50 mg/kg each) for 5 consecutive days. The 2nd group served as the vehicle-injected control.

On the 18th day of the experiment (12 days after the last 3-NP injection), the mice were deeply anesthetized with isoflurane (Forane; Abott Laboratories Hungary Ltd., Budapest, Hungary). After thoracotomy, 0.3–0.7 ml venous blood was obtained from the right ventricle by intracardial puncture, followed by perfusion with artificial cerebrospinal fluid (composition in mM: 122 NaCl, 3 KCl, 1 Na_2SO_4, 1.25 KH_2PO_4, 10 D-glucose*H_2O, 1 $MgCl_2$*$6H_2O$, 2 $CaCl_2$*$2H_2O$, 6 $NaHCO_3$) for 2 min by an automatic peristaltic pump. The blood samples were left to coagulate for 30 min, and were then centrifuged at 13709 RCF for 10 min at 4°C. The supernatant sera were pipetted into Eppendorf tubes and stored at - 80°C until further sample handling. After perfusion, the brains were rapidly removed on ice and stored at - 80°C until analysis. Before analysis, the CNS samples were weighed and then sonicated in an ice-cooled solution (250 µl) containing 2.5 w/w% PCA with 2 µM 3-NLT and 600 nM isoproterenol (IPR) as internal standards. The samples were next centrifuged at 13709 RCF for 10 min at 4°C, and the supernatants were collected.

Before analysis, the serum samples were thawed and, after a brief vortex 200 µl of serum sample was 'shot' onto 200 µl of precipitation solvent (containing 5 w/w% PCA with 4 µM 3-NLT and 2 µM IPR as internal standards). The samples were subsequently centrifuged at 13709 RCF for 10 min at 4°C, and the supernatants were collected.

The TRP, KYN and KYNA concentrations of the samples were quantified with the same equipment and method as described in paragraph 3.1 where the fluorescence detector was set at excitation and emission wavelengths of 254 nm and 398 nm for TRP, and the UV detector was set at 365 nm for the determination of KYN.

For determination of the concentrations of 3-OHK and its internal standard (IPR), we applied the Agilent 1100 HPLC system equipped with Model 105 electrochemical detector (Precision Instruments, Marseille, France). In brief, the working potential of the detector was set at +650 mV, using a glassy carbon electrode and an Ag/AgCl reference electrode. The mobile phase containing sodium octylsulfate (2.8 mM), sodium dihydrogenphosphate (75 mM) and disodium ethylenediaminetetraacetate (Na_2EDTA, 100 µM) was supplemented with ACN (5 v/v%) and the pH was adjusted to 3.0 with phosphoric acid (85 w/w%). The mobile phase was delivered at a rate of 1 ml/min at 40°C onto the reversed-phase column (HR-80 C18, 80 x 4.6mm, 3-µm particle size; ESA Biosciences, Chelmsford, MA, USA) after passage through a pre-column (Hypersil ODS, 20 x 2.1 mm, 5-µm particle size; Agilent Technologies, Santa Clara, CA, USA). 10 µl aliquots were injected by the auto-sampler with the cooling module set at 4°C.

Method validation was conducted the same way as described in paragraph 3.1. Calibrants were prepared at 6 different concentration levels, from 0.1 to 50 µM, 0.05 to 5 µM, 1 to 100 nM, 10 to 200 nM, 0.5 to 7.5 µM and 25 to 600 nM for TRP, KYN, KYNA, 3-OHK and the internal standards, 3-NLT and IPR, respectively. Very good linearity ($R^2 \leq 0.99$) was observed throughout the investigated concentration ranges for TRP, KYNA, KYN, 3-OHK and the internal standards when either fluorescence, UV or electrochemical detection was applied and all compounds could be detected in their own selected chromatograms without any significant interference. The LOD for CNS samples was 10, 40, 0.4 and 10 nM, while LLOQ was 20, 130, 1 and 30 nM for TRP, KYN, KYNA, and 3-OHK, respectively. The LOD for the serum samples was 15, 100, 1 and 10 nM, while LLOQ was 35, 275, 3.75 and 30 nM for TRP, KYN, KYNA and 3-OHK, respectively. Replicate HPLC analysis showed that CV was ≤ 2.2% for the peak area response and ≤ 0.1% for the retention time for TRP, KYN and KYNA, whereas in the case of 3-OHK the CV was ≤ 8.6% for the peak area response and ≤ 0.3% for the retention time. The recoveries for the CNS samples were 86 to 91%, 98 to 100%, 82 to 92% and 69 to 74% for TRP, KYN, KYNA and 3-OHK, respectively. The recoveries for the serum samples ranged from 77 to 90%, 77 to 82%, 103 to 108% and 28 to 34% for TRP, KYN, KYNA and 3-OHK, respectively. The peaks of the different compounds obtained during chromatographic analysis are presented in Figure 3.

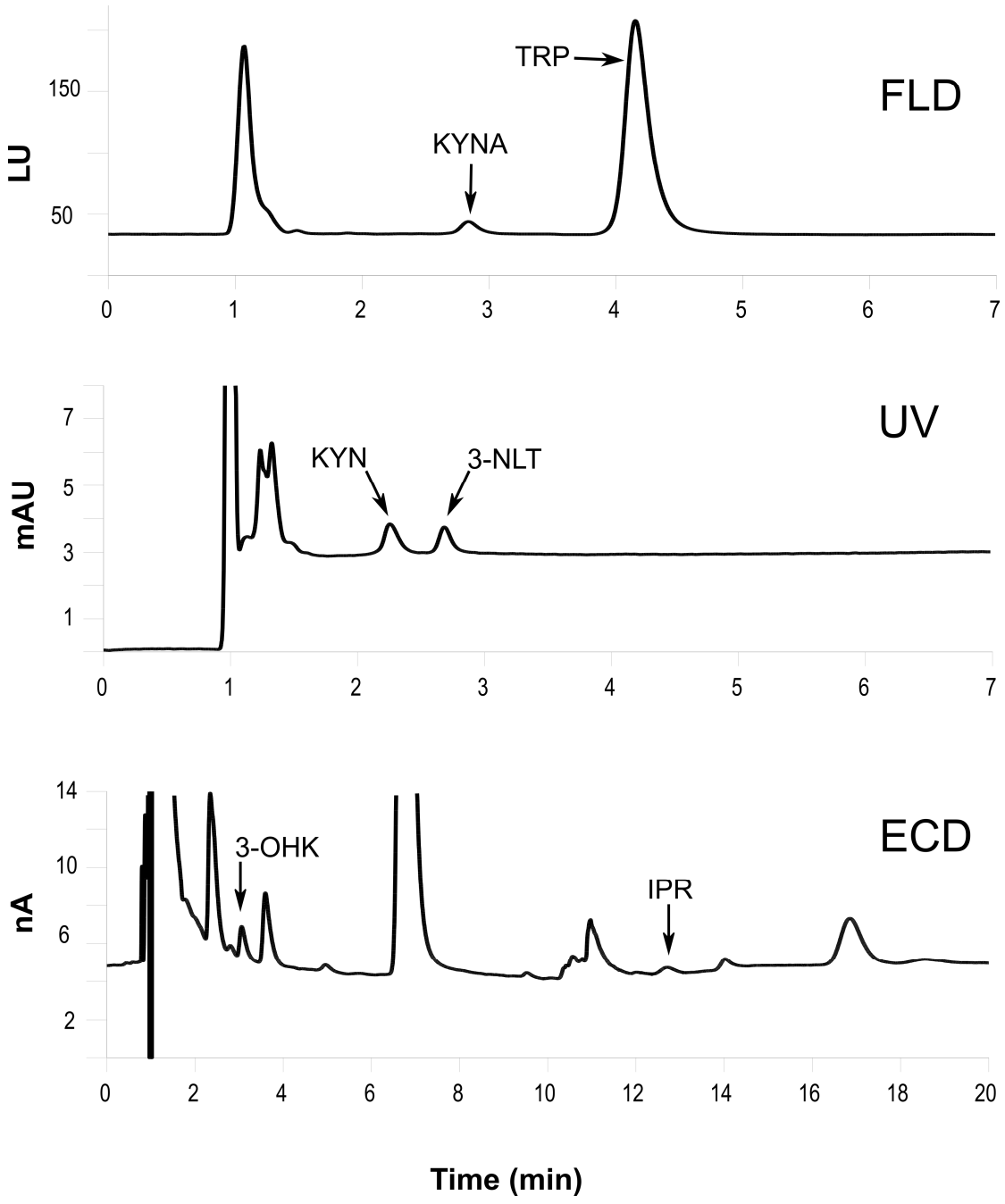

Figure 3 Chromatograms of the analyzed compounds of the kynurenine pathway of the tryptophan metabolism, from C57Bl/6 murine brain samples. *3-NLT* 3-nitro-L-tyrosine, *3-OHK* 3-hydroxykynurenine, *ECD* electrochemical detector, *FLD* fluorescence detector, *IPR* isoproterenol, *KYNA* kynurenic acid, *KYN* kynurenine, *TRP* tryptophan

3.3 Measurement of DA and its metabolites after MPTP treatment

12-week-old C57Bl/6 male mice were used in this study. The animals were housed in cages and maintained under standard laboratory conditions with 12-12 h light-dark cycle and free access to food and water. The experiments were carried out in accordance with the European Communities Council Directive (86/609/EEC) and were approved by the local animal care committee as well.

MPTP was dissolved in PBS (pH adjusted to 7.4) and was administered i.p. Animals were randomly divided into 6 groups (n = 7-8 in each group). The 1st and 2nd group received i.p. injection of 15 mg/kg body weight MPTP 5 times at 2 h intervals. The animals in the 1st group were deeply anesthetized with isoflurane (Forane®; Abott Laboratories Hungary Ltd., Budapest, Hungary) and the brains were dissected 90 min following the last MPTP injection (acute treatment – acute (day 1) assessment), while animals in the 2nd group were deeply anesthetized with isoflurane and the brains were dissected 1 week later (acute treatment - subacute (day 7) assessment). The mice in the 3rd group were injected i.p. with 15 mg/kg body weight MPTP once a day for 12 days (chronic treatment). 90 min following the last injection the animals were euthanized via isoflurane overdose as well. The 4th, 5th and 6th groups served as the respective control groups, and were injected with 0.1 M PBS according to the above-detailed treatment regimen. During the dissection process the brains were rapidly removed on ice and immediately halved at the midline. Following that, both hemispheres were further cut to obtain the striatum, cortex and cerebellum. Thereafter, these samples were stored at - 80ºC until the HPLC analysis.

The striata were weighted and then homogenized in an ice-cold solution (750 µl) containing PCA (2.5% w/w), sodium metabisulfite (0.1 M), Na_2EDTA (0.1 M), distilled water and 0.25 mM IPR for 30 sec. The homogenate was centrifuged at 13709 RCF for 10 min at 4ºC. The supernatant was stored at - 20ºC until the analysis. DA and its metabolites, DOPAC and HVA were measured with an Agilent 1100 HPLC system (Agilent Technologies, Santa Clara, CA, USA) combined with a Model 105 electrochemical detector (Precision Instruments, Marseille, France) under isocratic conditions. In brief, the working potential of the detector was set at +750 mV, using a glassy carbon electrode and an Ag/AgCl reference electrode. The mobile phase containing sodium dihydrogenphosphate (75 mM), sodium octylsulfate (2.8 mM) and Na_2EDTA (50 µM) was supplemented with ACN (10% v/v) and the pH was adjusted to 3.0

with phosphoric acid (85% w/w). The mobile phase was delivered at a rate of 1 ml/min at 40°C onto the reversed-phase column (HR-80 C18, 80 x 4.6 mm, 3 µm particle size; ESA Biosciences, Chelmsford, MA, USA) after passage through a pre-column (SecurityGuard, 4 x 3.0 mm I.D., 5 µm particle size, Phenomenex Inc., Torrance, CA, USA)). 10 µl aliquots were injected by the autosampler with the cooling module set at 4°C. With regard to method validation, which was conducted the same way as described in paragraph 3.1, the following parameters are reported briefly. Calibrants were prepared at 6 different concentration levels, from 2 to 200 ng/ml. Very good linearity ($R^2 \leq 0.99$) was observed throughout the investigated concentration ranges for DA, DOPAC and HVA and the internal standard (IPR) and all compounds could be detected in their own selected chromatograms without any significant interference. The LOD and LLOQ for the investigated compounds in the brain samples were 2 ng/ml and 10 ng/ml, respectively. With regard to precision, the CV was ≤ 3.25% for the peak area responses and ≤ 0.05% for the retention times. The recoveries ranged from 109 to 110%, 108 to 109% and 99 to 102% for DA, DOPAC and HVA, respectively. The peaks of the different compounds obtained during chromatographic analysis are presented in Figure 4.

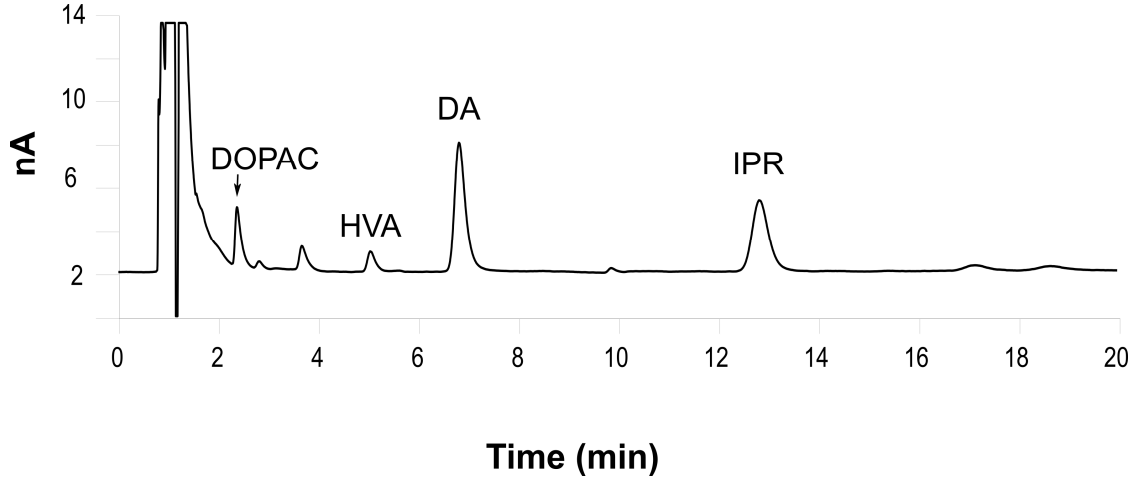

Figure 4 Chromatograms of the analyzed compounds of the dopamine metabolism in C57Bl/6 murine brain samples with electrochemical detection. *DA* dopamine, *DOPAC* 3,4-dihydroxyphenylacetic acid, *HVA* homovanillic acid, *IPR* isoproterenol

3.4 Tocopherol measurements from human serum

The study sample population comprised of 30 male (age range: 21-71 years, mean age: 49.50 year) and 30 female volunteer individuals (age range: 25-76 years, mean age: 50.03 year) without any major chronic illness and 30 male (age range: 18-73 years, mean age: 49.43 year) and 30 female (age range: 24-78 years, mean age: 49.60 year) patients with other neurological diseases (OND; main diagnoses for males were the following: ischemic stroke: 8, PD: 5, epilepsy: 5, lumbar disc disorder: 3, and other: 9; main diagnoses for females were the following: multiple sclerosis in remission: 8, ischemic stroke: 6, epilepsy: 5, and other: 11) where the presence of ataxia, myopathy or cognitive dysfunction was excluding criteria. The distribution of the age of the subjects was Gaussian in all groups ($p > 0.05$, Anderson-Darling test) and the variances were equal ($p = 0.98$, Levene test). There was no significant difference between the groups ($F = 0.01$, $p = 0.99$, one-way ANOVA). The recent regular intake of antihyperlipidemic agents or any kind of drugs or food supplements containing antioxidants was exclusion criteria as well in all groups. All participating individuals were of Hungarian origin and were enrolled in the Department of Neurology at the University of Szeged. The study was approved by the Ethics Committee of the Faculty of Medicine, University of Szeged (19/2014). All study participants gave their written informed consent, in accordance with the Declaration of Helsinki.

Blood was collected by venipuncture into gold-top vacutainers following fasting for 12 hours. The blood was immediately centrifuged at 1166 RCF for 10 min. 200 µL of the supernatant serum was shot into a solution containing 200 µL ascorbic acid (0.085 M) and 400 µL butylated hydroxytoluene (BHT, 1.14 mM) and the resulting solution was stored on - 80°C until measurement, while the remaining serum was aliquoted and stored on - 80°C as well.

Before HPLC measurement, 600 µL n-hexane containing 1.14 mM BHT and rac-tocol as internal standard were added to the freshly thawed serum samples treated with antioxidants (800 µL). This mixture was mixed for 1 min and then centrifuged at 1166 RCF for 5 min at 4°C. The hexane layer was transferred to a test vial and evaporated under nitrogen flow. The residue was reconstituted with 75 µL ACN and 50 µL ethanol/dioxane (1:1). The resulting solution was transferred into a 200 µL glass insert placed into an amber-colored vial for measurement.

Total cholesterol and triglyceride levels were determined by commercially available kits from Diasys (Diagnostics Systems GmbH, Holzheim, Germany) on Roche Modular P800 analyser (Roche, Rotkreuz, Switzerland) in the Department of Laboratory Medicine (Faculty of Medicine, Albert Szent-Györgyi Clinical Center, University of Szeged, Szeged, Hungary).

The concentrations of α-, β/γ-, δ-tocopherol were quantified with an Agilent 1200 HPLC system (Agilent Technologies, Santa Clara, CA, USA) equipped with an UV/VIS diode array detector (DAD) applying the modified method of Hess et al. (Hess et al. 1991). Chromatographic separations were performed on an Alltech Prevail C18 column, 150 x 4.6 mm I.D., 5 μm particle size (Alltech Associates Inc., Deerfield, IL, USA) after passage through a SecurityGuard pre-column, C18, 4 x 3.0 mm I.D., 5 μm particle size (Phenomenex Inc., Torrance, CA, USA) with a mobile phase composition of ACN/tetrahydrofurane/methanol/1 w/v% ammonium acetate/distilled water (684:220:68:28:28) applying isocratic elution. The flow rate and the injection volume were 2.1 mL/min and 50 μL, respectively. The detector was set at 292 (α-tocopherol) and 297 (β/γ-, δ-tocopherol, rac-tocol) nm.

The separation of β- and γ-tocopherol is challenging because they only differ in the position of a methyl group. With the use of a C18 column these 2 compounds have almost the same retention time (Saha et al. 2013). β- and γ-tocopherols can only be separated with the application of special columns and methods (Grebenstein and Frank 2012, Górnaś et al. 2014), the application of which may be challenging for the routine clinical practice. Accordingly, only γ-tocopherol was applied as standard compound for the establishment of the calibration curve in this study, and the concentrations at the corresponding retention time includes both substances and reported as β/γ-tocopherol.

With regard to method validation, which was conducted with minor changes compared to paragraph 3.1, the following parameters are reported briefly. Calibrants were prepared from serum samples spiked with 6 different concentration levels with concentration ranges of 0 – 40 μM, 0 – 6 μM, 0 – 6 μM and 0 – 24 μM for α-, β/γ-, δ-tocopherol and rac-tocol, respectively. Very good linearity ($R^2 \geq 0.99$) was observed throughout the concentration ranges for α-, β/γ-, δ-tocopherol and rac-tocol. For the determination of within-run precision, 5 samples for 4 concentration levels were applied (i.e., 20 replicates altogether). This measurement was repeated 2 more times with at least 1 week intervals to obtain between-run

precision. With regard to within-run precision the CV of the measured concentrations were 4.53%, 3.72% and 5.11% for α-, β/γ- and δ-tocopherols, respectively, whereas in case of between-run precision, they were 3.59%, 5.93% and 4.76% for α-, β/γ- and δ-tocopherol, respectively. The recoveries for the serum samples ranged from 86 to 105%, from 95 to 108% and from 116 to 124% for α-, β/γ- and δ-tocopherol, respectively. The peaks of the different compounds obtained during chromatographic analysis are presented in Figure 5.

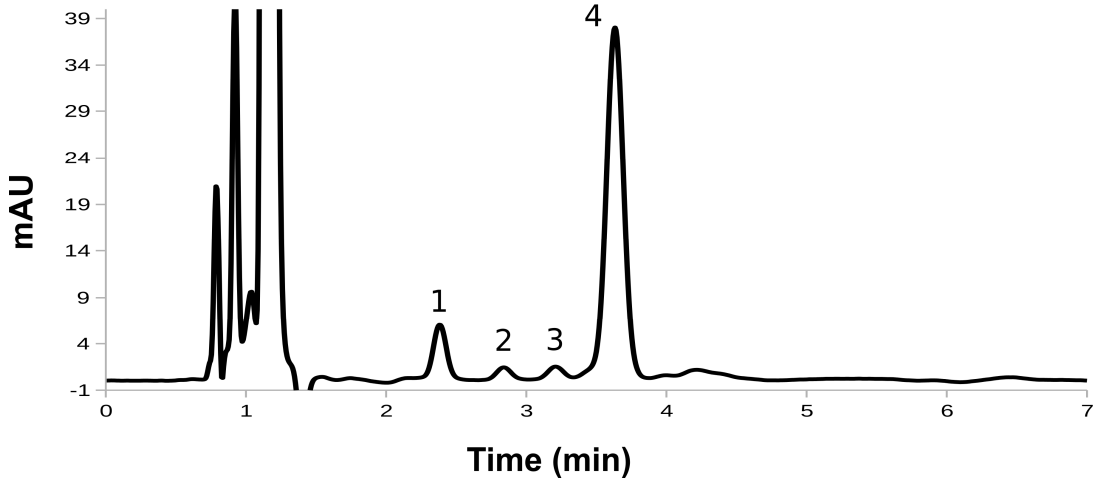

Figure 5 Chromatograms of the analyzed tocopherols from human serum with UV detection on 297 nm. rac-tocol (1), δ-tocopherol (2), γ-tocopherol (3) and α-tocopherol (4)

3.5 Statistics

All statistical analyses were performed with the use of the R software (R Development Core Team 2002). The pharmacokinetic data were evaluated with PKSolver, a freely available menu-driven add-in program for Microsoft Excel (Zhang et al. 2010).

We first checked the distribution of data populations with the Shapiro-Wilk test, and we also performed the Levene test for analysis of the homogeneity of variances. In the case of the analysis of 3-NP toxin model, due to the necessity of a large number of comparisons of data from the 2 groups obtained via a single measurement, two-sample t-tests via Monte-Carlo permutation (with 10,000 random permutations) were applied. With regard to the measurements for MPTP toxin model, all the data exhibited normal distribution and equal

variances were assumed, and therefore ANOVA was used with Bonferroni post hoc comparison.

To determine RI for tocopherol measurements, we took the IFCC (International Federation of Clinical Chemistry and Laboratory Medicine) and CLSI (Clinical and Laboratory Standards Institute) guidelines (Horowitz 2016) as a basis. According to these guidelines the minimum required number of individuals for the determination of RI with the bootstrap method is at least 100 samples. First we checked the distribution of our data with the Anderson-Darling test and we also performed the Levene test for analysis of the homogeneity of variances. If the distribution proved to be Gaussian and the variances were equal, one-way ANOVA was applied to compare the groups, otherwise Kruskal-Wallis test was utilized. To obtain the necessary quantiles and their confidence intervals for the determination of the reference intervals, the bootstrap method (1000 iterations) was applied. The correlation between the concentration of the measured compounds and the age of individuals in the sample population was examined with the nonparametric Spearman's test.

We rejected the null hypothesis when the corrected p values were < 0.05, and in such cases the differences were considered significant. Data with Gaussian or non-Gaussian distributions were plotted as means (± S.E.M. or ± S.D.) or medians (and interquartile range), respectively.

4 Results

4.1 Pharmacokinetic assessment of KYNA and KYNA amides

The concentrations of KYNA and KYNA amides measured in rat serum and CNS samples by HPLC are demonstrated in Table 1.

Table 1 The concentration of KYNA and KYNA amides in Sprague-Dawley male rat serum and CNS samples.

Serum

	KA-1 treatment		KA-2 treatment	
Time (min)	KA-1 (μM)	KYNA (nM)	KA-2 (μM)	KYNA (nM)
0 (control)	0	75.7 (72.8−90.4)	0	75.7 (72.8−90.4)
15	87.4 (0−191.2)	5517.9 (3287.2−6290.1)	2.6 (2.2−20.9)	287.9 (239.1−6753.5)
30	35.6 (0−140.4)	1159.3 (523.8−2397.9)	20.9 (17.4−22.6)	16709.5 (13796.6−17519)
60	39.6 (0−114.4)	464.1 (304.9−1342.3)	13.7 (13.7−14)	3375.8 (3332.7−4604.1)
120	19.5 (0−87.2)	561 (353.2−570.4)	3.2 (3−4.7)	334.6 (232.4−422.2)
300	3.1 (0−61.5)	103.6 (99.1−128.2)	0.5 (0.5−0.5)	149.3 (110.3−150.1)

CNS

	KA-1 treatment		KA-2 treatment	
Time (min)	KA-1 (pmol/g ww)	KYNA (pmol/g ww)	KA-2 (pmol/g ww)	KYNA (pmol/g ww)
0 (control)	0	5.33 (1.00−13.17)	0	5.33 (1.00 - 13.17)
15	< LOD	58.98 (53.37−277.22)	< LOD	17.41 (15.02−19.31)
30	< LOD	44.69 (29.43−104.13)	4.45 (3.88−4.67)	34.77 (25.01−50.53)
60	< LOD	58.61 (25.97−103.53)	6.44 (5.62−7.85)	65.70 (41.54−110.68)
120	< LOD	12.00 (11.07−15.68)	3.28 (2.75−3.31)	15.30 (10.81−18.47)
300	< LOD	13.73 (13.16−19.79)	1.98 (1.50−2.90)	22.43 (19.63−24.62)

The concentrations were measured with HPLC after pretreatment with KA-1 and KA-2. Sprague-Dawley male rats: n = 5 in each group; data are shown as median (interquartile range); *KYNA* kynurenic acid, *KA-1* N-(2-N,N-dimethylaminoethyl)-4-oxo-1H-quinoline-2-carboxamide hydrochloride, *KA-2* N-(2-N-pyrrolidinylethyl)-4-oxo-1H-quinoline-2-carboxamide hydrochloride, *LOD* limit of detection.

The time-course profile of the KYNA amides in the rat serum revealed that, after a steep increase in the concentration, a subsequent steep decrease occurred in the first hour, followed by a prolonged further gradual decrease (Figure 6).

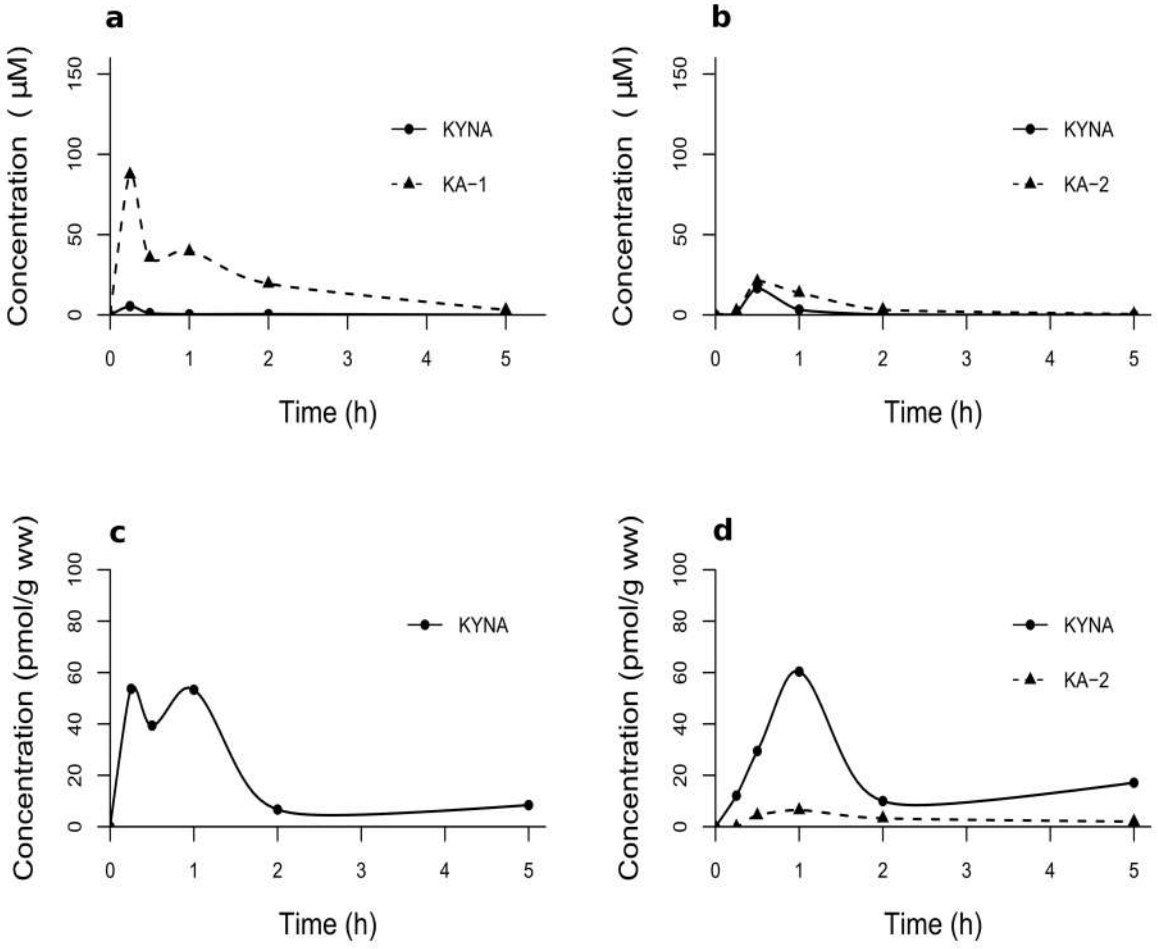

Figure 6 The concentrations of KYNA and KYNA amides in serum and CNS samples of Sprague-Dawley male rats. Figure 6a and 6b demonstrate the concentrations of KYNA and KYNA amides in rat serum with the course of time after injection. Figure 6c and 6d show the concentrations of KYNA and KYNA amides in the CNS samples of the same animals. KA-1 concentrations were under the limit of detection in the CNS samples. Sprague-Dawley male rats: n = 5 in each group; data are shown as medians; KYNA kynurenic acid, KA-1 N-(2-N,N-dimethylaminoethyl)-4-oxo-1H-quinoline-2-carboxamide hydrochloride, KA-2 N-(2-N-pyrrolidinylethyl)-4-oxo-1H-quinoline-2-carboxamide hydrochloride

Although the serum concentration of KA-2 did not show such a high level as that of KA-1, a slightly slower decrease in concentration was observed. These observations are consistent with the calculated serum pharmacokinetic parameters (C_{max}, T_{max}, area under the curve (AUC_{0-t}), the half-life ($t_{1/2}$), apparent total clearance (CL/F_{obs}) and apparent volume of distribution (Vz/F_{obs})) of KA-1 and KA-2, demonstrated in Table 2.

Table 2 Pharmacokinetic parameters of KYNA and KYNA amides in rat serum and CNS samples after intraperitoneal injection of KA-1 and KA-2.

Serum

	KA-1 treatment		KA-2 treatment	
Pharmacokinetic parameters	KA-1	KYNA	KA-2	KYNA
$t_{1/2}$ (h)	1.09	0.91	0.84	0.64
t_{max} (h)	0.25	0.25	0.50	0.50
C_{max} (µM)	87.44	5.44	20.87	16.63
AUC $_{0-t}$ (µM*h)	99.22	2.61	23.35	7.89
Vz/F_{obs} ((µmol/kg)/(µmol/l))	15.17	-	50.02	-
Cl/F_{obs} ((µmol/kg)/(µmol/l)/h)	9.61	-	41.81	-

CNS

	KA-1 treatment		KA-2 treatment	
Pharmacokinetic parameters	KA-1	KYNA	KA-2	KYNA
$t_{1/2}$ (h)	NA	1.67	2.61	3.45
t_{max} (h)	NA	0.25	1	1
C_{max} (pmol/g)	NA	53.66	6.44	60.37
AUC $_{0-t}$ (pmol/g*h)	NA	86.46	16.24	97.77
Vz/F_{obs} ((pmol/kg)/(pmol/l))	NA	-	158,88	-
Cl/F_{obs} ((pmol/kg)/(pmol/l)/h)	NA	-	42,22	-

The KYNA amides were applied in a dose of 1 mmol/kg. Sprague-Dawley male rats: n = 5 in each group; *KYNA* kynurenic acid, *KA-1* N-(2-N,N-dimethylaminoethyl)-4-oxo-1H-quinoline-2-carboxamide hydrochloride, *KA-2* N-(2-N-pyrrolidinylethyl)-4-oxo-1H-quinoline-2-carboxamide hydrochloride, *NA* not available

However, the increase in serum KYNA concentration following the i.p. injection of KA-2 was considerably higher (an approximately 200-fold maximal increase) as compared with that of KA-1 (an approximately 70-fold maximal increase), also well reflected by the above-mentioned pharmacokinetic parameters. To avoid the influence of the basal serum KYNA level on the calculated pharmacokinetic parameters, these basal concentrations were subtracted from the corresponding subsequent concentrations in the calculation of the pharmacokinetic parameters. The pharmacokinetic data therefore reflect only the KYNA amide-induced changes in KYNA concentrations. In the 5th hour, KA-1 and KA-2 were still present at 3.1 (0−61.5) μM and 0.5 (0.5−0.5) μM in the serum, respectively, while the KYNA levels had approximately returned to the baseline level, preferentially in the case of KA-1 treatment. In the rat CNS samples the KA-1 concentration was under LOD. However, KA-2 was present in detectable amounts in the CNS, reaching its maximum concentration (6.44 (5.62−7.85) pmol/g ww) after an hour which subsequently gradually decreased but in the 5th hour it was still present at 1.98 (1.50−2.90) pmol/g ww. The CNS pharmacokinetics of KYNA following KA-1 and KA-2 administration showed quite similar profiles, characterized by an approximately maximal 10-fold increase in basal concentration within the 1st hour. Vz/F_{obs} was relatively high in KA-1 and especially in KA-2. The apparent clearance was also high in the case of KA-2 relative to KA-1.

4.2 Measurement of TRP metabolites in the 3-NP toxin model of HD

As shown in Table 3, no difference was found in the KYNA concentration in the serum or in the investigated brain regions of the toxin-treated and control mice 12 days after the last injection, and there was no significant difference between the TRP levels of the serum samples of the toxin-treated and control mice, whereas in the case of KYN, a significant difference was detected in the cortex (2679 ± 110 pmol/g wet weight (ww); p = 0.017, permutation test) relative to the control value (3110 ± 112). However, significantly decreased TRP levels were found in the striatum (19,530 (17,700–20,440) pmol/g ww; p = 0.0002, permutation test), cortex (14,360 (13,540–16,300) pmol/g ww; p = 0.003, permutation test), hippocampus (16,550 (14,790–17,580) pmol/g ww (ww); p = 0.006, permutation test), cerebellum (14,930 (14,210–16,260) pmol/g ww; p = 0.0002, permutation test) and brainstem

(12,740 (12,280–14,100) pmol/g ww; $p = 0.0004$, permutation test) of 3-NP-treated mice as compared with the controls (27,950 (23,820–35,700); 22,860 (17,260–28,430); 26,590 (18,020–30,730); 24,810 (17,630–28,510); 20,960 (15,920–29,890) pmol/g ww, respectively).

Table 3 The concentrations of some metabolites of the KP in different brain regions and serum of control and 3-NP treated mice

		Serum	Str	Ctx	Hip	Cer	Stem
TRP	ctrl	102.8 (89.8 – 115.4)	27,950 (23,820 – 35,700)	22,860 (17,260 – 28,430)	26,590 (18,020 – 30,730)	24,810 (17,630 – 28,510)	20,960 (15,920 – 29,890)
	3-NP	88.6 (83.2 – 94.5)	19,530*** (17,700 – 20,440)	14,360** (13,540 – 16,300)	16,550** (14,790 – 17,580)	14,930*** (14,210 – 16,260)	12,740*** (12,280 – 14,100)
KYN	ctrl	1.39 ± 0.09	2922 ± 288	3110 ± 112	2914 ± 176	3060 ± 238	2389 ± 118
	3-NP	1.12 ± 0.12	3001 ± 309	2679* ± 110	2723 ± 208	2521 ± 182	2169 ± 111
KYNA	ctrl	0.19 (0.17 – 0.21)	5.73 (<LOD – 21.91)	5.07 (<LOD – 7.72)	<LOD (<LOD – 7.66)	<LOD (<LOD – 4.18)	<LOD
	3-NP	0.10 (0.09 – 0.18)	<LOD	6.67 (3.04 – 7.08)	<LOD (<LOD – 7.68)	<LOD (<LOD – 7.45)	<LOD
3-OHK	ctrl	<LOD	<LOD	<LOD	<LOD	66.84 (28.99 – 97.64)	<LOD (<LOD – 25.50)
	3-NP	<LOD	<LOD	<LOD	<LOD	<LOD**	<LOD

The concentration of TRP and some of its metabolites were measured from 5 different brain regions and serum of C57Bl/6 mice with HPLC. TRP levels were significantly decreased in all brain regions of 3-NP treated mice. In the cortex and cerebellum of toxin treated mice there was also a significant depletion in KYN and 3-OHK concentrations, respectively. Measurement unit was μM for serum and pmol/g wet weight for brain regions (*str* striatum; *ctx* cortex; *hip* hippocampus; *cer* cerebellum; *stem* brainstem). KYN results are expressed as mean ± S.E.M., the other substances are shown as median (interquartile range). *KP* kynurenine pathway, *TRP* tryptophan, *KYN* kynurenine, *KYNA* kynurenic acid, *3-OHK* 3-hydroxykynurenine, *3-NP* 3-nitropropionic acid, *ctrl* control, *LOD* limit of detection. * $p < 0.05$, ** $p < 0.01$, *** $p < 0.001$

The observed decreases in TRP level were generally associated with an increased KYN/TRP ratio, an index widely used to assess the metabolic activity of KP. Indeed, a significant increase in KYN/TRP ratio was observed in the striatum (0.156 ± 0.014; p = 0.008, permutation test), hippocampus (0.158 ± 0.008; p = 0.023, permutation test), cerebellum (0.166 ± 0.01; p = 0.008, permutation test) and brainstem (0.166 ± 0.008; p = 0.009, permutation test) as compared with the control values (0.102 ± 0.011; 0.122 ± 0.011; 0.129 ± 0.007; 0.117 ± 0.013, respectively; Figure 7); however, the difference in the cortex did not reach statistical significance.

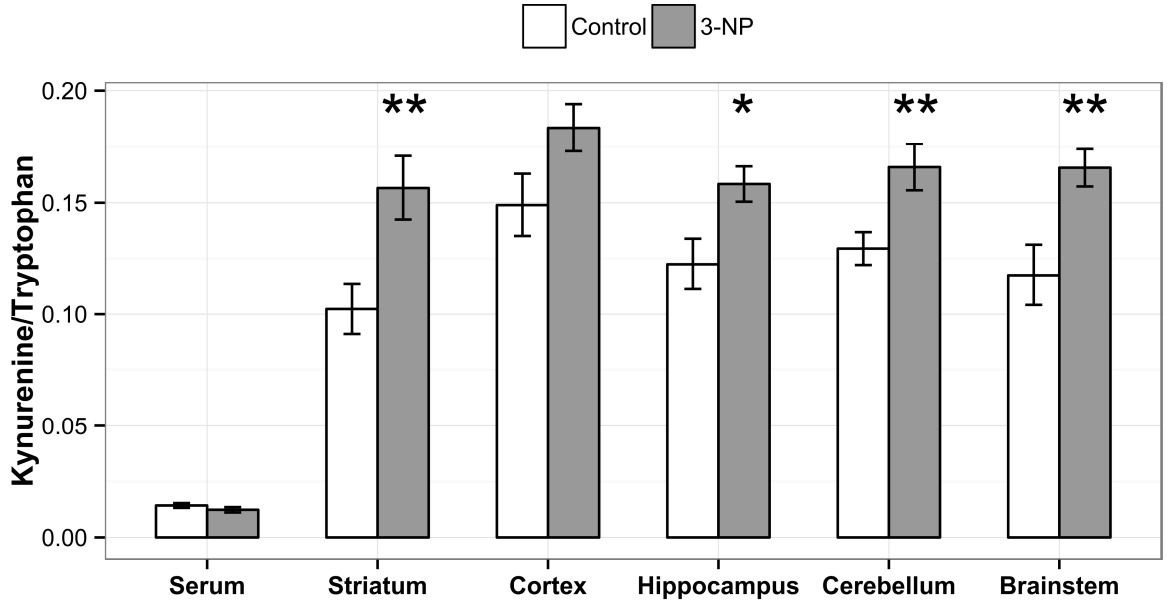

Figure 7 The effects of 3-NP treatment on the KYN/TRP ratio in the serum and different brain regions of C57Bl/6 mice. The KYN/TRP ratio was significantly elevated in the striatum, hippocampus, cerebellum and brainstem of the 3-NP-treated mice. The increase in the cortex did not reach the level of statistical significance. No alteration was observed in the serum. Data are means ± S.E.M; 3-NP 3-nitropropionic acid, KYN kynurenine, TRP tryptophan, * $p < 0.05$, ** $p < 0.01$

No difference in the KYN/TRP ratio was observed in the serum. With regard to 3-OHK levels, a significant decrease was observed in the cerebellum (to below the LOD; p = 0.005, permutation test) in the 3-NP-treated mice in comparison with the control value (66.84 (28.99–97.64) pmol/g ww), but not in the other brain regions.

4.3 Measurement of DA and its metabolites after MPTP treatment

The DA, DOPAC and HVA values in the respective control groups of the 3 treatment regimens were compared to each other, and there were no significant differences. Therefore, the values in these control groups were pooled for further comparisons with the MPTP-treated groups. The MPTP administration caused significant reductions in the striatal DA (ctrl: 8.08 ± 0.50, MPTP: 4.36 ± 0.92, p = 0.0005, ANOVA), DOPAC (ctrl: 2.57 ± 0.21, MPTP: 0.44 ± 0.08, $p = 3.78 \times 10^{-8}$, ANOVA) and HVA (ctrl: 2.18 ± 0.12, MPTP 0.67 ± 0.11, $p = 5.12 \times 10^{-10}$, ANOVA) levels compared to control values 90 min following its last administration in the acute treatment regimen (acute-1 day; Figure 8). Moreover, a significant reduction in metabolite levels was also observed 1 week after the last injection in the acute treatment regimen (acute-7 days; Figure 8) in the DA (ctrl: 8.08 ± 0.50, MPTP: 1.34 ± 0.43, $p = 4.86 \times 10^{-8}$, ANOVA), DOPAC (ctrl: 2.57 ± 0.21, MPTP: 0.76 ± 0.15, $p = 7 \times 10^{-6}$, ANOVA) and HVA (ctrl: 2.18 ± 0.12, MPTP: 0.81 ± 0.13, $p = 5.08 \times 10^{-8}$, ANOVA) values in the striatum of the MPTP-treated mice compared to the control animals. However, chronic MPTP treatment resulted in significant reductions of only striatal HVA (ctrl: 2.18 ± 0.12, MPTP: 1.40 ± 0.08, p = 0.0005, ANOVA) levels, striatal DA (ctrl: 8.08 ± 0.50, MPTP: 6.83 ± 0.48) and DOPAC (ctrl: 2.57 ± 0.21; MPTP: 1.99 ± 0.23) levels were not decreased significantly (Figure 8). 7 days following the acute treatment regimen the DA levels significantly decreased compared to those data from samples obtained 90 min following the last MPTP injection in the acute treatment regimen (p = 0.039, ANOVA).

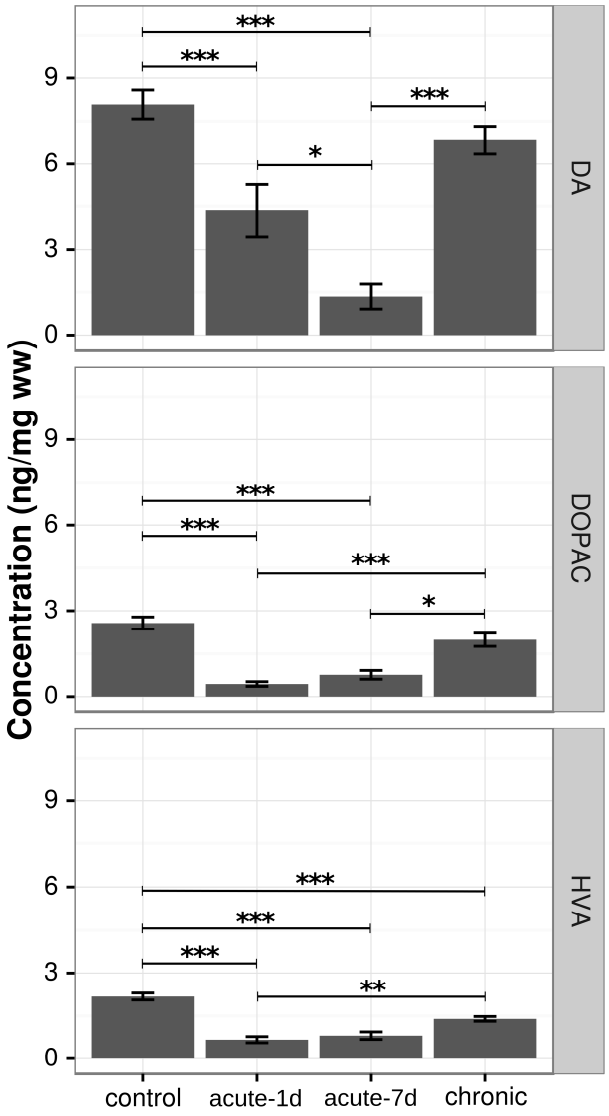

Figure 8 Striatal DA, DOPAC and HVA concentrations of MPTP-treated mice in 3 different treatment regimens. 90 min (acute-1d) and 7 days (acute-7d) following acute MPTP intoxication, DA, DOPAC and HVA levels significantly decreased in the striatum compared to the controls. The chronic (12 day) low dose MPTP treatment did not influence the striatal levels of DA and DOPAC, only HVA levels were significantly decreased. Values are plotted as means ± S.E.M; * $p < 0.05$, ** $p < 0.01$, *** $p < 0.001$; *DA* dopamine, *DOPAC* 3,4-dihydroxyphenylacetic acid, *HVA* homovanillic acid

4.4 Tocopherol measurements from human serum

The group-wise comparisons failed to detect any significant difference between groups regarding the concentrations of α-tocopherol ($p = 0.48$, $\chi^2 = 2.46$; Kruskal-Wallis test), β/γ-tocopherol ($p = 0.47$, $\chi^2 = 2.53$; Kruskal-Wallis test) or δ-tocopherol ($p = 0.82$, $\chi^2 = 0.94$; Kruskal-Wallis test; Table 4). Accordingly, in order to establish RI with appropriate subject numbers, the values for each measured compounds were pooled and the minimum required sample size (n = 120) was achieved.

Table 4 Serum tocopherol concentrations of subjects belonging to the control and OND groups.

	Controls (women)	Controls (men)	OND patients (women)	OND patients (men)	Group comparisons (*p*)
α-tocopherol (μM)	38.08 (33.70 – 44.10)	35.38 (31.35 – 45.83)	34.26 (29.40 – 41.60)	33.93 (30.54 – 41.08)	0.48 ($\chi^2 = 2.46$)
β/γ-tocopherol (μM)	1.83 (1.32 – 2.23)	1.68 (1.39 – 2.52)	1.57 (1.33 – 1.82)	1.75 (1.52 – 2.21)	0.47 ($\chi^2 = 2.53$)
δ-tocopherol (μM)	0.63 (0.52 – 0.86)	0.62 (0.53 – 0.78)	0.62 (0.55 – 0.82)	0.65 (0.57 – 0.75)	0.82 ($\chi^2 = 0.94$)

Group-wise comparisons (Kruskal-Wallis test) of the four groups failed to detect any significant difference between serum tocopherol levels. Data are presented as median and interquartile range. *OND* other neurological disease.

Table 5 The calculated uncorrected lower (2.5%) and upper (97.5%) reference intervals for tocopherols for the assessed Hungarian population.

	2.5%	S.E.	C.I. (95%)	97.5%	S.E.	C.I. (95%)
α-tocopherol (μM)	24.62	0.76	23.24 – 26.26	54.67	4.09	46.88 – 61.84
β/γ-tocopherol (μM)	0.81	0.13	0.60 – 1.11	3.69	0.45	2.71 – 4.55
δ-tocopherol (μM)	0.29	0.03	0.22 – 0.32	1.07	0.13	0.80 – 1.29

n = 120, *S.E.* standard error; *C.I.* confidence interval

For the determination of lower (2.5%) and upper (97.5%) RI with the corresponding confidence intervals and standard errors, the bootstrap method was applied and the results are demonstrated in Table 5. To obtain cholesterol-corrected tocopherol values as well, serum cholesterol concentrations were determined for each subject (median and interquartile range: 4.99 mM (4.31 – 5.54)) and the tocopherol/cholesterol ratios were calculated. The bootstrap method was applied again for the lipid corrected values (Table 6). To assess the incidental effect of age on measured serum lipid levels, Spearman test was performed. The cholesterol

levels positively correlated with the age of subjects ($p < 0.001$, Spearman's ρ = 0.34; Figure 10).

Table 6 The calculated cholesterol corrected lower (2.5%) and upper (97.5%) reference intervals for tocopherols for the assessed Hungarian population.

	2.5%	S.E.	C.I. (95%)	97.5%	S.E.	C.I. (95%)
α-tocopherol (μmol/mmol)	5.11	0.14	4.79 – 5.36	11.27	0.69	9.91 – 12.82
β/γ-tocopherol (μmol/mmol)	0.14	0.02	0.10 – 0.19	0.72	0.07	0.60 – 0.88
δ-tocopherol (μmol/mmol)	0.06	0.01	0.05 – 0.07	0.22	0.03	0.16 – 0.27

n = 120, *S.E.* standard error; *C.I.* confidence interval

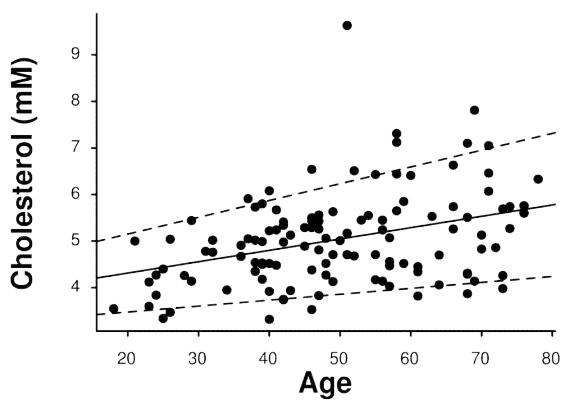

Figure 10 Serum cholesterol concentrations in function of age. There is a positive correlation between cholesterol levels and age ($p < 0.001$, Spearman's $\rho = 0.34$).

In case of uncorrected α- and β/γ-tocopherol concentrations this correlation with age is present as well (α-tocopherol: $p = 0.002$, Spearman's $\rho = 0.28$, Figure 11a; β/γ-tocopherol: $p = 0.001$, Spearman's $\rho = 0.29$, Figure 11c) whereas δ-tocopherol levels did not correlate with age ($p = 0.98$, Spearman's $\rho = 0.003$, Figure 11e). When tocopherol levels were normalized to cholesterol levels, all the correlations with age were eliminated (α-tocopherol: $p = 0.99$, Spearman's $\rho = -0.0007$, Figure 11b; β/γ-tocopherol: $p = 0.14$, Spearman's $\rho = 0.14$, Figure 11d; δ-tocopherol: $p = 0.051$, Spearman's $\rho = -0.18$, Figure 11f).

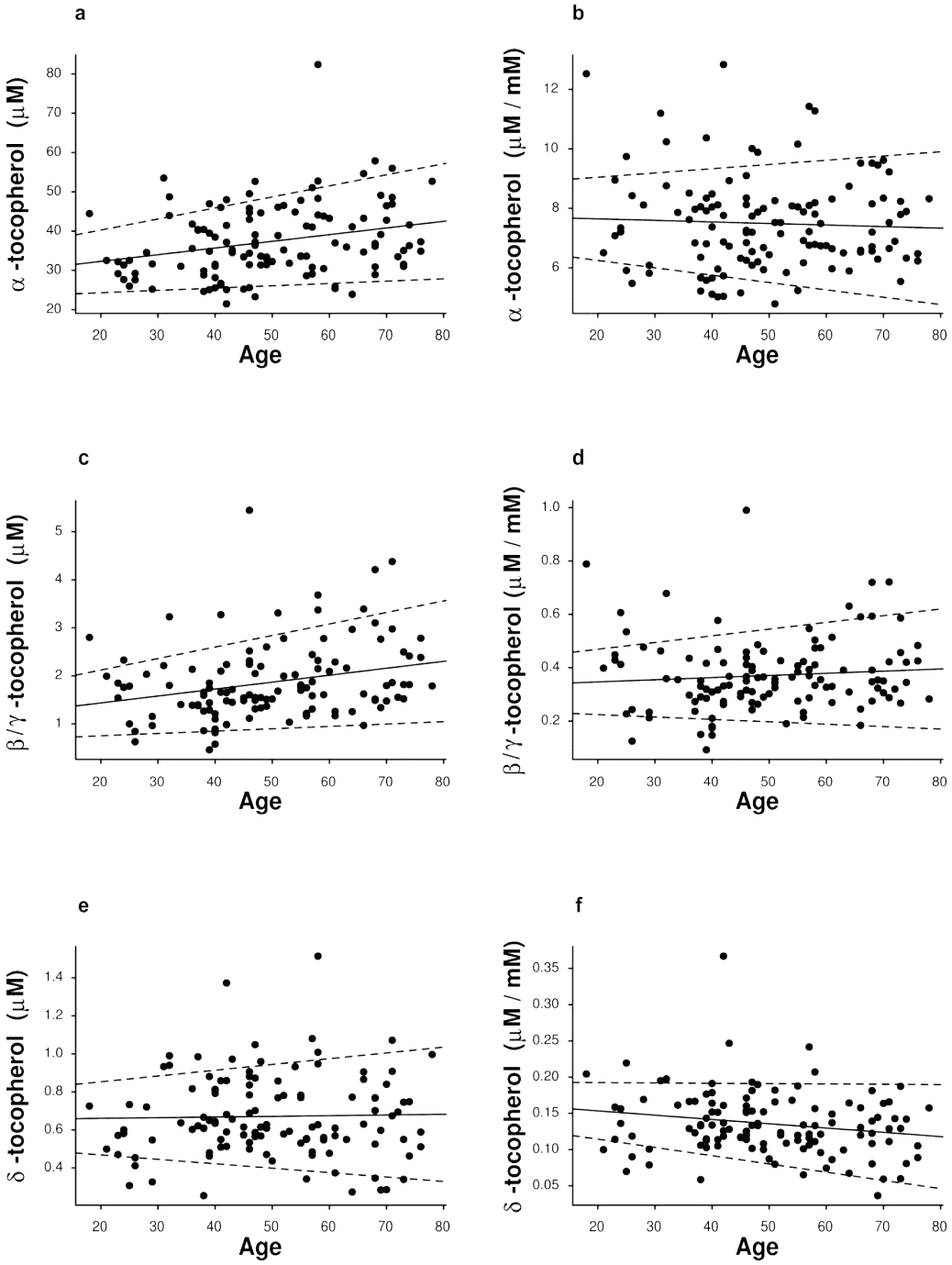

Figure 11 Serum tocopherol concentrations and tocopherol/cholesterol ratios plotted against the age of participants. The level of α-tocopherol positively correlates with age (p = 0.002, Spearman's ρ = 0.28; a), similarly to β/γ-tocopherol (p = 0.001, Spearman's ρ = 0.29; c), whereas δ-tocopherol levels do not correlate with age (p = 0.98, Spearman's ρ = 0.003; e). The cholesterol corrected values of α-tocopherol (p = 0.99, Spearman's ρ = - 0.0007; b) and β/γ-tocopherol (p = 0.14, Spearman's ρ = 0.14; d) do not further significantly correlate with age, and the correlation of δ-tocopherol levels with age also remained non-significant (p = 0.051, Spearman's ρ = - 0.18; f).

5 Discussion

Bioanalytical measurements play an essential role in differential diagnostics and may have prognostic value as well. Accordingly, numerous preclinical and clinical studies aim to discover novel biomarkers to monitor various pathological processes or the therapeutic effects of novel drugs. Amongst analytical methods, HPLC is one of the most popular options because it provides fast and robust determination of a wide range of compounds. However, these methods require substantial development of procedures in order to obtain valid, i.e., replicable, results.

For the investigation of the potential beneficial effects of KYNA amides in headache, a well-known model of trigeminal nociception, the orofacial formalin test, was applied. Immunohistochemical studies have revealed that formalin induces c-FOS and nNOS expression in the TNC, which suggests the activation and sensitization of that region (Hunt et al. 1987, Párdutz et al. 2000). Our aim was to give a pharmacokinetic explanation for the observed beneficial effects of 2 KYNA amides (KA-1 and KA-2) in the above-mentioned formalin model, which involves both peripheral and central components of pain processing. With regard to the serum concentrations of the analogs following their i.p. administration, the levels of KA-2 were considerably lower than those of KA-1 from the aspects of peak concentration and $AUC_{0\text{-}5h}$. In contrast, KA-1 could not be detected in the examined CNS region, and the concentration of KA-2 was likewise relatively low. On the other hand the serum pharmacokinetic data revealed that KA-2 decays into KYNA in larger amounts than KA-1, but nevertheless, in the examined CNS region, there is no major difference between KYNA levels following the treatments with KA-1 or KA-2. In view of these findings, the difference in the observed effects in behavioral and immunohistochemical studies (Veres et al. 2017) may be explained by the differences in the serum KYNA levels. From the aspect of a structure-activity relationship, the difference in peripheral conversion may stem from the structures of the 2 analogs, e.g., in the case of KA-2 the strained pyrrolidine moiety may influence the faster hydrolysis of the amide bond relative to the N,N-dimethyl function (KA-1). These findings suggest that the difference in the beneficial effects of the 2 analogs may be explained by the peripheral effect of elevated KYNA concentrations on formalin-induced pathological alterations. The molecular background would be the inhibition of NMDAR-

mediated neurotransmission at the strychnine-insensitive glycine-binding site (Szalárdy et al. 2012b) which is present on the peripheral process of the trigeminal nociceptors (Watanabe et al. 1994, Quartu et al. 2002). The observed peak serum KYNA concentration following KA-2 treatment during the experiment (16.71 μM) may be relevant with regard to the inhibition of glutamatergic neurotransmission via the above-mentioned pathway (Szalárdy et al. 2012b).

In another study, regarding the KP of TRP metabolism, we used the 3-NP toxin model of HD (Brouillet 2014). In contrast with genetic models (Guidetti et al. 2000, 2006, Sathyasaikumar et al. 2010, Mazarei et al. 2013), there are no available published data on the effects of 3-NP toxicity on the concentrations of TRP and KP metabolites under *in vivo* conditions in mice. One of the 2 studies on the effects of chronic 3-NP treatment in rats demonstrated a significant decrease in the number of kynurenine aminotransferase (KAT)-I-immunoreactive cells, predominantly in the striatum (Csillik et al. 2002). The other study on *ex vivo* rat cortical slices, demonstrated that 3-NP dose-dependently inhibited the production of KYNA and led to decreased KAT-I and KAT-II activities in the cortical tissue homogenates (Luchowski et al. 2002). No murine studies have been conducted previously to assess the effects of *in vivo* applied 3-NP on KP metabolism at the metabolite level per se, and there have been no studies of KP alterations due to 3-NP intoxication in the serum, which may allow the differentiation of systemic effects from those confined to the CNS. We have now quantitatively assessed the levels of 4 KP metabolites in the striatum, cortex, hippocampus, cerebellum and brainstem of mice, with a relatively high number of animals per group (n = 14-16).

Our findings indicated a decreased TRP level in association with an increased KYN/TRP ratio in most of the examined brain regions of C57Bl/6 mice treated with 3-NP, and also a reduced concentration of 3-OHK in the cerebellum. It is noteworthy that we did not detect any significant difference in serum samples, which suggests that the observed alterations are specific for the examined brain regions and are not affected by a systemic change and/or an altered permeability of the blood-brain barrier. Our results on 5-month-old 3-NP-treated animals resemble those from studies of 3-month-old transgenic YAC128 animals (Mazarei et al. 2013), which is known to be one of the best animal strains for the modeling of the alterations in human HD (Slow et al. 2003, Pouladi et al. 2013). The elevated KYN/TRP ratio is comparable with the previous finding of increased indolamine dioxigenase-1 activity in the

brain (but not in the serum) of YAC128 animals, an alteration reflecting that observed in several neurodegenerative diseases and their animal models (Vécsei et al. 2013), and which is suggested to contribute to the neurodegenerative process. In another study (Török et al. 2015) it has been confirmed with histochemical methods, that the sub-acute 3-NP treatment we used caused neuronal cell death in the striatum. The similarity of the findings of KP alterations in this 3-NP model with those observed previously in genetic models (Guidetti et al. 2000, 2006, Sathyasaikumar et al. 2010, Mazarei et al. 2013) leads us to presume that the KP alterations observed in transgenic animals might be secondary, at least partially, to a mitochondrial dysfunction, a well-known phenomenon in the pathogenesis of HD, and that 3-NP toxicity may comprise a useful and cheap tool for the screening of the efficacy of potential drug candidates before the application of more demanding genetic models.

With regard to DA measurements, our aim was to confirm that the applied acute MPTP treatment regimen was effective in decreasing striatal DA levels, while the chronic low dose administration of the toxin was not. In our study, we compared the above-mentioned MPTP treatment regimens. MPTP is typically administered to mice according to one of 2 protocols: acute treatment (typically 4 injections at 2-h intervals in 1 day (Jackson-Lewis et al. 1995, Przedborski and Vila 2003, Anderson et al. 2006)) or subacute treatment (sometimes also called ‘chronic’ (Furuya et al. 2004)), in which 1 or 2 injections per day are administered for 5 consecutive days. In our study, we tested an acute regimen similar to the others found in the literature (Jackson-Lewis et al. 1995) and furthermore, instead of the subacute treatment we applied a more prolonged low dose regimen to model drug-induced preconditioning. The preconditioning by MPTP is not intended to suggest a future direct therapeutic approach, but rather aimed at finding key players which may help to alleviate the pathological alterations. The situation may be similar to ischemic preconditioning where the outcome in myocardial infarction may depend substantially on which medications were applied with an influence on preconditioning (Tomai et al. 1999). Accordingly, the aim in the case of preconditioning with MPTP is the demonstration that this administration regimen does not cause significant decreases in striatal DA concentration.

90 min after the last MPTP injection of the high-dose acute treatment (75 mg/kg/day total dose) the concentration of DA and its metabolites, DOPAC and HVA, were significantly decreased compared to the controls. 7 days after the last injection this difference could still be

observed. Additionally, DA levels were notably lower compared to the animals processed after 90 min. With regard to the chronic low dose administration of MPTP (15 mg/kg/day), it did not induce significant DA depletion (i.e., neurotoxic effect at biochemical level), a meaningful decrease in concentration was observed only in the case of HVA.

These results demonstrated the presence of significant neurotoxicity in the case of the acute treatment regimen, associated with a sudden, but temporary, increase in PGC-1α expression, while the chronic low dose regimen failed to evoke any significant changes either in striatal DA concentration or in PGC-1α expression, suggesting that chronic low dose intoxication did not induce protective mechanisms with the involvement of PGC-1α.

The determination of exact serum tocopherol concentrations may be substantial for the diagnosis and therapeutic monitoring of certain conditions usually accompanied with neurological symptoms, such as ataxia, myopathy or cognitive deficiency (Muller 2010, Fata et al. 2014). Although the symptoms of genetically-determined disorders with tocopherol deficiency usually manifest during childhood (Raizman et al. 2014), malabsorption disorders and late-onset genetically determined metabolic conditions typically appear in adulthood, indicating the need for tocopherol measurement in adult population as well (Ueda et al. 2009). However, these concentrations alone hold little diagnostic value. For proper evaluation physicians need a well-established RI, which can vary considerably between populations (Appendix I). The underlying cause of this variation may be multifactorial, mainly including not standardized patient selection criteria and some methodological issues. The aim of our tocopherol measurements was to establish RIs for the adult Hungarian population and to compare the method of patient selection and the analytical procedure with that of previously published studies.

The investigated population in this study is homogeneously distributed with regard to age and covers a considerably wide age range of the adult population. The selection of a homogeneous study population may have a special importance, because the distribution of age can considerably influence reference values in light of the fact that the levels of certain tocopherols significantly increase with age (Figure 11; (Rifkind and Segal 1983)). Accordingly, when the investigated reference population includes young individuals, the results may be skewed to lower levels (Quesada et al. 2004, Ford et al. 2006, Paliakov et al. 2009, Zhao et al. 2014). Moving further to another qualitative aspect of the composition of the

study population, in addition to the involvement of subjects without any chronic illness, the group of assessed individuals also comprised patients with different neurological disorders where tocopherol levels were not previously reported to be abnormal (the establishment of the so called control group of OND). This study setup may ensure the absence of significant alterations of tocopherol levels in neurological cases lacking the symptoms of ataxia, myopathy and cognitive deficiency, which may be important for future screening studies. Thorough statistical assessment resulted in no significant differences, thus subgroups became suitable for pooling, i.e., the number of individuals in the reference population could be easily increased to the desired level. Several previous studies lack the setup of including well-detailed descriptions of the health condition of reference individuals, possibly introducing a bias into the reference values (Appendix I; (Quesada et al. 2004, Paliakov et al. 2009)). In the current study design, special attention was paid to dietary factors and to the intake of special medicines (e.g., statins) and food supplements as well, because these may considerably alter the levels of the assessed compounds (Colquhoun et al. 2005). The lack of this kind of standardization introduces another bias into the establishment of RIs (Appendix I; (Winbauer et al. 1999, Yuan et al. 2014)).

Tocopherol levels are often reported as tocopherol:cholesterol ratios based on the fact that there is a close relationship between the concentrations of tocopherols and lipids in the blood (Thurnham et al. 1986). However, under special circumstances, lipid corrected tocopherol levels can be misleading, because it was reported that malnutrition and infectious diseases in children can lower the levels of circulating cholesterol and its lipoprotein carriers, which alteration of which can mask decreased tocopherol levels if only corrected values are reported (Das et al. 1996, Sauerwein et al. 1997, Squali Houssaïni et al. 2001). Contrarily, when obese children were investigated, their α-tocopherol levels were normal while their tocopherol:cholesterol ratios were significantly lower compared to the control group (Strauss 1999). With regard to adults, in light of the fact that lipid status can vary with age (Figure 10; (Rifkind and Segal 1983)) the application of lipid corrected values may be necessary for the characterization of vitamin E status (Horwitt et al. 1972, Thurnham et al. 1986). Nevertheless, the report of serum tocopherol concentrations with lipid ratios may be practical for the proper evaluation of tocopherol status. However, only one third of the papers reported both of them (Appendix I).

During bioanalytical measurements there are several things to consider regarding the robustness and reproducibility of the method. An important matter is the validation of the applied analytical procedure, which can provide valuable information about the robustness of the measurement and the validity of the reported values. For scientific publications, at least a partial method validation is required (ICH 1995). Without method validation, the reliability of the presented data are questionable. With regard to the tocopherol measurements approximately 20% of the previous studies presenting human tocopherol concentrations are not validated (Appendix I).

To compensate between the true and the measured concentrations, the use of an internal standard in known quantity also seems to be obligatory in bioanalytical methods, because during sample preparation slight changes in the concentration may occur. These changes can be more pronounced as the complexity of the method increases (e.g., tissue homogenization, liquid-liquid extraction, evaporation under N_2). Of course, internal standards are required in other measurements as well, to enhance the quality and reproducibility of the procedures. Furthermore, applying these compounds for measurements from tissue samples allows correction for the weight of the sample so concentration can be determined precisely as g / wet weight tissue. With regard to sample collection, it needs to be considered that serum or plasma samples should be used, e.g. during tocopherol measurements the application of oxalate, citrate or ethylenediaminetetraacetic acid for plasma collection can reduce tocopherol concentration (Nierenberg and Lester 1985).

6 Conclusion

Our results from KP metabolite measurements in the orofacial pain model draw attention to the role of the glutamatergic system in the alleviation of peripheral sensitization, which can be utilized for future drug development. The possibility of targeting the peripheral component of pain processing may provide an option for pharmaceutical drug design without necessitating good penetration of the BBB, but other pharmacokinetic parameters, such as solubility and clearance, must be kept in mind. The present results and previous preclinical findings indicate that the KYNA amides, via their probable direct effects (KA-1 (Zádori et al. 2011a)) or as prodrugs (KA-2 in the current pharmacokinetic study), may be promising drug candidates in

neurological disorders with a high socioeconomic burden, including those involving pain and headache. Furthermore, we detected marked persistent increases in the KYN/TRP ratio in the striatum, hippocampus, cerebellum and brainstem and a slight reduction in the level of 3-OHK in the cerebellum in mice when we applied the subacute 3-NP model of HD. Such alterations have not been reported earlier in 3-NP studies and are similar to those seen in young genetic animal models (especially in 3-month-old YAC128 transgenic mice (Mazarei et al. 2013)). In the era of advanced genetic models of HD, our findings demonstrate the continued relevance and applicability of toxin models, which may provide cost-effective and rapid ways of screening potential drug candidates to treat this currently intractable disease.

Similarly to the 3-NP toxin model for HD, the MPTP toxin treatment serves as a good model for PD for the rapid testing of novel compounds and for the observation of various biochemical changes. Measuring the DA concentration in the striatum is a reliable method for the evaluation of possible neuroprotective effects.

Glutamatergic excitotoxicity and mitochondrial disturbances play essential roles in the pathomechanism of several neurological diseases (Zádori et al. 2012) and they are almost always accompanied by the formation of RS (Szalárdy et al. 2015). Accordingly, we were interested in the characterization of the antioxidant mechanisms, more specifically the serum tocopherol levels. First we had to establish proper RIs for the adult Hungarian population, which are presented here with their corresponding cholesterol corrected values. These results can facilitate the diagnostic process for certain neurological conditions, such as ataxia with vitamin E deficiency. Moreover, we draw attention to the importance of a thoroughly designed protocol associated with the establishment of these RIs and the possible pitfalls of tocopherol measurements.

7 Acknowledgments

I would like to express my gratitude to my supervisor Dr. Dénes Zádori, Assistant Professor at the Department of Neurology, University of Szeged, to Prof. Dr. László Vécsei, Member of the Hungarian Academy of Sciences, Head of the Department of Neurology, University of Szeged and to Prof. Dr. Péter Klivényi, Full Professor at the Department of Neurology,

University of Szeged for their excellent scientific guidance and continuous support of my research activities.

I would also like to thank all colleagues with whom I performed the experiments, especially Rita Maszlag-Török, Dr. Zsuzsanna Bohár, Dr. Annamária Fejes-Szabó, Máté Molnár, Evelin Vágvölgyi-Sümegi and Dr. Levente Szalárdy, present and former Ph.D. students at the Department of Neurology, University of Szeged, and Dr István Mándity, Assistant Professor at the Institute of Pharmaceutical Chemistry, University of Szeged, for performing the HPLC-MS measurements, Attila Bajtai and Márton Szentirmai, who carried out scientific research activities as students under my practical supervision at the Department of Neurology, University of Szeged.

I would like to express my special thanks to Dr. István Ilisz, Associate Professor at the Department of Inorganic and Analytical Chemisrty, for his guidance in HPLC method development, and also, to Dr. István Szatmári, Senior Lecturer at the Department of Pharmaceutical Chemistry, University of Szeged, and to Prof. Dr. Ferenc Fülöp, Member of the Hungarian Academy of Sciences, Head of the Department of Pharmaceutical Chemistry, University of Szeged, for providing us the KYNA amide analogs.

Last but not least, I would like to express my special gratitude to my family for their continuous support throughout my studies and work.

8 References

Afridi, S.K., Giffin, N.J., Kaube, H., and Goadsby, P.J. 2013. A randomized controlled trial of intranasal ketamine in migraine with prolonged aura. Neurology **80**(7): 642–647. doi:10.1212/WNL.0b013e3182824e66.

Alt, A., Weiss, B., Ogden, A.M., Li, X., Gleason, S.D., Calligaro, D.O., Bleakman, D., and Witkin, J.M. 2006. In vitro and in vivo studies in rats with LY293558 suggest AMPA/kainate receptor blockade as a novel potential mechanism for the therapeutic treatment of anxiety disorders. Psychopharmacology (Berl.) **185**(2): 240–247. doi:10.1007/s00213-005-0292-0.

Anderson, D.W., Bradbury, K.A., and Schneider, J.S. 2006. Neuroprotection in Parkinson models varies with toxin administration protocol. Eur. J. Neurosci. **24**(11): 3174–3182. doi:10.1111/j.1460-9568.2006.05192.x.

Beal, M.F., Matson, W.R., Storey, E., Milbury, P., Ryan, E.A., Ogawa, T., and Bird, E.D. 1992. Kynurenic acid concentrations are reduced in Huntington's disease cerebral cortex. J. Neurol. Sci. **108**(1): 80–87.

Beal, M.F., Matson, W.R., Swartz, K.J., Gamache, P.H., and Bird, E.D. 1990. Kynurenine pathway measurements in Huntington's disease striatum: evidence for reduced formation of kynurenic acid. J. Neurochem. **55**(4): 1327–1339. doi:10.1111/j.1471-4159.1990.tb03143.x.

Bose, A., and Beal, M.F. 2016. Mitochondrial dysfunction in Parkinson's disease. J. Neurochem. **139**: 216–231. doi:10.1111/jnc.13731.

Breidert, T., Callebert, J., Heneka, M.T., Landreth, G., Launay, J.M., and Hirsch, E.C. 2002. Protective action of the peroxisome proliferator-activated receptor-γ agonist pioglitazone in a mouse model of Parkinson's disease. J. Neurochem. **82**(3): 615–624. doi:10.1046/j.1471-4159.2002.00990.x.

Brouillet, E. 2014. The 3-NP model of striatal neurodegeneration. Curr. Protoc. Neurosci. **67**: 9.48.1-14. doi:10.1002/0471142301.ns0948s67.

Carpenter, M.B., and Sutin, J. 1983. Human neuroanatomy. Williams & Wilkins, Baltimore.

Chen, N., Luo, T., Wellington, C., Metzler, M., McCutcheon, K., Hayden, M.R., and Raymond, L.A. 1999. Subtype-specific enhancement of NMDA receptor currents by mutant huntingtin. J. Neurochem. **72**(5): 1890–1898.

Chiba, K., Trevor, A., and Castagnoli, N. 1984. Metabolism of the neurotoxic tertiary amine, MPTP, by brain monoamine oxidase. Biochem. Biophys. Res. Commun. **120**(2): 574–578.

Chichorro, J.G., Porreca, F., and Sessle, B. 2017. Mechanisms of craniofacial pain. Cephalalgia Int. J. Headache **37**(7): 613–626. doi:10.1177/0333102417704187.

Choo, Y.S., Johnson, G.V.W., MacDonald, M., Detloff, P.J., and Lesort, M. 2004. Mutant huntingtin directly increases susceptibility of mitochondria to the calcium-induced permeability transition and cytochrome c release. Hum. Mol. Genet. **13**(14): 1407–1420. doi:10.1093/hmg/ddh162.

Clavelou, P., Dallel, R., Orliaguet, T., Woda, A., and Raboisson, P. 1995. The orofacial formalin test in rats: effects of different formalin concentrations. Pain **62**(3): 295–301.

Colquhoun, D.M., Jackson, R., Walters, M., Hicks, B.J., Goldsmith, J., Young, P., Strakosch, C., and Kostner, K.M. 2005. Effects of simvastatin on blood lipids, vitamin E, coenzyme Q10 levels and left ventricular function in humans. Eur. J. Clin. Invest. **35**(4): 251–258. doi:10.1111/j.1365-2362.2005.01486.x.

Csillik, A., Knyihár, E., Okuno, E., Krisztin-Péva, B., Csillik, B., and Vécsei, L. 2002. Effect of 3-nitropropionic acid on kynurenine aminotransferase in the rat brain. Exp. Neurol. **177**(1): 233–241.

Das, B.S., Thurnham, D.I., and Das, D.B. 1996. Plasma alpha-tocopherol, retinol, and carotenoids in children with falciparum malaria. Am. J. Clin. Nutr. **64**(1): 94–100.

Dehmer, T., Heneka, M.T., Sastre, M., Dichgans, J., and Schulz, J.B. 2004. Protection by pioglitazone in the MPTP model of Parkinson's disease correlates with I kappa B alpha induction and block of NF kappa B and iNOS activation. J. Neurochem. **88**(2): 494–501.

Dézsi, L., and Vécsei, L. 2017. Monoamine oxidase B inhibitors in Parkinson's disease. CNS Neurol. Disord. Drug Targets.

Diener, H.-C., Charles, A., Goadsby, P.J., and Holle, D. 2015. New therapeutic approaches for the prevention and treatment of migraine. Lancet Neurol. **14**(10): 1010–1022. doi:10.1016/S1474-4422(15)00198-2.

Fata, G., Weber, P., and Mohajeri, M. 2014. Effects of vitamin E on cognitive performance during ageing and in Alzheimer's disease. Nutrients **6**(12): 5453–5472. doi:10.3390/nu6125453.

Ford, E.S., Schleicher, R.L., Mokdad, A.H., Ajani, U.A., and Liu, S. 2006. Distribution of serum concentrations of alpha-tocopherol and gamma-tocopherol in the US population. Am. J. Clin. Nutr. **84**(2): 375–383.

Forno, L.S. 1996. Neuropathology of Parkinson's disease. J. Neuropathol. Exp. Neurol. **55**(3): 259–272. doi:10.1097/00005072-199603000-00001.

Forno, L.S., DeLanney, L.E., Irwin, I., and Langston, J.W. 1993. Similarities and differences between MPTP-induced parkinsonsim and Parkinson's disease. Neuropathologic considerations. Adv. Neurol. **60**: 600–608.

Fülöp, F., Szatmári, I., Vámos, E., Zádori, D., Toldi, J., and Vécsei, L. 2009. Syntheses, transformations and pharmaceutical applications of kynurenic acid derivatives. Curr. Med. Chem. **16**(36): 4828–4842.

Furuya, T., Hayakawa, H., Yamada, M., Yoshimi, K., Hisahara, S., Miura, M., Mizuno, Y., and Mochizuki, H. 2004. Caspase-11 mediates inflammatory dopaminergic cell death in the 1-methyl-4-phenyl-1,2,3,6-tetrahydropyridine mouse model of Parkinson's disease. J. Neurosci. **24**(8): 1865–1872. doi:10.1523/JNEUROSCI.3309-03.2004.

Górnaś, P., Siger, A., Czubinski, J., Dwiecki, K., Segliņa, D., and Nogala-Kalucka, M. 2014. An alternative RP-HPLC method for the separation and determination of tocopherol and tocotrienol homologues as butter authenticity markers: A comparative study between two European countries: Tocopherols - authenticity markers of butter. Eur. J. Lipid Sci. Technol.: n/a-n/a. doi:10.1002/ejlt.201300319.

Grebenstein, N., and Frank, J. 2012. Rapid baseline-separation of all eight tocopherols and tocotrienols by reversed-phase liquid-chromatography with a solid-core pentafluorophenyl column and their sensitive quantification in plasma and liver. J. Chromatogr. A **1243**: 39–46. doi:10.1016/j.chroma.2012.04.042.

Guidetti, P., Bates, G.P., Graham, R.K., Hayden, M.R., Leavitt, B.R., MacDonald, M.E., Slow, E.J., Wheeler, V.C., Woodman, B., and Schwarcz, R. 2006. Elevated brain 3-hydroxykynurenine and quinolinate levels in Huntington disease mice. Neurobiol. Dis. **23**(1): 190–197. doi:10.1016/j.nbd.2006.02.011.

Guidetti, P., Reddy, P.H., Tagle, D.A., and Schwarcz, R. 2000. Early kynurenergic impairment in Huntington's disease and in a transgenic animal model. Neurosci. Lett. **283**(3): 233–235.

Hacquebard, M., and Carpentier, Y.A. 2005. Vitamin E: absorption, plasma transport and cell uptake. Curr. Opin. Clin. Nutr. Metab. Care **8**(2): 133–138.

Hallman, H., Olson, L., and Jonsson, G. 1984. Neurotoxicity of the meperidine analogue N-methyl-4-phenyl-1,2,3,6-tetrahydropyridine on brain catecholamine neurons in the mouse. Eur. J. Pharmacol. **97**(1–2): 133–136.

Harris, J.B., and Blain, P.G. 2004. Neurotoxicology: what the neurologist needs to know. J. Neurol. Neurosurg. Psychiatry **75**(suppl 3): iii29-iii34. doi:10.1136/jnnp.2004.046318.

Hervé, C., Beyne, P., Jamault, H., and Delacoux, E. 1996. Determination of tryptophan and its kynurenine pathway metabolites in human serum by high-performance liquid chromatography with simultaneous ultraviolet and fluorimetric detection. J. Chromatogr. B. Biomed. Sci. App. **675**(1): 157–161. doi:10.1016/0378-4347(95)00341-X.

Hess, D., Keller, H.E., Oberlin, B., Bonfanti, R., and Schüep, W. 1991. Simultaneous determination of retinol, tocopherols, carotenes and lycopene in plasma by means of high-performance liquid chromatography on reversed phase. Int. J. Vitam. Nutr. Res. **61**(3): 232–238.

Heyes, M.P., Saito, K., Crowley, J.S., Davis, L.E., Demitrack, M.A., Der, M., Dilling, L.A., Elia, J., Kruesi, M.J., and Lackner, A. 1992. Quinolinic acid and kynurenine pathway metabolism in inflammatory and non-inflammatory neurological disease. Brain J. Neurol. **115 (Pt 5)**: 1249–1273.

Horowitz, G.L. 2016. Establishment and use of reference values. *In* Tietz Textbook of Clinical Chemistry and Molecular Diagnostics, 5th ed. Elsevier, Oxford.

Horwitt, M.K., Harvey, C.C., Dahm, C.H., and Searcy, M.T. 1972. Relationship between tocopherol and serum lipid levels for determination of nutritional adequacy. Ann. N. Y. Acad. Sci. **203**: 223–236.

Hunt, S.P., Pini, A., and Evan, G. 1987. Induction of c-fos-like protein in spinal cord neurons following sensory stimulation. Nature **328**(6131): 632–634. doi:10.1038/328632a0.

ICH. 1995. ICH harmonised tripartite guideline, validation of analytical procedures. Fed Regist: 60:11260.

Jackson-Lewis, V., Jakowec, M., Burke, R.E., and Przedborski, S. 1995. Time course and morphology of dopaminergic neuronal death caused by the neurotoxin 1-methyl-4-phenyl-1,2,3,6-tetrahydropyridine. Neurodegeneration **4**(3): 257–269.

Jackson-Lewis, V., and Przedborski, S. 2007. Protocol for the MPTP mouse model of Parkinson's disease. Nat. Protoc. **2**(1): 141–151. doi:10.1038/nprot.2006.342.

Jauch, D., Urbańska, E.M., Guidetti, P., Bird, E.D., Vonsattel, J.-P.G., Whetsell, W.O., and Schwarcz, R. 1995. Dysfunction of brain kynurenic acid metabolism in Huntington's disease: focus on kynurenine aminotransferases. J. Neurol. Sci. **130**(1): 39–47. doi:10.1016/0022-510X(94)00280-2.

Javitch, J.A., D'Amato, R.J., Strittmatter, S.M., and Snyder, S.H. 1985. Parkinsonism-inducing neurotoxin, N-methyl-4-phenyl-1,2,3,6 -tetrahydropyridine: uptake of the metabolite N-methyl-4-phenylpyridine by dopamine neurons explains selective toxicity. Proc. Natl. Acad. Sci. U. S. A. **82**(7): 2173–2177.

Jellinger, K.A. 2001. Cell death mechanisms in neurodegeneration. J. Cell. Mol. Med. **5**(1): 1–17. doi:10.1111/j.1582-4934.2001.tb00134.x.

Kalinderi, K., Bostantjopoulou, S., and Fidani, L. 2016. The genetic background of Parkinson's disease: current progress and future prospects. Acta Neurol. Scand. **134**(5): 314–326. doi:10.1111/ane.12563.

Karg, E., Klivényi, P., Németh, I., Bencsik, K., Pintér, S., and Vécsei, L. 1999. Nonenzymatic antioxidants of blood in multiple sclerosis. J. Neurol. **246**(7): 533–539.

Klivényi, P., and Vécsei, L. 2010. Novel therapeutic strategies in Parkinson's disease. Eur. J. Clin. Pharmacol. **66**(2): 119–125. doi:10.1007/s00228-009-0742-4.

Knutti, D., and Kralli, A. 2001. PGC-1, a versatile coactivator. Trends Endocrinol. Metab. **12**(8): 360–365. doi:10.1016/S1043-2760(01)00457-X.

Kurosaki, R., Muramatsu, Y., Kato, H., and Araki, T. 2004. Biochemical, behavioral and immunohistochemical alterations in MPTP-treated mouse model of Parkinson's disease. Pharmacol. Biochem. Behav. **78**(1): 143–153. doi:10.1016/j.pbb.2004.03.006.

Lam, D.K., Sessle, B.J., and Hu, J.W. 2009a. Glutamate and capsaicin effects on trigeminal nociception I: Activation and peripheral sensitization of deep craniofacial nociceptive afferents. Brain Res. **1251**: 130–139. doi:10.1016/j.brainres.2008.11.029.

Lam, D.K., Sessle, B.J., and Hu, J.W. 2009b. Glutamate and capsaicin effects on trigeminal nociception II: Activation and central sensitization in brainstem neurons with deep craniofacial afferent input. Brain Res. **1253**: 48–59. doi:10.1016/j.brainres.2008.11.056.

Lopes da Silva, S., Vellas, B., Elemans, S., Luchsinger, J., Kamphuis, P., Yaffe, K., Sijben, J., Groenendijk, M., and Stijnen, T. 2014. Plasma nutrient status of patients with Alzheimer's disease: Systematic review and meta-analysis. Alzheimers Dement. **10**(4): 485–502. doi:10.1016/j.jalz.2013.05.1771.

Luchowski, P., Luchowska, E., Turski, W.A., and Urbanska, E.M. 2002. 1-Methyl-4-phenylpyridinium and 3-nitropropionic acid diminish cortical synthesis of kynurenic acid via interference with kynurenine aminotransferases in rats. Neurosci. Lett. **330**(1): 49–52.

Mazarei, G., Budac, D.P., Lu, G., Adomat, H., Tomlinson Guns, E.S., Möller, T., and Leavitt, B.R. 2013. Age-dependent alterations of the kynurenine pathway in the YAC128 mouse model of Huntington disease. J. Neurochem. **127**(6): 852–867. doi:10.1111/jnc.12350.

Milnerwood, A.J., Gladding, C.M., Pouladi, M.A., Kaufman, A.M., Hines, R.M., Boyd, J.D., Ko, R.W.Y., Vasuta, O.C., Graham, R.K., Hayden, M.R., Murphy, T.H., and Raymond, L.A. 2010. Early increase in extrasynaptic NMDA receptor signaling and expression contributes to phenotype onset in Huntington's disease mice. Neuron **65**(2): 178–190. doi:10.1016/j.neuron.2010.01.008.

Morley, S., Panagabko, C., Shineman, D., Mani, B., Stocker, A., Atkinson, J., and Manor, D. 2004. Molecular determinants of heritable vitamin E deficiency. Biochemistry (Mosc.) **43**(14): 4143–4149. doi:10.1021/bi0363073.

Muller, D.P.R. 2010. Vitamin E and neurological function. Mol. Nutr. Food Res. **54**(5): 710–718. doi:10.1002/mnfr.200900460.

Näsström, J., Karlsson, U., and Post, C. 1992. Antinociceptive actions of different classes of excitatory amino acid receptor antagonists in mice. Eur. J. Pharmacol. **212**(1): 21–29.

Nicklas, W.J., Vyas, I., and Heikkila, R.E. 1985. Inhibition of NADH-linked oxidation in brain mitochondria by 1-methyl-4-phenyl-pyridine, a metabolite of the neurotoxin, 1-methyl-4-phenyl-1,2,5,6-tetrahydropyridine. Life Sci. **36**(26): 2503–2508.

Nierenberg, D.W., and Lester, D.C. 1985. Determination of vitamins A and E in serum and plasma using a simplified clarification method and high-performance liquid chromatography. J. Chromatogr. **345**(2): 275–284.

Obermann, M., Holle, D., Naegel, S., Burmeister, J., and Diener, H.-C. 2015. Pharmacotherapy options for cluster headache. Expert Opin. Pharmacother. **16**(8): 1177–1184. doi:10.1517/14656566.2015.1040392.

Oshinsky, M.L., and Luo, J. 2006. Neurochemistry of trigeminal activation in an animal model of migraine. Headache **46 Suppl 1**: S39-44.

Paliakov, E.M., Crow, B.S., Bishop, M.J., Norton, D., George, J., and Bralley, J.A. 2009. Rapid quantitative determination of fat-soluble vitamins and coenzyme Q-10 in human serum by reversed phase ultra-high pressure liquid chromatography with UV detection. J. Chromatogr. B **877**(1–2): 89–94. doi:10.1016/j.jchromb.2008.11.012.

Párdutz, Á., Fejes, A., Bohár, Z., Tar, L., Toldi, J., and Vécsei, L. 2012. Kynurenines and headache. J. Neural Transm. **119**(2): 285–296. doi:10.1007/s00702-011-0665-y.

Párdutz, Á., Krizbai, I., Multon, S., Vécsei, L., and Schoenen, J. 2000. Systemic nitroglycerin increases nNOS levels in rat trigeminal nucleus caudalis: NeuroReport **11**(14): 3071–3075. doi:10.1097/00001756-200009280-00008.

Parihar, M.S., Parihar, A., Fujita, M., Hashimoto, M., and Ghafourifar, P. 2008. Mitochondrial association of alpha-synuclein causes oxidative stress. Cell. Mol. Life Sci. **65**(7–8): 1272–1284. doi:10.1007/s00018-008-7589-1.

Patel, V., Chisholm, D., Dua, T., Laxminarayan, R., and Medina-Mora, M.L. (*Editors*). 2016. Disease control priorities: mental, neurological, and substance use disorders. *In* 3rd ed. The World Bank. doi:10.1596/978-1-4648-0426-7.

Pearson, S.J., and Reynolds, G.P. 1992. Increased brain concentrations of a neurotoxin, 3-hydroxykynurenine, in Huntington's disease. Neurosci. Lett. **144**(1–2): 199–201. doi:10.1016/0304-3940(92)90749-W.

Pereira, E.F.R., Hilmas, C., Santos, M.D., Alkondon, M., Maelicke, A., and Albuquerque, E.X. 2002. Unconventional ligands and modulators of nicotinic receptors. J. Neurobiol. **53**(4): 479–500. doi:10.1002/neu.10146.

Pouladi, M.A., Morton, A.J., and Hayden, M.R. 2013. Choosing an animal model for the study of Huntington's disease. Nat. Rev. Neurosci. **14**(10): 708–721. doi:10.1038/nrn3570.

Prescott, C., Weeks, A.M., Staley, K.J., and Partin, K.M. 2006. Kynurenic acid has a dual action on AMPA receptor responses. Neurosci. Lett. **402**(1–2): 108–112. doi:10.1016/j.neulet.2006.03.051.

Przedborski, S., and Vila, M. 2003. The 1-methyl-4-phenyl-1,2,3,6-tetrahydropyridine mouse model: a tool to explore the pathogenesis of Parkinson's disease. Ann. N. Y. Acad. Sci. **991**: 189–198.

Quartu, M., Serra, M.P., Ambu, R., Lai, M.L., and Del Fiacco, M. 2002. AMPA-type glutamate receptor subunits 2/3 in the human trigeminal sensory ganglion and subnucleus caudalis from prenatal ages to adulthood. Mech. Ageing Dev. **123**(5): 463–471.

Quesada, J.M., Mata-Granados, J.M., and Luque de Castro, M.D. 2004. Automated method for the determination of fat-soluble vitamins in serum. J. Steroid Biochem. Mol. Biol. **89**–**90**: 473–477. doi:10.1016/j.jsbmb.2004.03.056.

R Development Core Team. 2008. R: A Language and Environment for Statistical Computing. R Foundation for Statistical Computing, Vienna, Austria. Available from http://www.R-project.org.

Raboisson, P., and Dallel, R. 2004. The orofacial formalin test. Neurosci. Biobehav. Rev. **28**(2): 219–226. doi:10.1016/j.neubiorev.2003.12.003.

Raizman, J.E., Cohen, A.H., Teodoro-Morrison, T., Wan, B., Khun-Chen, M., Wilkenson, C., Bevilaqua, V., and Adeli, K. 2014. Pediatric reference value distributions for vitamins A and E in the CALIPER cohort and establishment of age-stratified reference intervals. Clin. Biochem. **47**(9): 812–815. doi:10.1016/j.clinbiochem.2014.03.025.

Rifkind, B.M., and Segal, P. 1983. Lipid Research Clinics Program reference values for hyperlipidemia and hypolipidemia. JAMA **250**(14): 1869–1872.

Saha, S., Walia, S., Kundu, A., and Pathak, N. 2013. Effect of mobile phase on resolution of the isomers and homologues of tocopherols on a triacontyl stationary phase. Anal. Bioanal. Chem. **405**(28): 9285–9295. doi:10.1007/s00216-013-7336-9.

Sahara, Y., Noro, N., Iida, Y., Soma, K., and Nakamura, Y. 1997. Glutamate receptor subunits GluR5 and KA-2 are coexpressed in rat trigeminal ganglion neurons. J. Neurosci. **17**(17): 6611–6620.

Sang, C.N., Ramadan, N.M., Wallihan, R.G., Chappell, A.S., Freitag, F.G., Smith, T.R., Silberstein, S.D., Johnson, K.W., Phebus, L.A., Bleakman, D., Ornstein, P.L., Arnold, B., Tepper, S.J., and Vandenhende, F. 2004. LY293558, a novel AMPA/GluR5 antagonist, is efficacious and well-tolerated in acute migraine. Cephalalgia Int. J. Headache **24**(7): 596–602. doi:10.1111/j.1468-2982.2004.00723.x.

Sathyasaikumar, K.V., Stachowski, E.K., Amori, L., Guidetti, P., Muchowski, P.J., and Schwarcz, R. 2010. Dysfunctional kynurenine pathway metabolism in the R6/2 mouse model of Huntington's disease. J. Neurochem. **113**(6): 1416–1425. doi:10.1111/j.1471-4159.2010.06675.x.

Sauerwein, R.W., Mulder, J.A., Mulder, L., Lowe, B., Peshu, N., Demacker, P.N., van der Meer, J.W., and Marsh, K. 1997. Inflammatory mediators in children with protein-energy malnutrition. Am. J. Clin. Nutr. **65**(5): 1534–1539.

Schwarcz, R., Okuno, E., White, R.J., Bird, E.D., and Whetsell, W.O. 1988. 3-Hydroxyanthranilate oxygenase activity is increased in the brains of Huntington disease victims. Proc. Natl. Acad. Sci. **85**(11): 4079–4081.

Sies, H. 1993. Strategies of antioxidant defense. Eur. J. Biochem. **215**(2): 213–219.

Sies, H. 1997. Oxidative stress: oxidants and antioxidants. Exp. Physiol. **82**(2): 291–295.

Slow, E.J., van Raamsdonk, J., Rogers, D., Coleman, S.H., Graham, R.K., Deng, Y., Oh, R., Bissada, N., Hossain, S.M., Yang, Y.-Z., Li, X.-J., Simpson, E.M., Gutekunst, C.-A., Leavitt, B.R., and Hayden, M.R. 2003. Selective striatal neuronal loss in a YAC128 mouse model of Huntington disease. Hum. Mol. Genet. **12**(13): 1555–1567.

Squali Houssaïni, F.Z., Foulon, T., Payen, N., Iraqi, M.R., Arnaud, J., and Groslambert, P. 2001. Plasma fatty acid status in Moroccan children: increased lipid peroxidation and

impaired polyunsaturated fatty acid metabolism in protein-calorie malnutrition. Biomed. Pharmacother. **55**(3): 155–162.

Stahl, W.L., and Swanson, P.D. 1974. Biochemical abnormalities in Huntington's chorea brains. Neurology **24**(9): 813–819.

Stovner, L., Hagen, K., Jensen, R., Katsarava, Z., Lipton, R., Scher, A., Steiner, T., and Zwart, J.-A. 2007. The global burden of headache: A documentation of headache prevalence and disability worldwide. Cephalalgia **27**(3): 193–210. doi:10.1111/j.1468-2982.2007.01288.x.

St-Pierre, J., Drori, S., Uldry, M., Silvaggi, J.M., Rhee, J., Jäger, S., Handschin, C., Zheng, K., Lin, J., Yang, W., Simon, D.K., Bachoo, R., and Spiegelman, B.M. 2006. Suppression of reactive oxygen species and neurodegeneration by the PGC-1 transcriptional coactivators. Cell **127**(2): 397–408. doi:10.1016/j.cell.2006.09.024.

Strauss, R.S. 1999. Comparison of serum concentrations of alpha-tocopherol and beta-carotene in a cross-sectional sample of obese and nonobese children (NHANES III). National Health and Nutrition Examination Survey. J. Pediatr. **134**(2): 160–165.

Swanson, C.R., Du, E., Johnson, D.A., Johnson, J.A., and Emborg, M.E. 2013. Neuroprotective Properties of a Novel Non-Thiazoledinedione Partial PPAR-γ Agonist against MPTP. PPAR Res. **2013**. doi:10.1155/2013/582809.

Szalárdy, L., Klivényi, P., Zádori, D., Fülöp, F., Toldi, J., and Vécsei, L. 2012a. Mitochondrial disturbances, tryptophan metabolites and neurodegeneration: medicinal chemistry aspects. Curr. Med. Chem. **19**(13): 1899–1920.

Szalárdy, L., Zádori, D., Klivényi, P., Toldi, J., and Vécsei, L. 2015. Electron transport disturbances and neurodegeneration: from Albert Szent-Györgyi's concept (Szeged) till novel approaches to boost mitochondrial bioenergetics. Oxid. Med. Cell. Longev. **2015**: 1–19. doi:10.1155/2015/498401.

Szalárdy, L., Zádori, D., Toldi, J., Fülöp, F., Klivényi, P., and Vécsei, L. 2012b. Manipulating kynurenic acid levels in the brain - on the edge between neuroprotection and cognitive dysfunction. Curr. Top. Med. Chem. **12**(16): 1797–1806.

Tallaksen-Greene, S.J., Young, A.B., Penney, J.B., and Beitz, A.J. 1992. Excitatory amino acid binding sites in the trigeminal principal sensory and spinal trigeminal nuclei of the rat. Neurosci. Lett. **141**(1): 79–83. doi:10.1016/0304-3940(92)90339-9.

The Huntington's Disease Collaborative Research Group. 1993. A novel gene containing a trinucleotide repeat that is expanded and unstable on Huntington's disease chromosomes. Cell **72**(6): 971–983. doi:10.1016/0092-8674(93)90585-E.

Thurnham, D.I., Davies, J.A., Crump, B.J., Situnayake, R.D., and Davis, M. 1986. The use of different lipids to express serum tocopherol: lipid ratios for the measurement of vitamin E status. Ann. Clin. Biochem. **23 (Pt 5)**: 514–520. doi:10.1177/000456328602300505.

Tomai, F., Crea, F., Chiariello, L., and Gioffrè, P.A. 1999. Ischemic preconditioning in humans: models, mediators, and clinical relevance. Circulation **100**(5): 559–563.

Török, R., Kónya, J.A., Zádori, D., Veres, G., Szalárdy, L., Vécsei, L., and Klivényi, P. 2015. mRNA expression levels of PGC-1α in a transgenic and a toxin model of Huntington's disease. Cell. Mol. Neurobiol. **35**(2): 293–301. doi:10.1007/s10571-014-0124-z.

Túnez, I., Tasset, I., Pérez-De La Cruz, V., and Santamaría, A. 2010. 3-Nitropropionic acid as a tool to study the mechanisms involved in Huntington's disease: Past, present and future. Molecules **15**(2): 878–916. doi:10.3390/molecules15020878.

Ueda, N., Suzuki, Y., Rino, Y., Takahashi, T., Imada, T., Takanashi, Y., and Kuroiwa, Y. 2009. Correlation between neurological dysfunction with vitamin E deficiency and gastrectomy. J. Neurol. Sci. **287**(1–2): 216–220. doi:10.1016/j.jns.2009.07.020.

Vécsei, L., Szalárdy, L., Fülöp, F., and Toldi, J. 2013. Kynurenines in the CNS: recent advances and new questions. Nat. Rev. Drug Discov. **12**(1): 64–82. doi:10.1038/nrd3793.

Veres, G., Fejes-Szabó, A., Zádori, D., Nagy-Grócz, G., László, A.M., Bajtai, A., Mándity, I., Szentirmai, M., Bohár, Z., Laborc, K., Szatmári, I., Fülöp, F., Vécsei, L., and Párdutz, Á. 2017. A comparative assessment of two kynurenic acid analogs in the formalin model of trigeminal activation: a behavioral, immunohistochemical and pharmacokinetic study. J. Neural Transm. **124**(1): 99–112. doi:10.1007/s00702-016-1615-5.

Vikelis, M., and Mitsikostas, D.D. 2007. The role of glutamate and its receptors in migraine. CNS Neurol. Disord. Drug Targets **6**(4): 251–257.

Watanabe, M., Mishina, M., and Inoue, Y. 1994. Distinct gene expression of the N-methyl-D-aspartate receptor channel subunit in peripheral neurons of the mouse sensory ganglia and adrenal gland. Neurosci. Lett. **165**(1–2): 183–186.

Weatherall, M.W. 2015. Drug therapy in headache. Clin. Med. **15**(3): 273–279. doi:10.7861/clinmedicine.15-3-273.

Winbauer, A.N., Pingree, S.S., and Nuttall, K.L. 1999. Evaluating serum alpha-tocopherol (vitamin E) in terms of a lipid ratio. Ann. Clin. Lab. Sci. **29**(3): 185–191.

Yuan, C., Burgyan, M., Bunch, D.R., Reineks, E., Jackson, R., Steinle, R., and Wang, S. 2014. Fast, simple, and sensitive high-performance liquid chromatography method for measuring vitamins A and E in human blood plasma: Liquid Chromatography. J. Sep. Sci. **37**(17): 2293–2299. doi:10.1002/jssc.201301373.

Zádori, D., Ilisz, I., Klivényi, P., Szatmári, I., Fülöp, F., Toldi, J., Vécsei, L., and Péter, A. 2011a. Time-course of kynurenic acid concentration in mouse serum following the administration of a novel kynurenic acid analog. J. Pharm. Biomed. Anal. **55**(3): 540–543. doi:10.1016/j.jpba.2011.02.014.

Zádori, D., Klivényi, P., Plangár, I., Toldi, J., and Vécsei, L. 2011b. Endogenous neuroprotection in chronic neurodegenerative disorders: with particular regard to the kynurenines. J. Cell. Mol. Med. **15**(4): 701–717. doi:10.1111/j.1582-4934.2010.01237.x.

Zádori, D., Klivényi, P., Szalárdy, L., Fülöp, F., Toldi, J., and Vécsei, L. 2012. Mitochondrial disturbances, excitotoxicity, neuroinflammation and kynurenines: Novel therapeutic strategies for neurodegenerative disorders. J. Neurol. Sci. **322**(1): 187–191. doi:10.1016/j.jns.2012.06.004.

Zhang, Y., Huo, M., Zhou, J., and Xie, S. 2010. PKSolver: An add-in program for pharmacokinetic and pharmacodynamic data analysis in Microsoft Excel. Comput. Methods Programs Biomed. **99**(3): 306–314. doi:10.1016/j.cmpb.2010.01.007.

Zhao, Y., Monahan, F.J., McNulty, B.A., Gibney, M.J., and Gibney, E.R. 2014. Effect of vitamin E intake from food and supplement sources on plasma α- and γ-tocopherol concentrations in a healthy Irish adult population. Br. J. Nutr. **112**(09): 1575–1585. doi:10.1017/S0007114514002438.

Appendix

I.

Population	Population description	Age range (year)	Sample size	α-tocopherol (μM) [corrected values (μmol/mmol)]	γ-tocopherol (μM) [corrected values (μmol/mmol)]	δ-tocopherol (μM) [corrected values (μmol/mmol)]	Cholesterol measurement	Sample type	ISTD	Validation
Arabian[1]	detailed	32.5 (18 – 58)[a]	159 M	21.3 ± 0.6[b]			+	serum	+	+
				[5.6 ± 0.2]						
		33.3 (18 – 63)	101 F	17.3 ± 0.5						
				[4.3 ± 0.1]						
Dutch[16]	detailed	31.2 (24 – 45)[a]	33 M	23.9 (13.2 – 41.3)[a]	2.3 (0.98 – 5.20)[a]		+	serum	+	+
				[4.97 (2.65 – 7.01)]						
		33.1 (24 – 43)	39 F	25.5 (18.3 – 39.2)	2.32 (1.17 – 4.30)					
				[5.37 (3.21 – 9.32)]						
English[22]	none	44 (19 – 62)[a]	45 M	30.0 ± 7.4[b]			-	plasma	+	+
			66 F	30.4 ± 7.1						

English[8]	detailed	70.2 ± 2.0[b]	264 M	[5.5 ± 1.3][c]			+	plasma	+	+
		70.2 ± 2.1	204 F	[5.4 ± 1.4]						
Europian[10]	detailed	58.0 ± 7.8[b]	446	27.9 (17.6 – 45.1)[d]	3.1 (1.0 – 8.6)[d]		-	plasma	+	-
Europian[11]	detailed	59 (49.5 – 67.2)[e]	898	27.7 (20.50 – 37.92)[f]	1.49 (0.79 – 3.01)[f]	0.13 (0.05 – 0.36)[f]	-	plasma	+	+
Finnish[12]	detailed	71.3 (65.4 – 79.1)[a]	76	29.26 ± 2.99[b]	1.88 ± 0.17[b]	0.27 ± 0.01[b]	+	serum	-	+
				[5.13 ± 1.02]	[0.33 ± 0.06]	[0.047 ± 0.01]				
French[3]	detailed	52.1 ± 4.7[b]	1487 M	27.5 (24.1 – 31.7)[g]			+	serum	+	+
		47.1 ± 6.7	2034 F	28.2 (24.5 – 32.4)						
French[7]	detailed	<45	1307 M	-			+	serum	-	+
		45 – 50		31.8 ± 7.5[b]						
		50 – 55		31.8 ± 8.0						
		>55		31.7 ± 7.7						

French[7]	detailed	<45	1821 F	29.4 ± 6.9			+	serum	-	+
		45 – 50		30.7 ± 7.5						
		50 – 55		31.9 ± 6.4						
		>55		33.5 ± 8.5						
French[16]	detailed	34.7 (24 – 45)[a]	38 M	26.9 (17.9 – 37.8)[a]	1.28 (0.17 – 2.90)[a]		+	serum	+	+
				[6.12 (4.93 – 9.12)]						
		35.9 (25 – 45)	37 F	26.5 (16.7 – 39.9)	1.05 (0.31 – 2.50)					
				[5.89 (4.78 – 9-96)]						
Indian[4]	detailed	55 ± 4.7[b]	291	20.63 ± 5.37[b]	2.54 ± 0.84[b]		+	NA	-	-
				[4.44 ± 1.13]	[0.55 ± 0.18]					
Irish[27]	detailed	18 – 35	363	21.83 ± 4.81[b]	1.61 ± 0.77[b]		-	plasma	+	+
		36 – 50	283	26.73 ± 6.48	1.84 ± 0.96					

Irish[27]	detailed	51 – 64	165	28.37 ± 7.14	2.05 ± 0.96		-	plasma	+	+
		> 64	110	26.67 ± 7.43	1.79 ± 0.95					
Irish[16]	detailed	30.7 (24 – 44)[a]	40 M	26.2 (20.7 – 23.2)[a]	1.87 (0.81 – 3.51)[a]		+	serum	+	+
				[7.62 (4.95 – 12.97)]						
		31.9 (24 – 45)	33 F	26.5 (19.0 – 33.4)	1.74 (0.73 – 4.19)					
				[7.82 (5.94 – 14.17)]						
Italian[19]	detailed	73.7 ± 6.1[b]	666	[6. 0 ± 1.8][b]	[0.37 ± 0.11][b]	[0.05 ± 0.01][b]	+	plasma	+	-
Japanese[28]	detailed	41 (23 – 67)[l]	206 M	15.09 (3.94 – 35.75)[l]	1.20 (0.24 – 10.08)[l]		+	serum	-	+
North American[26]	none	19 – 64	51	13.93 – 53.40[h]	0.72 – 7.68[h]		-	NA	+	+
North American[17]	none	≥13	160	9.84 – 69.67[i]	0.17 – 8.06[i]		-	serum	+	+
		0 – 12	120	8.82 – 54.02	0.048 – 5.13					
North American[5]	detailed	71 ± 6.8[b]	272	30.49 (23.74 – 39.50)[g]	3.56 (1.63 – 5.75)[g]		-	plasma	+	-

North American[24]	basic	51 ± 18[b]	307	11.61 – 41.79[h]			+	serum	+	+
				[not calculated]						
North American[14]	detailed	70 ± 7.5[b]	538	33.57 (26.44 – 45.09)[g]	4.06 (2.35 – 6.53)[g]	0.60 (0.50 – 0.77)[g]	+		+	+
North American[20]	detailed	60.6 ± 10.9[b]	777 M	32.30 ± 14.58[b]			-	NA	+	+
		59.3 ± 10.3	839 F	34.83 ± 16.25						
North American[6]	detailed	20 – 29	442 – 770	20.92[k]	4.97[k]		+	serum	+	+
				[4.48]	[1.07]					
		30 – 39		24.17	4.88					
				[4.87]	[0.98]					
		40 – 49		28.54	5.04					
				[5.35]	[0.95]					
		50 – 59		32.50	4.89					
				[5.95]	[0.90]					

North American[6]	detailed	60 – 69	442 – 770	35.14 [6.26]	4.36 [0.78]		+	serum	+	+
		≥ 70		35.01 [6.49]	4.16 [0.77]					
North American[21]	none	NA	221	34.45 (4.71 – 65.42)[a]	3.05 (0.55 – 9.36)[a]	0.15 (0.02 – 0.57)[a]	-	plasma	+	+
North Irish[16]	detailed	34.7 (26 – 46)[a]	32 M	26.0 (16.5 – 46.4)[a] [7.12 (1.31 – 14.04)]	1.64 (0.55 – 6.93)[a]		+	serum	+	+
		35.1 (19 – 45)	33 F	27.6 (18.1 – 40.4) [7.60 (2.96 – 16.23)]	1.55 (0.51 – 4.22)					
Norwegian[9]	detailed	65 – 79	418 M	29.5 ± 11.8[b]			+	serum	+	+
			1016 F	32.1 ± 14.2						

Spanish[15]	basic	32 (5 – 79)[l]	210 M	18.34 – 45.97[i]			+	serum	+	+
				[3.85 – 7.56]						
		32.5 (5 – 79)	240 F	17.65 – 41.33						
				[4.83 – 7.13]						
Spanish[13]	none	18 – 65	215	22.13 ± 8.3[b]			-	serum	+	+
Spanish[18]	none	18 – 27	120 M	10.91 (5.57 – 18.57)[a]			-	serum	+	+
		28 – 37		12.07 (3.25 – 23.22)						
		38 – 47		13.70 (2.79 – 24.61)						
		48 – 65		14.86 (6.04 – 22.75)						
		18 – 27	120 F	9.29 (4.88 – 14.86)						
		28 – 37		12.54 (3.25 – 26.70)						
		38 – 47		11.38 (4.18 – 16.25)						
		48 – 65		13.23 (6.73 – 22.75)						

Spanish[16]	detailed	36 (25 – 45)[a]	32 M	27.4 (18.1 – 38.8)[a] [7.04 (4.60 – 14.79)]	1.14 (0.39 – 4.16)[a]		+	serum	+	+
		36.1 (25 – 45)	32 F	28.3 (17.6 – 41.6) [6.53 (4.83 – 11.38)]	0.88 (0.37 – 2.44)					
Swiss[25]	basic	12.6 (0.4 – 38.7)[l]	208	[4.29 – 6.76][j]			+	plasma	-	+
Taiwanese[2]	detailed	46 (44.77 – 47.03)[m]	176 M	28.60 ± 14.34[b]			+	serum	+	+
		44 (42.41 – 44.64)	118 F	23.72 ± 15.16						
Taiwanese[23]	detailed	41.0 (25.0 – 53.0)[l]	14 M	18.73 (2.62-28.30)[l] [3.52 (2.73 – 4.15)]			+	serum	-	-
		40 (16.0 – 60.0)	58 F	18.53 (5.30 – 30.28) [3.41 (0.81 – 7.78)]						

Footnotes to Supplementary table 1

1 Abbreviations

F – female

M – male

NA – not available

RA – retinol acetate

TA – tocopherol acetate

2 Notes

a – mean (range)

b – mean ± standard deviation

c – geometric mean ± standard deviation

d – median (5-95th percentile)

e – median (10-90th percentile)

f – geometric mean (10-90th percentile)

g – median (interquartile range)

h – reference interval

i – reference interval (95%)

j – reference interval (90%)

k – geometric mean

l – median (range)

m – median (95% confidence interval)

* - retinyl butyrate and nonapreno-β-carotene

3 Methods

PubMed (MEDLINE) and Web of Science™ were used as search engines for articles. The key terms for searching were: tocopherol, human, reference interval, vitamin E. Papers reporting only measurement data of subjects under the age of 18 years or those with a control group consisting less than 50 individuals were excluded. With regard to population description three levels were determined: descriptions without details were assigned to ‘none’; when only few specific criteria for patient enrollment were presented, ‘basic’ was applied; if the study population parameters were thoroughly delineated with special attention to vitamin E consumption and medications, the description was considered as ‘detailed’. There was not applied any differentiation between the depth of validation process, only methods without any reported validation were considered as unvalidated.

4 References

[1] C. Abiaka, S. Olusi, A. Simbeye, Serum concentrations of micronutrient antioxidants in an adult Arab population, Asia Pac. J. Clin. Nutr. 11 (2002) 22–27. doi:10.1046/j.1440-6047.2002.00260.x.

[2] P. Boonsiri, J. Pooart, R. Tangrassameeprasert, P. Hongsprabhas, Serum beta-carotene, lycopene and alpha-tocopherol levels of healthy people in northeast Thailand., Asia Pac. J. Clin. Nutr. 16 Suppl 1 (2007) 47–51. http://www.ncbi.nlm.nih.gov/pubmed/17392076.

[3] L. Dauchet, S. Péneau, S. Bertrais, A.C. Vergnaud, C. Estaquio, E. Kesse-Guyot, S. Czernichow, A. Favier, H. Faure, P. Galan, S. Hercberg, Relationships between different types of fruit and vegetable consumption and serum concentrations of antioxidant vitamins., Br. J. Nutr. 100 (2008) 633–41. doi:10.1017/S000711450892170X.

[4] M. Dherani, G.V.S. Murthy, S.K. Gupta, I.S. Young, G. Maraini, M. Camparini, G.M. Price, N. John, U. Chakravarthy, A.E. Fletcher, Blood Levels of Vitamin C, Carotenoids and Retinol Are Inversely Associated with Cataract in a North Indian Population, Investig. Opthalmology Vis. Sci. 49 (2008) 3328. doi:10.1167/iovs.07-1202.

[5] M. Epplein, A.A. Franke, R. V. Cooney, J.S. Morris, L.R. Wilkens, M.T. Goodman, S.P. Murphy, B.E. Henderson, L.N. Kolonel, L. Le Marchand, Association of plasma micronutrient levels and urinary isoprostane with risk of lung cancer: The Multiethnic Cohort Study, Cancer Epidemiol. Biomarkers Prev. 18 (2009) 1962–1970. doi:10.1158/1055-9965.EPI-09-0003.

[6] E.S. Ford, R.L. Schleicher, A.H. Mokdad, U.A. Ajani, S. Liu, Distribution of serum concentrations of alpha-tocopherol and gamma-tocopherol in the US population., Am. J. Clin. Nutr. 84 (2006) 375–83. http://www.ncbi.nlm.nih.gov/pubmed/16895886.

[7] P. Galan, F.E. Viteri, S. Bertrais, S. Czernichow, H. Faure, J. Arnaud, D. Ruffieux, S. Chenal, N. Arnault, A. Favier, A.-M. Roussel, S. Hercberg, Serum concentrations of beta-carotene, vitamins C and E, zinc and selenium are influenced by sex, age, diet, smoking status, alcohol consumption and corpulence in a general French adult population, Eur. J. Clin. Nutr. 59 (2005) 1181–1190. doi:10.1038/sj.ejcn.1602230.

[8] C.R. Gale, H.E. Ashurst, H.J. Powers, C.N. Martyn, Antioxidant vitamin status and carotid atherosclerosis in the elderly., Am. J. Clin. Nutr. 74 (2001) 402–408.

[9] K. Holvik, C.G. Gjesdal, G.S. Tell, G. Grimnes, B. Schei, E.M. Apalset, S.O. Samuelsen, R. Blomhoff, K. Michaëlsson, H.E. Meyer, Low serum concentrations of alpha-tocopherol are associated with increased risk of hip fracture. A NOREPOS study, Osteoporos. Int. 25 (2014) 2545–2554. doi:10.1007/s00198-014-2802-6.

[10] S.M. Jeurnink, M.M. Ros, M. Leenders, F.J.B. van Duijnhoven, P.D. Siersema, E.H.J.M. Jansen, C.H. van Gils, M.F. Bakker, K. Overvad, N. Roswall, A. Tjønneland, M.-C. Boutron-Ruault, A. Racine, C. Cadeau, V. Grote, R. Kaaks, K. Aleksandrova, H. Boeing, A. Trichopoulou, V. Benetou, E. Valanou, D. Palli, V. Krogh, P. Vineis, R. Tumino, A. Mattiello, E. Weiderpass, G. Skeie, J.M.H. Castaño, E.J. Duell, A.

Barricarte, E. Molina-Montes, M. Argüelles, M. Dorronsoro, D. Johansen, B. Lindkvist, M. Sund, F.L. Crowe, K. Khaw, M. Jenab, V. Fedirko, E. Riboli, H.B. Bueno-de-Mesquita, Plasma carotenoids, vitamin C, retinol and tocopherols levels and pancreatic cancer risk within the European Prospective Investigation into Cancer and Nutrition: A nested case-control study, Int. J. Cancer. 136 (2015) E665–E676. doi:10.1002/ijc.29175.

[11] M. Leenders, A.M. Leufkens, P.D. Siersema, F.J.B. van Duijnhoven, A. Vrieling, P.J.M. Hulshof, C.H. van Gils, K. Overvad, N. Roswall, C. Kyrø, M.-C. Boutron-Ruault, G. Fagerhazzi, C. Cadeau, T. Kühn, T. Johnson, H. Boeing, K. Aleksandrova, A. Trichopoulou, E. Klinaki, A. Androulidaki, D. Palli, S. Grioni, C. Sacerdote, R. Tumino, S. Panico, M.F. Bakker, G. Skeie, E. Weiderpass, P. Jakszyn, A. Barricarte, J. María Huerta, E. Molina-Montes, M. Argüelles, I. Johansson, I. Ljuslinder, T.J. Key, K.E. Bradbury, K. Khaw, N.J. Wareham, P. Ferrari, T. Duarte-Salles, M. Jenab, M.J. Gunter, A. Vergnaud, P.A. Wark, H.B. Bueno-de-Mesquita, Plasma and dietary carotenoids and vitamins A, C and E and risk of colon and rectal cancer in the European Prospective Investigation into Cancer and Nutrition, Int. J. Cancer. 135 (2014) 2930–2939. doi:10.1002/ijc.28938.

[12] F. Mangialasche, A. Solomon, I. Kareholt, B. Hooshmand, R. Cecchetti, L. Fratiglioni, H. Soininen, T. Laatikainen, P. Mecocci, M. Kivipelto, Serum levels of vitamin E forms and risk of cognitive impairment in a Finnish cohort of older adults, Exp. Gerontol. 48 (2013) 1428–1435. doi:10.1016/j.exger.2013.09.006.

[13] J.M. Mata-Granados, M.D. Luque de Castro, J.M. Quesada Gomez, Inappropriate serum levels of retinol, α-tocopherol, 25 hydroxyvitamin D3 and 24,25 dihydroxyvitamin D3 levels in healthy Spanish adults: Simultaneous assessment by HPLC, Clin. Biochem. 41 (2008) 676–680. doi:10.1016/j.clinbiochem.2008.02.003.

[14] Y. Morimoto, N.J. Ollberding, R. V. Cooney, L.R. Wilkens, A.A. Franke, L. Le Marchand, M.T. Goodman, B.Y. Hernandez, L.N. Kolonel, G. Maskarinec, Prediagnostic serum tocopherol levels and the risk of non-Hodgkin lymphoma: the multiethnic cohort, Cancer Epidemiol. Biomarkers Prev. 22 (2013) 2075–2083. doi:10.1158/1055-9965.EPI-13-0522.

[15] B. Olmedilla, F. Granado, E. Gil-Martinez, I. Blanco, E. Rojas-Hidalgo, Reference values for retinol, tocopherol, and main carotenoids in serum of control and insulin-dependent diabetic Spanish subjects, Clin. Chem. 43 (1997) 1066–1071.

[16] B. Olmedilla, F. Granado, S. Southon, A.J.A. Wright, I. Blanco, E. Gil-Martinez, H. van den Berg, B. Corridan, A. Roussel, M. Chopra, D.I. Thurnham, Serum concentrations of carotenoids and vitamins A, E, and C in control subjects from five European countries, Br. J. Nutr. 85 (2001) 227. doi:10.1079/BJN2000248.

[17] E.M. Paliakov, B.S. Crow, M.J. Bishop, D. Norton, J. George, J.A. Bralley, Rapid quantitative determination of fat-soluble vitamins and coenzyme Q-10 in human serum by reversed phase ultra-high pressure liquid chromatography with UV detection, J. Chromatogr. B. 877 (2009) 89–94. doi:10.1016/j.jchromb.2008.11.012.

[18] J.M. Quesada, J.M. Mata-Granados, M.D. Luque De Castro, Automated method for the determination of fat-soluble vitamins in serum, J. Steroid Biochem. Mol. Biol. 89–90 (2004) 473–477. doi:10.1016/j.jsbmb.2004.03.056.

[19] G. Ravaglia, P. Forti, A. Lucicesare, N. Pisacane, E. Rietti, F. Mangialasche, R. Cecchetti, C. Patterson, P. Mecocci, Plasma tocopherols and risk of cognitive impairment in an elderly Italian cohort., Am. J. Clin. Nutr. 87 (2008) 1306–13. http://www.ncbi.nlm.nih.gov/pubmed/18469254.

[20] H.J. Schünemann, B.J.B. Grant, J.L. Freudenheim, P. Muti, R.W. Browne, J.A. Drake, R.A. Klocke, M. Trevisan, The relation of serum levels of antioxidant vitamins C and E, retinol and carotenoids with pulmonary function in the general population, Am. J. Respir. Crit. Care Med. 163 (2001) 1246–1255. doi:10.1164/ajrccm.163.5.2007135.

[21] D. Siluk, R. V. Oliveira, M. Esther-Rodriguez-Rosas, S. Ling, A. Bos, L. Ferrucci, I.W. Wainer, A validated liquid chromatography method for the simultaneous determination of vitamins A and E in human plasma, J. Pharm. Biomed. Anal. 44 (2007) 1001–1007. doi:10.1016/j.jpba.2007.03.033.

[22] D. Talwar, T.K. Ha, J. Cooney, C. Brownlee, D.S. O'Reilly, A routine method for the simultaneous measurement of retinol, alpha-tocopherol and five carotenoids in human

plasma by reverse phase HPLC., Clin. Chim. Acta. 270 (1998) 85–100. http://www.ncbi.nlm.nih.gov/pubmed/9544447.

[23] D. Viroonudomphol, P. Pongpaew, R. Tungtrongchitr, S. Changbumrung, A. Tungtrongchitr, B. Phonrat, N. Vudhivai, F.P. Schelp, The relationships between anthropometric measurements, serum vitamin A and E concentrations and lipid profiles in overweight and obese subjects., Asia Pac. J. Clin. Nutr. 12 (2003) 73–9. http://www.ncbi.nlm.nih.gov/pubmed/12737014.

[24] A.N. Winbauer, S.S. Pingree, K.L. Nuttall, Evaluating serum alpha-tocopherol (vitamin E) in terms of a lipid ratio., Ann. Clin. Lab. Sci. 29 (1999) 185–91. http://www.ncbi.nlm.nih.gov/pubmed/10440582.

[25] B.M. Winklhofer-Roob, M.A. Van'T Hof, D.H. Shmerling, Reference values for plasma concentrations of vitamin E and A and carotenoids in a swiss population from infancy to adulthood, adjusted for seasonal influences, Clin. Chem. 43 (1997) 146–153.

[26] C. Yuan, M. Burgyan, D.R. Bunch, E. Reineks, R. Jackson, R. Steinle, S. Wang, Fast, simple, and sensitive high-performance liquid chromatography method for measuring vitamins A and E in human blood plasma., J. Sep. Sci. 37 (2014) 2293–9. doi:10.1002/jssc.201301373.

[27] Y. Zhao, F.J. Monahan, B. a McNulty, M.J. Gibney, E.R. Gibney, Effect of vitamin E intake from food and supplement sources on plasma α- and γ-tocopherol concentrations in a healthy Irish adult population., Br. J. Nutr. 112 (2014) 1575–85. doi:10.1017/S0007114514002438.

[28] Y. Zou, D. Wang, N. Sakano, Y. Sato, S. Iwanaga, K. Taketa, M. Kubo, K. Takemoto, C. Masatomi, K. Inoue, K. Ogino, Associations of serum retinol, α-tocopherol, and γ-tocopherol with biomarkers among healthy japanese men, Int. J. Environ. Res. Public Health. 11 (2014) 1647–1660. doi:10.3390/ijerph110201647.

II.

J Neural Transm
DOI 10.1007/s00702-016-1615-5

A comparative assessment of two kynurenic acid analogs in the formalin model of trigeminal activation: a behavioral, immunohistochemical and pharmacokinetic study

Gábor Veres[1,4] · Annamária Fejes-Szabó[1] · Dénes Zádori[1] · Gábor Nagy-Grócz[1,5] · Anna M. László[3] · Attila Bajtai[1] · István Mándity[2] · Márton Szentirmai[1] · Zsuzsanna Bohár[1,4] · Klaudia Laborc[1] · István Szatmári[2] · Ferenc Fülöp[2] · László Vécsei[1,4] · Árpád Párdutz[1]

Received: 6 May 2016 / Accepted: 31 August 2016

Abstract Kynurenic acid (KYNA) has well-established protective properties against glutamatergic neurotransmission, which plays an essential role in the activation and sensitization process during some primary headache disorders. The goal of this study was to compare the effects of two KYNA analogs, *N*-(2-*N*,*N*-dimethylaminoethyl)-4-oxo-1H-quinoline-2-carboxamide hydrochloride (KA-1) and N-(2-N-pyrrolidinylethyl)-4-oxo-1H-quinoline-2-carboxamide hydrochloride (KA-2), in the orofacial formalin test of trigeminal pain. Following pretreatment with KA-1 or KA-2, rats were injected with subcutaneous formalin solution in the right whisker pad. Thereafter, the rubbing activity and c-Fos immunoreactivity changes in the spinal trigeminal nucleus pars caudalis (TNC) were investigated. To obtain pharmacokinetic data, KA-1, KA-2 and KYNA concentrations were measured following KA-1 or KA-2 injection. Behavioral tests demonstrated that KA-2 induced larger amelioration of formalin-evoked alterations as compared with KA-1 and the assessment of c-Fos immunoreactivity in the TNC yielded similar results. Although KA-1 treatment resulted in approximately four times larger area under the curve values in the serum relative to KA-2, the latter resulted in a higher KYNA elevation than in the case of KA-1. With regard to TNC, the concentration of KA-1 was under the limit of detection, while that of KA-2 was quite small and there was no major difference in the approximately tenfold KYNA elevations. These findings indicate that the differences between the beneficial effects of KA-1 and KA-2 may be explained by the markedly higher peripheral KYNA levels following KA-2 pretreatment. Targeting the peripheral component of trigeminal pain processing would provide an option for drug design which might prove beneficial in headache conditions.

Keywords Kynurenic acid analog · Rat · Trigeminal pain · Formalin test · Pharmacokinetics

Introduction

The kynurenine pathway (KP) of the tryptophan (TRP) metabolism is extensively studied, mostly because of the well-established endogenous protective properties of kynurenic acid (KYNA) against the excitotoxic effect of other KP metabolites, such as quinolinic acid and 3-hydroxy-L-kynurenine (Vécsei et al. 2013; Zádori et al. 2011b). Thus, KYNA has become a molecule of interest for central nervous system (CNS) drug development for several disorders (Schwarcz 2004). The application of KYNA in in vivo preclinical studies would be difficult due to its chemical and pharmacokinetic properties. There are problems with its solubility in higher doses, it cannot pass the blood–brain barrier in an acceptable quantity and it has

G. Veres and A. Fejes-Szabó contributed equally to this work.

✉ László Vécsei
vecsei.laszlo@med.u-szeged.hu

[1] Department of Neurology, Faculty of Medicine, Albert Szent-Györgyi Clinical Center, University of Szeged, Semmelweis u. 6, 6725 Szeged, Hungary

[2] Institute of Pharmaceutical Chemistry, University of Szeged, Szeged, Hungary

[3] Department of Biometrics and Agricultural Informatics, Faculty of Horticultural Science, Szent Istvan University, Budapest, Hungary

[4] MTA-SZTE Neuroscience Research Group, Szeged, Hungary

[5] Faculty of Health Sciences and Social Studies, University of Szeged, Szeged, Hungary

Published online: 14 September 2016

a rapid clearance from the CNS and in the periphery, mediated by organic anion transporters (Bahn et al. 2005; Fukui et al. 1991). Several analogs, derivatives and prodrugs have been synthesized with the aim of mitigating these disadvantages and of improving the utility of the molecule in preclinical studies (Fülöp et al. 2009). Among our newly synthesized KYNA amides, two lead compounds have been identified (Patent number #P0900281/PCT/HU2010/00050).

With regard to in vitro electrophysiology studies, *N*-(2-*N*,*N*-dimethylaminoethyl)-4-oxo-1H-quinoline-2-carboxamide hydrochloride (KA-1, Fig. 1a) has been demonstrated to be an even more effective inhibitor of hippocampal excitatory synaptic transmission than KYNA (Nagy et al. 2011). Accordingly, in an in vivo model of trigeminal activation, KA-1 displayed better efficacy than that of its parent compound, KYNA (Knyihár-Csillik et al. 2008). Following this comparative study, KA-1 was tested in several experimental setups and proved to have beneficial effects (Gellért et al. 2012, 2011; Knyihár-Csillik et al. 2008; Marosi et al. 2010; Vámos et al. 2010, 2009; Zádori et al. 2011c). In contrast with the electrophysiological findings with KA-1, *N*-(2-*N*-pyrrolidinylethyl)-4-oxo-1H-quinoline-2-carboxamide hydrochloride (KA-2, Fig. 1b) did not decrease, but rather slightly increased the amplitudes of field excitatory postsynaptic potentials (fEPSPs) (Nagy et al. 2011). However, in a recent study, pretreatment with KA-2 was also able to attenuate the effects of nitroglycerine (NTG) in an experimental model of migraine (Fejes-Szabó et al. 2014).

The modes of action of these two compounds are still not fully understood. The two main possibilities are the following: (1) the intact structure is necessary for the mechanism of action, which would mimic some effects of the parent compound, KYNA; (2) the KYNA amides serve as prodrugs and dissociate into KYNA, which can exert its

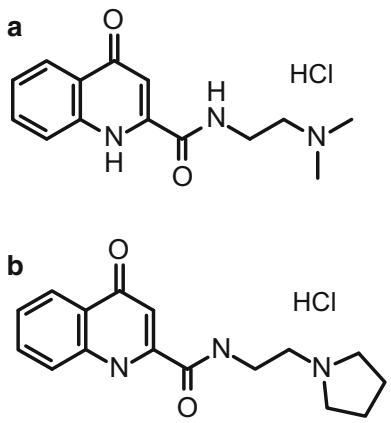

Fig. 1 The chemical structure of *N*-(2-*N*,*N*-dimethylaminoethyl)-4-oxo-1H-quinoline-2-carboxamide hydrochloride (KA-1, **a**) and *N*-(2-*N*-pyrrolidinylethyl)-4-oxo-1H-quinoline-2-carboxamide hydrochloride (KA-2, **b**)

pharmacological effects. With regard to the clarification of this issue, only one pharmacokinetic study is available to date (Zádori et al. 2011a). In that study, KYNA and KA-1 levels were measured with high-performance liquid chromatography (HPLC) in C57B/6 mouse serum following the intraperitoneal administration of KA-1. The time-course profile of KA-1 exhibited a steep increase in concentration followed by a rapid decrease in the first hour. Although the concentration of KYNA also increased from the basal serum level following KA-1 administration, this increase was considerably less than that in the case of KA-1. It may therefore be concluded that only a small proportion of KA-1 is metabolized to KYNA. These findings and the results of electrophysiology studies led to the assumption that it is less likely that KA-1 acts as a prodrug. Similar pharmacokinetic studies relating to KA-2 have not yet been made, but in view of the results of the electrophysiology studies, it seems to have a different mode of action.

The trigeminal system is responsible for most of the pain processing originating from the area of the head (Carpenter and Sutin 1983), and its activation therefore plays an important role in the pathomechanism of several neurological disorders, including primary headaches and trigeminal pain syndromes. These disorders, including migraine cause an enormous burden to the society (Olesen et al. 2012) underlining the need of new treatment options with a possible different mechanism of action. On the basis of its antagonistic influence on *N*-methyl-D-aspartate (NMDA), α-amino-3-hydroxy-5-methyl-4-isoxazolepropionic acid (AMPA) and kainate receptors (Pereira et al. 2002), it is assumed that KYNA has a modifying effect on nociception (Näsström et al. 1992; Párdutz et al. 2012), and thus might possibly be a future candidate in headache treatment.

One aim of this study was to investigate the effects of KA-1 and KA-2 in the orofacial formalin test to quantify the nociception in the trigeminal region of the rat (Clavelou et al. 1995; Raboisson and Dallel 2004). A further aim was to perform a comparative pharmacokinetic study so as to further clarify the possible modes of action of these two KYNA amides.

Materials and methods

Animals

During the experiments, adult male Sprague–Dawley rats weighing 200–250 g were used. The animals were housed under standard laboratory conditions (in an air-conditioned, humidity-controlled and ventilated room) and were allowed free access to drinking water and regular rat chow on a 12 h–12 h dark–light cycle. The procedures used in

this study followed the guidelines of the International Association for the Study of Pain and the directive of the European Economic Community (86/609/ECC). They were approved by the Committee of Animal Research at the University of Szeged (I-74-12/2012) and the Scientific Ethics Committee for Animal Research of the Protection of Animals Advisory Board (XXIV./352/2012.).

Materials

The new KYNA amides (patent number #P0900281/PCT/HU2010/00050), KA-1 and KA-2, were synthesized in the Department of Pharmaceutical Chemistry, University of Szeged. The reference compounds [KYNA and 3-nitro-L-tyrosine (3-NLT)], zinc acetate dihydrate, chloral hydrate and 3,3′-diaminobenzidine were purchased from Sigma-Aldrich (Saint Louis, MO, USA), acetonitrile, H_2O_2, nickel ammonium sulfate and perchloric acid (PCA) were purchased from Scharlau (Barcelona, Spain), acetic acid and Triton X-100 were purchased from VWR International (Radnar, PA, USA), and paraformaldehyde was purchased from Merck (Darmstadt, Germany). The HPLC–MS grade acetonitrile and acetic acid were obtained from VWR International (Radnar, PA, USA).

Behavioral testing

To produce and quantify nociception in the trigeminal region of the rat, we used the orofacial formalin test.

The animals were divided into three groups ($n = 27$–28 per group) and received an intraperitoneal (i.p.) injection of phosphate-buffered saline (PBS, 0.1 M, pH 7.4) in the Control group or an i.p. injection of KA-1 (1 mmol/kg body weight; pH 7.4) in the KA-1 group or an i.p. injection of KA-2 (1 mmol/kg body weight; pH 7.4) in the KA-2 group. One hour after pretreatment, the animals were divided further into two subgroups ($n = 13$–15 per subgroup), half of the rats receiving a subcutaneous (s.c.) injection of 50 µl physiological saline without formalin (control, KA-1 and KA-2), while the other half of the rats were injected s.c. with 50 µl 1.5 % formalin solution containing 0.55 % formaldehyde (control–formalin, KA-1–formalin and KA-2–formalin), administered via a 26-gauge needle into the right whisker pad.

The testing procedures were performed during the light phase (between 8 a.m. and 2 p.m.) in a quiet room. The test box was a 30 × 30 × 30 cm glass terrarium with mirrored walls. For the offline analysis of rubbing activity directed to the whisker pad, the behavior of the individually tested rats was recorded with a video camera (Logitech HD Webcam C615) situated 1 m above the terrarium. One hour after pretreatment and following a 10-min habituation period in the test box, the whisker pads of the rats were injected s.c. with physiological saline or formalin and the animals were immediately replaced in the chamber for 45-min. The rats did not receive any food or water during the observation period. The test box was cleaned and decontaminated after each animal. An observer blind to the experimental procedures analyzed the recorded videos. The 45-min recording period was divided into 15 × 3-min blocks, and we distinguished two phases following formalin injection [Phase 1 (time block 1, i.e., 0–3 min) and Phase 2 (time blocks 5–15, i.e., 12–45 min)] according to the previously published methods (Clavelou et al. 1995; Raboisson and Dallel 2004), and the total time (number of seconds) spent in rubbing/scraping the injected area with the ipsilateral fore- or hindpaw was measured in each block and defined as the nociceptive score for that block. Earlier literature findings led us to use the grooming activity of animals in the control subgroup as control (Clavelou et al. 1995).

Immunohistochemistry

Four hours after the formalin injection, the rats were perfused transcardially with 100 ml PBS, followed by 500 ml 4 % paraformaldehyde in phosphate buffer under deep chloral hydrate (0.4 g/kg body weight) anesthesia. The medullary segment containing the spinal trigeminal nucleus pars caudalis (TNC) between +1 and −5 mm from the obex was removed, postfixed overnight for immunohistochemistry in the same fixative and cryoprotected (10 % sucrose for 2 h, 20 % sucrose until the blocks sank, and 30 % sucrose overnight). Before sectioning, each segment was marked with a small incision on the ventral and left (contralateral) side of the tissue block, allowing side discrimination during the quantification process. 30-µm transverse cryostat sections were cut through the rostrocaudal axis from the beginning of the TNC and were serially collected in wells containing cold PBS. Each well contained every tenth section at 0.3-mm intervals along the rostrocaudal axis (15 levels = sections). The free-floating sections were rinsed in PBS and immersed in 0.3 % H_2O_2 in PBS for 30 min to suppress endogenous peroxidase activity. After several rinses in PBS containing 1 % Triton X-100 (PBST), sections were incubated at room temperature overnight in PBST containing rabbit anti-rat c-Fos polyclonal antibody (Santa Cruz Biotechnology, sc-52) at a dilution of 1:2000. The immunohistochemical reaction was visualized using Vectastain Elite avidin–biotin kits (Vector Laboratories, PK6101). Briefly, the sections were incubated at room temperature for 2 h in PBST containing goat anti-rabbit biotinylated secondary antibody. After several rinses in PBST, and incubation at room temperature for 2 h in PBST containing avidin and biotinylated horseradish peroxidase, the sections were stained with 3,3′-

diaminobenzidine intensified with nickel ammonium sulfate. The specificity of the immune reactions was checked by omitting the primary antiserum.

The immunoreactive (IR) cells in the superficial layer of the TNC were counted by an observer blind to the experimental procedures under the 10× objective of a Nikon Optiphot-2 (Nikon Instruments, Melville, NY, USA) light microscope in every tenth transverse section in each animal. Before the counting, the location of each section along the rostrocaudal axis and the location of the TNC on each medullary section were determined by means of The Rat Brain in Stereotaxic Coordinates Atlas (Paxinos and Watson 2007). The c-Fos neurons with obvious specific nuclear staining were taken into consideration and were counted in the TNC both ipsilaterally and contralaterally to the formalin injection.

HPLC measurements

Sample preparation

At set time points (15, 30, 60, 120 and 300 min) following the i.p. injection with the KYNA amides (1 mmol/kg), the rats were deeply anesthetized with i.p. injection of chloral hydrate (0.4 g/kg, Sigma-Aldrich). Blood samples were collected from vena cava caudalis and centrifuged at 13709 RCF (relative centrifugal force) for 10 min at 4 °C. The supernatants, i.e., the serum samples, were collected and centrifuged at 13709 RCF for 10 min at 4 °C again and the supernatants were stored at −80 °C until use. After the collection of blood samples, the animals were transcardially perfused with 100 ml 0.1 M PBS for 5 min. The CNS samples containing the medullary segment of the TNC were then removed and stored at −80 °C until measurements. The animals in the Control group underwent a similar procedure with one measurement point at 300 min.

For the measurement of KYNA concentration, the CNS samples were cut in half, weighed and then sonicated for 1.5 min in an ice-cooled solution (250 µl) comprising PCA (2.5 % w/w), 3-NLT (10 or 2 µM) and distilled water in an Eppendorf tube. The content of the Eppendorf tube was centrifuged at 13709 RCF for 10 min at 4 °C and the supernatant was measured. Before analysis, the serum samples were thawed and, after a brief vortex, the serum sample was 'shot' onto a precipitation solvent (containing PCA with 3-NLT as internal standard, with resulting concentrations of 2.5 w/w% and 2 µM, respectively). The samples were subsequently centrifuged at 13709 RCF for 10 min at 4 °C, and the supernatants were collected for measurement.

For the analysis of KYNA amides, the other half of the CNS samples were weighed and then sonicated in ice-cold (250 µl) distilled water for 1.5 min and centrifuged at 13709 RCF for 10 min at 4 °C. From the supernatant, 100 µl was transferred to an Eppendorf tube containing 750 µl HPLC gradient grade acetonitrile and 150 µl distilled water. After a brief vortex, the samples were centrifuged at 13709 RCF for 10 min at 4 °C and 900 µl of supernatant was evaporated in a vacuum centrifuge. After thawing and brief stirring with a vortex, 200 µl of serum sample was transferred to an Eppendorf tube containing 700 µl HPLC gradient grade acetonitrile and 100 µl distilled water. After a brief vortex, the samples were centrifuged at 13709 RCF for 10 min at 4 °C and 900 µl of supernatant was evaporated in a vacuum centrifuge. The evaporated CNS and serum samples were stored at 4 °C until use.

Chromatographic conditions

The KYNA concentrations of the CNS samples were quantified on the basis of a slight modification of a literature method (Hervé et al. 1996) as described in detail with method validation in our previous article (Fejes-Szabó et al. 2014). For the measurement of concentration of the above-mentioned metabolite from serum samples we applied the same method with a slight modification. Furthermore, we applied the method validation procedures to the serum samples too. Briefly, we used an Agilent 1100 HPLC system (Agilent Technologies, Santa Clara, CA, USA) equipped with fluorescence and a UV detector; the former was applied for the determination of KYNA and the latter for the determination of the internal standard (3-NLT). Chromatographic separations were performed on an Onyx Monolithic C18 column, 100 mm × 4.6 mm I.D. (Phenomenex Inc., Torrance, CA, USA) after passage through a SecurityGuard pre-column C18, 4 × 3.0 mm I.D., 5 µm particle size (Phenomenex Inc., Torrance, CA, USA) with a mobile phase composition of 0.2 M zinc acetate/ACN = 95/5 (v/v), the pH of which was adjusted to 6.2 with acetic acid, applying isocratic elution. The flow rate was 1.5 ml/min and the injection volume was 20 µl for serum, and 50 µl for CNS samples. The fluorescence detector was set at excitation and emission wavelengths of 344 and 398 nm. The UV detector was set at a wavelength of 365 nm.

For the determination of KYNA amides, a Thermo LCQFleet ion trap mass spectrometer was used equipped with an ESI ion source combined with a Dionex Ultimate 3000 HPLC system. The ionization parameters were as follows: heater temperature: 500 °C, sheath gas flow rate: 60, auxiliary gas flow rate: 20, spray voltage: 4 kV, capillary temperature: 400 °C. Chromatographic separations were performed on a Kinetex C18 column, 100 mm × 4.6 mm, 2.6 µm particle size (Phenomenex Inc., Torrance, CA, USA) after passage through a SecurityGuard pre-

column C18, 4 × 3.0 mm, 5 µm particle size (Phenomenex Inc., Torrance, CA, USA), with a mobile phase composition of 0.05 % aqueous CH_3COOH/ACN = 90/10 (v/v), applying isocratic elution. The flow rate and the injection volume were 1 ml/min and 50 µl, respectively.

Calibration curve and linearity

Calibrants were prepared at six different concentration levels, from 1 to 100 nM, 0.5 to 5 µM and 0.01 to 100 µM for KYNA, 3-NLT and the KYNA amides, respectively. Three parallel injections of each solution were made under the chromatographic conditions described above. The peak area responses were plotted against the corresponding concentration, and the linear regression computations were carried out by the least square method with the freely available R software (R Development Core Team 2002). Very good linearity was observed throughout the investigated concentration ranges for KYNA, 3-NLT and the KYNA amides when either fluorescence, UV or MS detection was applied.

Selectivity

The selectivity of the method was checked by comparing the chromatograms of KYNA, KYNA amides and the internal standard for a blank serum and CNS sample and those for a spiked sample. All compounds could be detected in their own selected chromatograms without any significant interference.

LOD and LLOQ

The limit of detection (LOD) and the lower limit of quantification (LLOQ) were determined via the signal-to-noise ratio with a threshold of 3 and 10, respectively, according to the ICH guidelines (ICH 1995). The LOD and LLOQ for KYNA in the serum samples were 1 and

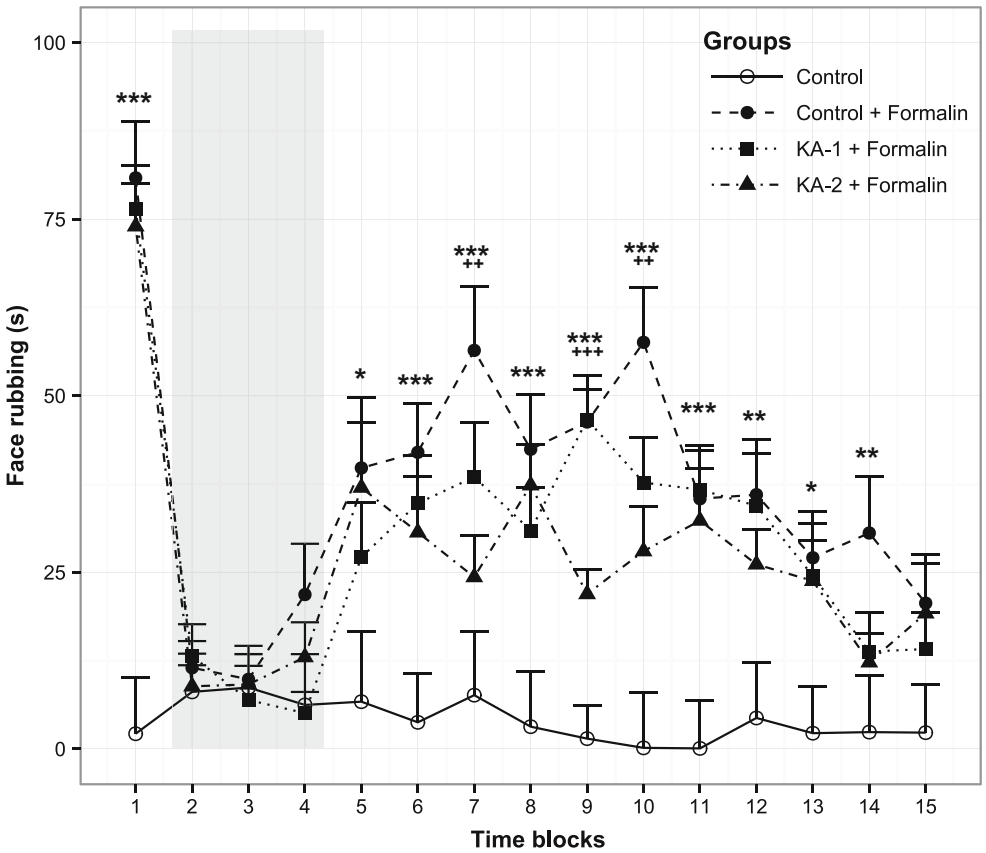

Fig. 2 The effects of formalin and KYNA amide treatments on Sprague–Dawley male rats in the orofacial formalin tests. Following formalin injection, the recording period was 45-min and this time period was divided into 15 × 3-min time blocks. Phase 1 (time block 1) of the test is before the grayed out area, while Phase 2 (time blocks 5–15) is after the grayed out area. The two phases of formalin action in the control + formalin group are well demonstrated when compared to the control group (*$p < 0.05$; **$p < 0.01$; ***$p < 0.001$). The KA-2 pretreatment significantly reduced the formalin-induced nociceptive behavior relative to the control + formalin group ($^{++}p < 0.01$; $^{+++}p < 0.001$). Sprague–Dawley male rats: $n = 13$–15 in each group; data are shown as mean ± SEM; *KA-1 N*-(2-*N*,*N*-dimethylaminoethyl)-4-oxo-1H-quinoline-2-carboxamide hydrochloride; *KA-2 N*-(2-*N*-pyrrolidinylethyl)-4-oxo-1H-quinoline-2-carboxamide hydrochloride

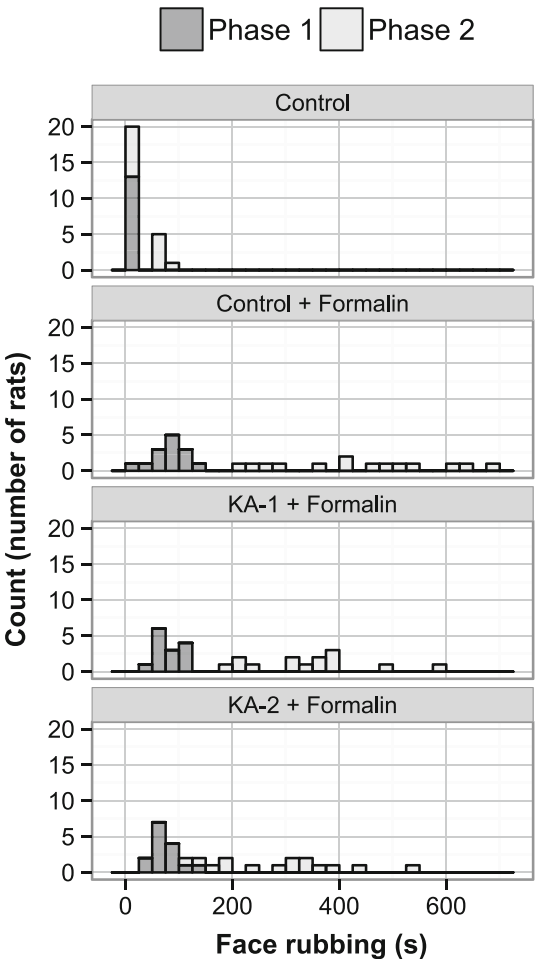

Fig. 3 Distribution of rubbing activity by groups in Phase 1 and 2 of the orofacial formalin test. The recording period was 45-min, Phase 1 is the first 3-min, while Phase 2 is the overall rubbing activity from min 12 to the end of the examination. Sprague–Dawley male rats: $n = 13$–15 in each group; *KA-1* *N*-(2-*N*,*N*-dimethylaminoethyl)-4-oxo-1H-quinoline-2-carboxamide hydrochloride; *KA-2* *N*-(2-*N*-pyrrolidinylethyl)-4-oxo-1H-quinoline-2-carboxamide hydrochloride

3.75 nM, respectively, while in the CNS samples they were 0.4 and 1 nM, respectively. The LOD and LLOQ for the samples in MS detection were 0.001 and 0.015 μM, respectively.

Precision

Replicate HPLC analysis showed that the relative standard deviation was ≤2.2 % for the peak area response and ≤0.1 % for the retention time for KYNA and the KYNA amides.

Recovery

The relative recoveries were estimated by measuring spiked samples of KYNA and the KYNA amides at two concentrations with three replicates of each. No significant differences were observed for the lower and higher concentrations. The recoveries for the serum samples ranged from 103 to 108 %, 81 to 94 % and 79 to 80 % for KYNA, KA-1 and KA-2, respectively. The recoveries for the CNS samples ranged from 82 to 92 % and 78 to 84 % for KYNA and KA-2, respectively.

Data evaluation

To compare the means of jaw rubbing counts (orofacial formalin tests) in the different treatment groups (control, control–formalin, KA-1, KA-1–formalin, KA-2, KA-2–formalin) on rats during 15 3-min time periods ($n = 13$–15 animals in each group), two-way repeated measures ANOVA were run. Treatment with six groups was used as between-subject factor and time with 15 time points as within-subject factor for the analysis.

When Levene's test for homogeneity of variance was significant in the Phase data (Phase 1 is the first 3 min, while Phase 2 is the overall rubbing from min 12 to the end of the examination, min 45, i.e., which is from the fifth 3-min time period to the 15th), the Welch test was run to compare mean rubbing counts. Pairwise comparisons were estimated by the Sidak test. The effect size (EF, f) was calculated according to Cohen J. (Cohen 1988) with regard to the ANOVA tests comparing the effects of compounds on behavioral data in Phase 1 and 2.

In the case of the immunohistochemistry data, the numbers of c-Fos-containing nuclei were assessed. Three-way repeated measures ANOVA was used to analyze group means across 15 adjacent measuring sites (consequent slices from the medullary segment of the CNS containing the TNC) among sides (contralateral and ipsilateral) and between pretreatment groups (control, KA-1 and KA-2) all with formalin injections. Measuring sites and sides were used as within-subject factor, while pretreatment was the between-subject factor in the general linear model.

In the ANOVA models when Mauchly's test of sphericity was significant, the Greenhouse–Geisser correction was performed. In the event of the significant interaction of factors, effects could not be reported independently. Moreover, owing to the significant interaction, group differences could be examined separately over the within-subject factor based on estimated marginal means for multiple comparisons with the Sidak adjustment.

Statistical analyses were carried out with IBM SPSS Statistics, version 21 (IBM Corporation, Armonk, NY, USA) software. All tests were two-sided, and $p < 0.05$ was considered to be statistically significant. The pharmacokinetic data were evaluated with PKSolver, a freely available menu-driven add-in program for Microsoft Excel (Zhang et al. 2010).

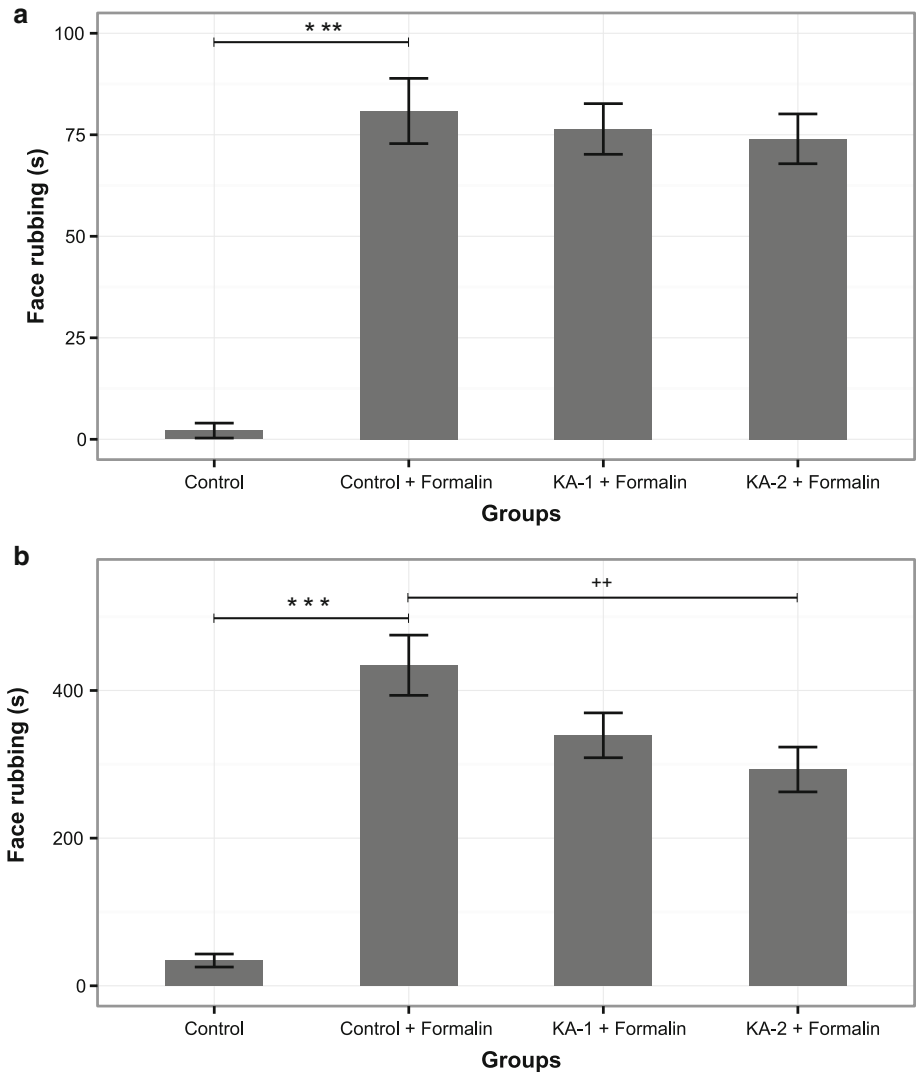

Fig. 4 Diagrams showing the rubbing activity in the first (**a**) and the second (**b**) phase in the orofacial formalin test. In the control + formalin group, the subcutaneous formalin injection induced a significant increase in rubbing activity in both Phase 1 and 2 (***$p < 0.001$) as compared to the control group. In Phase 2, pretreatment with KA-2 had a significant effect on mitigating the formalin-induced increase in the time spent with rubbing ($^{++}p < 0.01$) as compared with the control + formalin group. Sprague–Dawley male rats: $n = 13$–15 in each group; data are presented as mean ± SEM; *KA-1* *N*-(2-*N*,*N*-dimethylaminoethyl)-4-oxo-1H-quinoline-2-carboxamide hydrochloride; *KA-2* *N*-(2-*N*-pyrrolidinylethyl)-4-oxo-1H-quinoline-2-carboxamide hydrochloride

Results

Behavioral assessment

The results of orofacial formalin testing are demonstrated in Figs. 2, 3 and 4. To simplify the presentation of group comparisons for better transparency, the groups of KA-1 and KA-2 were omitted from Figs. 2, 3 and 4. Pairwise comparisons revealed that face rubbing activity in the control, KA-1 and in the KA-2-treated groups was significantly lower in both Phase 1 and Phase 2 compared with the control–formalin (ES of Phase 1, −1.88 and Phase 2, −2.17), KA-1–formalin (ES of Phase 1, −1.75 and Phase 2, −1.56) and KA-2–formalin (ES of Phase 1, −1.64 and Phase 2, −1.26) groups. With regard to the comparison of the face rubbing activity in the KA-1–formalin (ES of Phase 1, 0.11 and Phase 2, 0.51) and KA-2–formalin (ES of Phase 1: 0.16 and Phase 2: 0.76) groups with that in the control–formalin group, although KA-1 decreased face rubbing activity as well (demonstrated by the corresponding left-skewed histogram in Fig. 3), only KA-2 treatment resulted in a significant reduction in the middle of Phase 2 (Figs. 2, 4).

Immunohistochemistry

The results of immunohistochemical analysis are demonstrated in Figs. 5 and 6. The comparison of the ipsilateral and the contralateral sides of the slices from the medullary segment of the rat CNS containing the TNC demonstrated that the mean number of c-Fos IR neurons was significantly higher on the ipsilateral side than on the contralateral side in the control–formalin, KA-1–formalin and KA-2–formalin groups (the two latter groups are not demonstrated to simplify the presentation of group comparisons for better transparency in Fig. 6). With regard to the comparison of the ipsilateral sides of the KA-1–formalin and KA-2–formalin groups with the control–formalin group from the

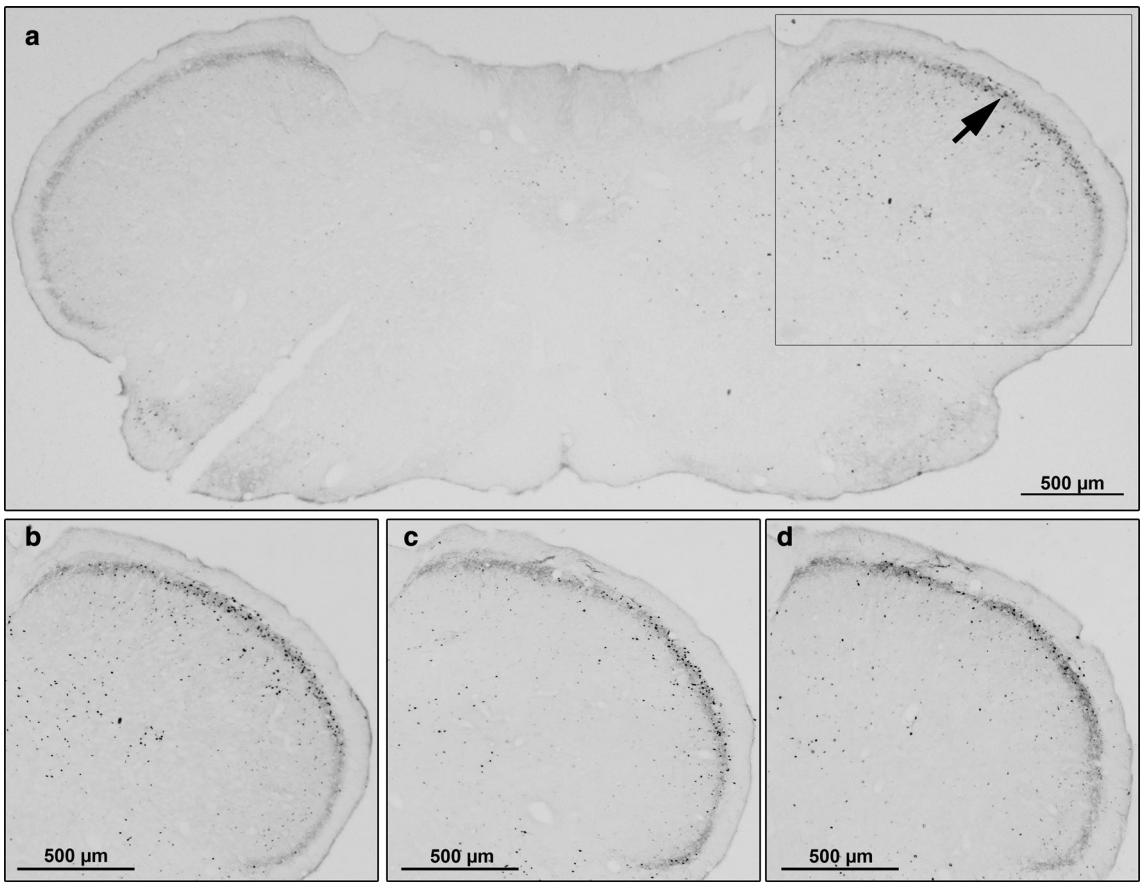

Fig. 5 Representative histological images following c-Fos immunostaining in Sprague–Dawley male rats. Subcutaneous formalin injection induced an increase in the number of c-Fos IR neurons on the ipsilateral side demonstrated on the transverse section of medulla containing the TNC from the control + formalin subgroup (**a**, **b**; contralateral side is indicated with an incision on the ventral side of the section). The pretreatments (KA-1: **c**; KA-2: **d**), reduced the amount of IR cells in the superficial layers of TNC as compared with control + formalin group (**b**). *Black arrow* c-Fos IR neurons in the superficial laminae; *black frame* magnified area, which can be seen in images **b**–**d**; *TNC* trigeminal nucleus pars caudalis, *IR* immunoreactive, *KA-1 N*-(2-*N*,*N*-dimethylaminoethyl)-4-oxo-1H-quinoline-2-carboxamide hydrochloride, *KA-2 N*-(2-*N*-pyrrolidinylethyl)-4-oxo-1H-quinoline-2-carboxamide hydrochloride

aspect of the mean number of c-Fos IR neurons, the treatments, preferentially with KA-2, resulted in significant reductions in IR cell count at certain levels of the assessed region (the c-Fos changes followed the somatotopic representation of the trigeminal nociceptors in the injected whisker pad area; Strassman and Vos 1993). Besides the observed significant differences, the effects of the treatment are well demonstrated by the curves in Fig. 6.

HPLC measurements and pharmacokinetics

The concentrations of KYNA and KYNA amides measured in rat serum and CNS samples by HPLC are demonstrated in Table 1. The time-course profile of the KYNA amides in the rat serum revealed that after a steep increase in the concentration, a subsequent steep decrease occurred in the first hour, followed by a prolonged further gradual decrease (Fig. 7). Although the serum concentration of KA-2 did not show such a high level as that of KA-1, a slightly slower decrease in concentration was observed. These observations are consistent with the calculated serum pharmacokinetic parameters (C_{max}, T_{max}, area under the curve (AUC_{0-t}), the half-life ($t_{1/2}$), apparent total clearance (CL/F_{obs}) and apparent volume of distribution (Vz/F_{obs})) of KA-1 and KA-2, demonstrated in Table 2. However, the increase in serum KYNA concentration following the i.p. injection of KA-2 was considerably higher (an approximately 200-fold maximal increase) as compared with that of KA-1 (an approximately 70-fold maximal increase), also well reflected by the above-mentioned pharmacokinetic parameters. To avoid the influence of the basal serum KYNA level on the calculated pharmacokinetic parameters, these basal concentrations were subtracted from the corresponding subsequent concentrations in the calculation of the pharmacokinetic parameters. The pharmacokinetic data therefore reflect only the KYNA amide-induced changes in KYNA concentrations. In the fifth hour, KA-1 and KA-2 were still present at 3.1 (0–61.5) µM and 0.5 (0.5–0.5) µM in the serum,

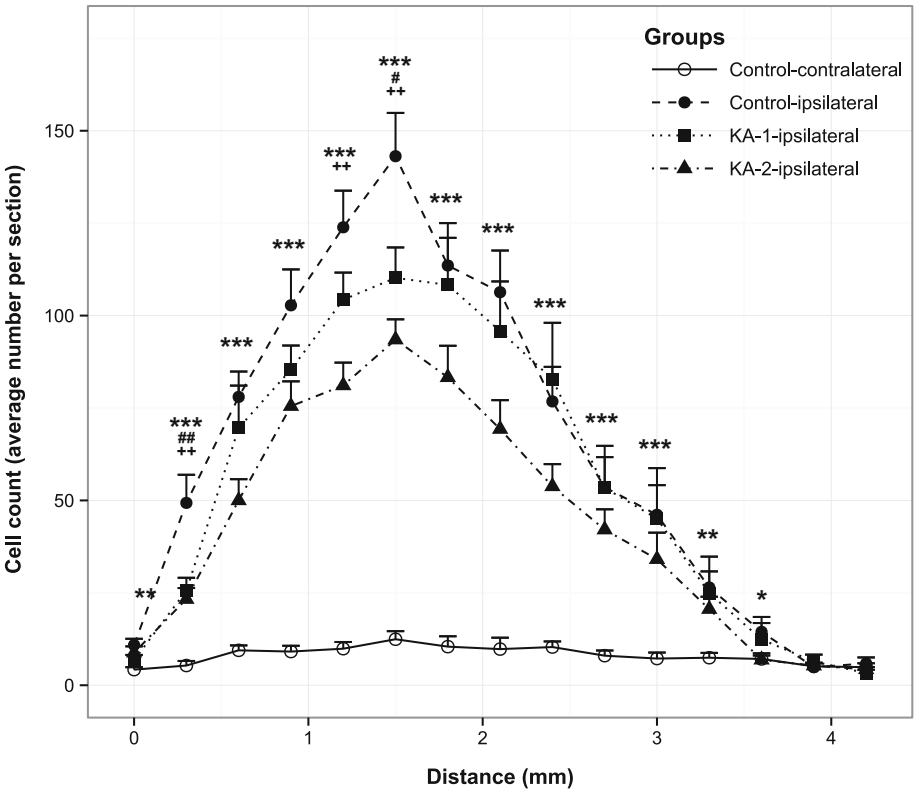

Fig. 6 The average number of c-Fos immunoreactive cells per section of TNC in Sprague–Dawley male rats after formalin injection with KYNA amide pretreatments. The distance was calculated caudally from the starting point of TNC. Subcutaneous formalin injection resulted in a higher number of c-Fos-IR neurones on the ipsilateral side compared with the contralateral side in the control + formalin group (*$p < 0.05$; **$p < 0.01$; ***$p < 0.001$). The pretreatments (KA-1: $^{\#}p < 0.05$, $^{\#\#}p < 0.01$; KA-2: $^{++}p < 0.01$), reduced the amount of IR cells in the superficial layers of TNC as compared with the ipsilateral side in the control + formalin group. Sprague–Dawley male rats: $n = 9$–10 in each group; data are shown as mean ± SEM; *IR* immunoreactive, *TNC* trigeminal nucleus pars caudalis, *KA-1* *N*-(2-*N*,*N*-dimethylaminoethyl)-4-oxo-1H-quinoline-2-carboxamide hydrochloride, *KA-2* *N*-(2-*N*-pyrrolidinylethyl)-4-oxo-1H-quinoline-2-carboxamide hydrochloride

respectively, while the KYNA levels had approximately returned to the baseline level, preferentially in the case of KA-1 treatment. In the rat CNS samples, the KA-1 concentration was under LOD. However, KA-2 was present in detectable amounts in the CNS, reaching its maximum concentration (6.44 (5.62–7.85) pmol/g ww) after an hour which subsequently gradually decreased, but in the fifth hour it was still present at 1.98 (1.50–2.90) pmol/g ww. The CNS pharmacokinetics of KYNA following KA-1 and KA-2 administration showed quite similar profiles, characterized by an approximately maximal tenfold increase in basal concentration within the first hour. Vz/F_{obs} was relatively high in KA-1 and especially in KA-2. The apparent clearance was also high in the case of KA-2 relative to KA-1.

Discussion

Headache, one of the most common disorders of the nervous system, is a major health problem worldwide. The global prevalence for the adult population of active headache disorder is 46 % for headache in general, 11 % for migraine, 42 % for tension-type headache and 3 % for chronic daily headache (Stovner et al. 2007). The treatment of primary headache disorders is challenging requiring both acute and preventive therapeutic strategies (Weatherall 2015). The efficacy of these treatments is not always satisfactory and the contraindications and side effects often limit the options of the physician (Diener et al. 2015; Obermann et al. 2015). There is therefore a constant need to study and develop new molecules. In addition to the currently available drugs, e.g., NSAIDs, triptans, anticonvulsants, verapamil, propranolol, etc. (National Institute for Health and Care Excellence 2012), the pipeline of pharmaceutical research in this field involves the development of novel agents acting on the glutamatergic system due to its essential role in the nociceptive process (Dickenson et al. 1997; Diener et al. 2015). Animal and human studies have revealed that glutamate receptors are present in various parts of the trigeminal system (Quartu et al. 2002; Sahara et al. 1997; Tallaksen-Greene et al. 1992), and stimulation of the trigeminal nerve results in elevated

Table 1 The concentration of KYNA and KYNA amides in Sprague–Dawley male rat serum and CNS samples

Serum					CNS			
Time (min)	KA-1 treatment		KA-2 treatment		KA-1 treatment		KA-2 treatment	
	KA-1 (μM)	KYNA (nM)	KA-2 (μM)	KYNA (nM)	KA-1 (pmol/g ww)	KYNA (pmol/g ww)	KA-2 (pmol/g ww)	KYNA (pmol/g ww)
0 (control)	0	75.7 (72.8–90.4)	0	75.7 (72.8–90.4)	0	5.33 (1.00–13.17)	0	5.33 (1.00–13.17)
15	87.4 (0–191.2)	5517.9 (3287.2–6290.1)	2.6 (2.2–20.9)	287.9 (239.1–6753.5)	<LOD	58.98 (53.37–277.22)	<LOD	17.41 (15.02–19.31)
30	35.6 (0–140.4)	1159.3 (523.8–2397.9)	20.9 (17.4–22.6)	16,709.5 (13,796.6–17,519)	<LOD	44.69 (29.43–104.13)	4.45 (3.88–4.67)	34.77 (25.01–50.53)
60	39.6 (0–114.4)	464.1 (304.9–1342.3)	13.7 (13.7–14)	3375.8 (3332.7–4604.1)	<LOD	58.61 (25.97–103.53)	6.44 (5.62–7.85)	65.70 (41.54–110.68)
120	19.5 (0–87.2)	561 (353.2–570.4)	3.2 (3–4.7)	334.6 (232.4–422.2)	<LOD	12.00 (11.07–15.68)	3.28 (2.75–3.31)	15.30 (10.81–18.47)
300	3.1 (0–61.5)	103.6 (99.1–128.2)	0.5 (0.5–0.5)	49.3 (110.3–150.1)	<LOD	13.73 (13.16–19.79)	1.98 (1.50–2.90)	22.43 (19.63–24.62)

The concentrations were measured with HPLC after pretreatment with KA-1 and KA-2. Sprague–Dawley male rats: $n = 5$ in each group; data are shown as median (interquartile range)

KYNA kynurenic acid, *KA-1 N*-(2-*N*,*N*-dimethylaminoethyl)-4-oxo-1H-quinoline-2-carboxamide hydrochloride, *KA-2 N*-(2-*N*-pyrrolidinylethyl)-4-oxo-1H-quinoline-2-carboxamide hydrochloride, *LOD* limit of detection

glutamate levels in the TNC (Oshinsky and Luo 2006). The peripheral application of glutamate to deep craniofacial tissue proved to be able to activate and sensitize nociceptive afferents and neurons in the upper cervical cord (Lam et al. 2009a, b). These findings suggest that excitatory amino acid receptors (and NMDA in particular) play an important role in pain processing and the sensitization process which is also present in migraineurs (Vikelis and Mitsikostas 2007). Ketamine, an NMDA antagonist, is so far the only promising treatment option for patients with severe or long-lasting migraine aura (Afridi et al. 2013). Another novel substance, tezampanel, which acts on the AMPA and kainate subtypes of ionotropic glutamate receptors (Alt et al. 2006), has also shown promising results in acute migraine therapy (Sang et al. 2004).

As regards the preclinical models of headache disorders, NTG is the most frequently used substance to trigger a delayed migraine-like attack (Sicuteri et al. 1987). Animal experiments have revealed that NTG can activate the trigeminal system and stimulate the second-order trigeminal neurons, which lead to increased c-Fos and neuronal nitric oxide synthase (nNOS) expression in the affected area (Párdutz et al. 2000; Tassorelli et al. 1997). NTG is also able to sensitize the trigeminal system in humans (Di Clemente et al. 2009). Together, these results confirm that NTG administration can model the central trigeminal nociceptor sensitization demonstrated in migraine patients (Burstein et al. 2000). With regard to the above-mentioned therapeutic strategy with the aim of neurotransmission modulation via the glutamatergic system, earlier studies revealed that KA-1 is able to attenuate the effects of NTG on the number of nNOS, calcium/calmodulin-dependent protein kinase II type alpha (CamKIIα) and calcitonin gene related peptide (CGRP) IR cells in the TNC, markers related to the activation and sensitization of the nociceptors (Vámos et al. 2010, 2009). KA-2 was later also tested in the NTG model and proved to be able to increase the KYNA concentration both in the C1–C2 region and in the serum. Pretreatment with KA-2 (0.5 and 1 mmol/kg) significantly reduced the effects of NTG on the CGRP-, c-Fos-, nNOS- and CaMKIIα-related changes in the C1–C2 region (Fejes-Szabó et al. 2014). To date, there has been only one study of the pharmacokinetic properties of KYNA amides, which found that only a small proportion of KA-1 decays into KYNA in the serum of C57B/6 mice (Zádori et al. 2011a).

In this study, we used another well-known model of trigeminal nociception, the orofacial formalin test. Formalin solution administered s.c. into the upper lip of rats causes tissue injury, inflammation and nociception (Clavelou et al. 1995). Immunohistochemical studies have revealed that formalin induces c-Fos and nNOS expression in the TNC, similarly as in the NTG model, which suggests

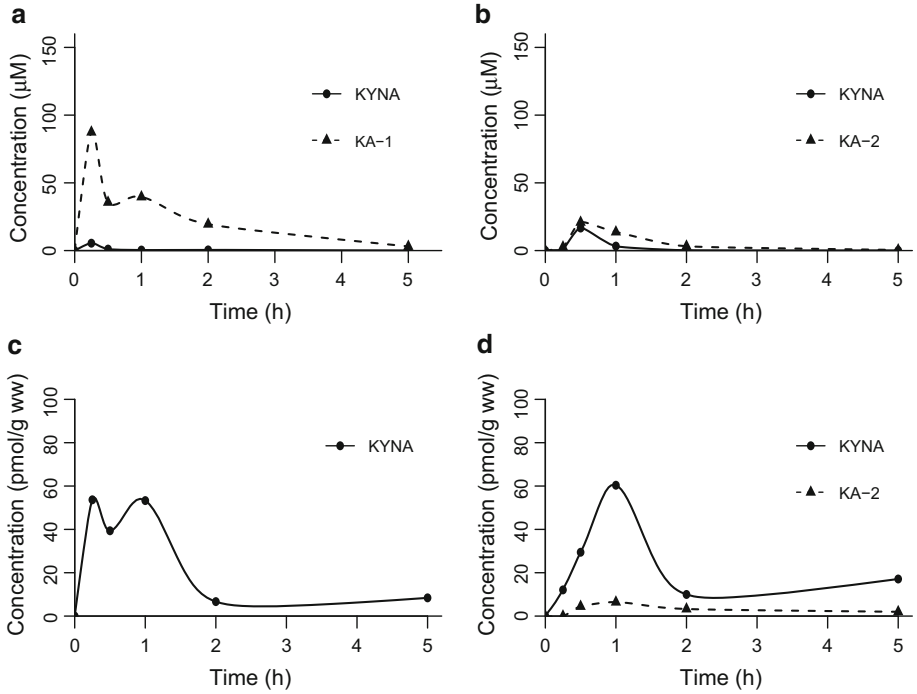

Fig. 7 The concentrations of KYNA and KYNA amides in serum and CNS samples of Sprague–Dawley male rats. **a**, **b** Concentrations of KYNA and KYNA amides in rat serum with the course of time after injection. **c**, **d** Concentrations of KYNA and KYNA amides in the CNS samples of the same animals. KA-1 concentrations were under the limit of detection in the CNS samples. Sprague–Dawley male rats: $n = 5$ in each group; data are shown as medians; *KYNA* kynurenic acid, *KA-1 N*-(2-*N*,*N*-dimethylaminoethyl)-4-oxo-1H-quinoline-2-carboxamide hydrochloride, *KA-2 N*-(2-*N*-pyrrolidinylethyl)-4-oxo-1H-quinoline-2-carboxamide hydrochloride

Table 2 Pharmacokinetic parameters of KYNA and KYNA amides in rat serum and CNS samples after intraperitoneal injection of KA-1 and KA-2

Serum					CNS				
Pharmacokinetic parameters	KA-1 treatment		KA-2 treatment		Pharmacokinetic parameters	KA-1 treatment		KA-2 treatment	
	KA-1	KYNA	KA-2	KYNA		KA-1	KYNA	KA-2	KYNA
$t_{1/2}$ (h)	1.09	0.91	0.84	0.64	$t_{1/2}$ (h)	NA	1.67	2.61	3.45
t_{max} (h)	0.25	0.25	0.50	0.50	t_{max} (h)	NA	0.25	1	1
C_{max} (μM)	87.44	5.44	20.87	16.63	C_{max} (pmol/g)	NA	53.66	6.44	60.37
AUC_{0-t} (μM h)	99.22	2.61	23.35	7.89	AUC_{0-t} (pmol/g h)	NA	86.46	16.24	97.77
Vz/F_{obs} ((μmol/kg)/(μmol/l))	15.17	–	50.02	–	Vz/F_{obs} ((pmol/kg)/(pmol/l))	NA	–	158,879.15	–
Cl/F_{obs} ((μmol/kg)/(μmol/l)/h)	9.61	–	41.81	–	Cl/F_{obs} ((pmol/kg)/(pmol/l)/h)	NA	–	42,220.03	–

The KYNA amides were applied in a dose of 1 mmol/kg. Sprague–Dawley male rats: $n = 5$ in each group

KYNA kynurenic acid, *KA-1 N*-(2-*N*,*N*-dimethylaminoethyl)-4-oxo-1H-quinoline-2-carboxamide hydrochloride, *KA-2 N*-(2-*N*-pyrrolidinylethyl)-4-oxo-1H-quinoline-2-carboxamide hydrochloride

the activation and sensitization of the area (Hunt et al. 1987; Párdutz et al. 2000). The behavioral effect of formalin is biphasic, with a short period of rubbing activity immediately after injection and then a tonic prolonged (20–22 min) second phase after a quiescent period (Raboisson and Dallel 2004). Using the formalin model, our aim was to compare the two compounds (KA-1 and KA-2) in an assessment method which involves both peripheral and central components of pain processing, with special interest in the pharmacokinetic explanation of the observed differences.

Our results indicated that KA-2 has more significant beneficial effects on the formalin-induced behavioral and immunohistochemical alterations. We carried out a comparative pharmacokinetic study to clarify this difference between the two analogs. With regard to the serum concentrations of the analogs following their i.p. administration, the levels of KA-2 were considerably lower than those of KA-1 from the aspects of peak concentration and AUC_{0-5h}. In contrast, KA-1 could not be detected in the examined CNS region, and the concentration of KA-2 was likewise relatively low. On the other hand, the serum pharmacokinetic data revealed that KA-2 decays into KYNA in larger amount as compared with KA-1, but nevertheless, in the examined CNS region, there is no major difference between KYNA levels following the treatments with KA-1 or KA-2. Summarizing these findings, the peak elevation of KYNA in the CNS

(approximately tenfold of the basal concentration) is considerably lower (by one order of magnitude) than that of peak elevation of KYNA in the serum (approximately 70–200-fold of the basal concentration) following the administration of KA-1 and KA-2, and with respect to CNS samples, there are no differences between KYNA levels. In view of these findings, the difference in the observed effects in behavioral and immunohistochemical studies could be explained by the differences in serum KYNA levels. From the aspect of a structure–activity relationship, the difference in peripheral conversion may stem from the structures of the two analogs, e.g., in the case of KA-2 the strained pyrrolidine moiety may influence the faster hydrolysis of the amide bond relative to the N,N-dimethyl function (KA-1). These findings suggest that the difference in the beneficial effects of the two analogs may be explained by the peripheral effect of elevated KYNA concentrations on formalin-induced pathological alterations. The molecular background would be the inhibition of NMDA receptor-mediated neurotransmission at the strychnine-insensitive glycine-binding site (Szalárdy et al. 2012) which is present on the peripheral process of the trigeminal nociceptors (Quartu et al. 2002; Watanabe et al. 1994). The observed peak serum KYNA concentration following KA-2 treatment during the experiment (16.71 μM) would be relevant with regard to the inhibition of glutamatergic neurotransmission via the above-mentioned possibility (Szalárdy et al. 2012).

In conclusion, our results draw attention to the role of influencing the glutamatergic system in the alleviation of peripheral sensitization, which can be utilized during future drug development. The possibility of targeting the peripheral component of pain processing would provide an option of pharmaceutical drug design without the obligation of good penetration through the BBB, but other pharmacokinetic parameters, such as solubility and clearance, must be kept in mind. The present results and previous preclinical findings indicate that the KYNA amides, via their probable direct effects (KA-1; Zádori et al. 2011a) or serving as prodrugs (KA-2 in the current pharmacokinetic study), would be promising drug candidates in neurological disorders, including those involving pain and headache, with a high socioeconomic burden.

Acknowledgments This research was supported by the Hungarian Brain Research Program—Grant No. KTIA_13_NAP-A_III/9, in the frame of EUROHEADPAIN FP7—Project Number: 602633 and TÁMOP 4.2.4. A/2-11-1-2012-0001. Dr. Árpád Párdutz and Dr. Dénes Zádori were supported by the János Bolyai Research Scholarship of the Hungarian Academy of Sciences.

Compliance with ethical standards

Conflict of interest The authors declare that there is no conflict of interest.

References

Afridi SK, Giffin NJ, Kaube H, Goadsby PJ (2013) A randomized controlled trial of intranasal ketamine in migraine with prolonged aura. Neurology 80:642–647. doi:10.1212/WNL.0b013e3182824e66

Alt A, Weiss B, Ogden AM, Li X, Gleason SD, Calligaro DO, Bleakman D, Witkin JM (2006) In vitro and in vivo studies in rats with LY293558 suggest AMPA/kainate receptor blockade as a novel potential mechanism for the therapeutic treatment of anxiety disorders. Psychopharmacology 185:240–247. doi:10.1007/s00213-005-0292-0

Bahn A, Ljubojevic M, Lorenz H, Schultz C, Ghebremedhin E, Ugele B, Sabolic I, Burckhardt G, Hagos Y (2005) Murine renal organic anion transporters mOAT1 and mOAT3 facilitate the transport of neuroactive tryptophan metabolites. Am J Physiol Cell Physiol 289:C1075–C1084. doi:10.1152/ajpcell.00619.2004

Burstein R, Cutrer MF, Yarnitsky D (2000) The development of cutaneous allodynia during a migraine attack clinical evidence for the sequential recruitment of spinal and supraspinal nociceptive neurons in migraine. Brain 123:1703–1709

Carpenter M, Sutin J (1983) Human neuroanatomy, 8th edn. Williams & Wilkins, Baltimore

Clavelou P, Dallel R, Orliaguet T, Woda A, Raboisson P (1995) The orofacial formalin test in rats: effects of different formalin concentrations. Pain 62:295–301

Cohen J (1988) Statistical power analysis for the behavioral sciences, 2nd edn. Lawrence Erlbaum Associates Inc, Hillsdale. ISBN 0-8058-0283-5

Di Clemente L, Coppola G, Magis D, Gérardy P-Y, Fumal A, De Pasqua V, Di Piero V, Schoenen J (2009) Nitroglycerin sensitises in healthy subjects CNS structures involved in migraine pathophysiology: evidence from a study of nociceptive blink reflexes and visual evoked potentials. Pain 144:156–161. doi:10.1016/j.pain.2009.04.018

Dickenson AH, Chapman V, Green GM (1997) The pharmacology of excitatory and inhibitory amino acid-mediated events in the transmission and modulation of pain in the spinal cord. Gen Pharmacol 28:633–638. doi:10.1016/S0306-3623(96)00359-X

Diener H-C, Charles A, Goadsby PJ, Holle D (2015) New therapeutic approaches for the prevention and treatment of migraine. Lancet Neurol 14:1010–1022. doi:10.1016/S1474-4422(15)00198-2

Fejes-Szabó A, Bohár Z, Vámos E, Nagy-Grócz G, Tar L, Veres G, Zádori D, Szentirmai M, Tajti J, Szatmári I, Fülöp F, Toldi J, Párdutz Á, Vécsei L (2014) Pre-treatment with new kynurenic acid amide dose-dependently prevents the nitroglycerine-induced neuronal activation and sensitization in cervical part of trigemino-cervical complex. J Neural Transm 121:725–738. doi:10.1007/s00702-013-1146-2

Fukui S, Schwarcz R, Rapoport SI, Takada Y, Smith QR (1991) Blood brain barrier transport of kynurenines: implications for brain synthesis and metabolism. J Neurochem 56:2007–2017. doi:10.1111/j.1471-4159.1991.tb03460.x

Fülöp F, Szatmári I, Vámos E, Zádori D, Toldi J, Vécsei L (2009) Syntheses, transformations and pharmaceutical applications of kynurenic acid derivatives. Curr Med Chem 16:4828–4842. doi:10.2174/092986709789909602

Gellért L, Fuzik J, Göblös A, Sárközi K, Marosi M, Kis Z, Farkas T, Szatmári I, Fülöp F, Vécsei L, Toldi J (2011) Neuroprotection with a new kynurenic acid analog in the four-vessel occlusion model of ischemia. Eur J Pharmacol 667:182–187. doi:10.1016/j.ejphar.2011.05.069

Gellért L, Varga D, Ruszka M, Toldi J, Farkas T, Szatmári I, Fülöp F, Vécsei L, Kis Z (2012) Behavioural studies with a newly

developed neuroprotective KYNA-amide. J Neural Transm 119:165–172. doi:10.1007/s00702-011-0692-8

Hervé C, Beyne P, Jamault H, Delacoux E (1996) Determination of tryptophan and its kynurenine pathway metabolites in human serum by high-performance liquid chromatography with simultaneous ultraviolet and fluorimetric detection. J Chromatogr B Biomed Appl 675:157–161

Hunt SP, Pini A, Evan G (1987) Induction of c-fos-like protein in spinal cord neurons following sensory stimulation. Nature 328:632–634. doi:10.1038/328632a0

ICH (1995) ICH harmonised tripartite guideline, validation of analytical procedures. Fed Regist 60:11260

Knyihár-Csillik E, Mihaly A, Krisztin-Peva B, Robotka H, Szatmari I, Fulop F, Toldi J, Csillik B, Vécsei L (2008) The kynurenate analog SZR-72 prevents the nitroglycerol-induced increase of c-fos immunoreactivity in the rat caudal trigeminal nucleus: comparative studies of the effects of SZR-72 and kynurenic acid. Neurosci Res 61:429–432. doi:10.1016/j.neures.2008.04.009

Lam DK, Sessle BJ, Hu JW (2009a) Glutamate and capsaicin effects on trigeminal nociception I: activation and peripheral sensitization of deep craniofacial nociceptive afferents. Brain Res 1251:130–139. doi:10.1016/j.brainres.2008.11.029.Glutamate

Lam DK, Sessle BJ, Hu JW (2009b) Glutamate and capsaicin effects on trigeminal nociception II: activation and central sensitization in brainstem neurons with deep craniofacial afferent input. Brain Res 1253:48–59. doi:10.1016/j.brainres.2008.11.056

Marosi M, Nagy D, Farkas T, Kis Z, Rózsa É, Robotka H, Fülöp F, Vécsei L, Toldi J (2010) A novel kynurenic acid analogue: a comparison with kynurenic acid. An in vitro electrophysiological study. J Neural Transm 117:183–188. doi:10.1007/s00702-009-0346-2

Nagy K, Plangár I, Tuka B, Gellért L, Varga D, Demeter I, Farkas T, Kis Z, Marosi M, Zádori D, Klivényi P, Fülöp F, Szatmári I, Vécsei L, Toldi J (2011) Synthesis and biological effects of some kynurenic acid analogs. Bioorg Med Chem 19:7590–7596. doi:10.1016/j.bmc.2011.10.029

Näsström J, Karlsson U, Post C (1992) Antinociceptive actions of different classes of excitatory amino acid receptor antagonists in mice. Eur J Pharmacol 212:21–29

National Institute for Health and Care Excellence (2012) Headaches in over 12 s: diagnosis and management. https://www.nice.org.uk

Obermann M, Holle D, Naegel S, Burmeister J, Diener H-C (2015) Pharmacotherapy options for cluster headache. Expert Opin Pharmacother 16:1177–1184. doi:10.1517/14656566.2015.1040392

Olesen J, Gustavsson A, Svensson M, Wittchen H-U, Jönsson B, on behalf of the CDBE2010 study group, the European Brain Council (2012) The economic cost of brain disorders in Europe. Eur J Neurol 19:155–162. doi:10.1111/j.1468-1331.2011.03590.x

Oshinsky ML, Luo J (2006) Neurochemistry of trigeminal activation in an animal model of migraine. Headache 46(Suppl 1):S39–S44

Párdutz Á, Krizbai I, Multon S, Vécsei L, Schoenen J (2000) Systemic nitroglycerin increases nNOS levels in rat trigeminal nucleus caudalis. Neuroreport 11:3071–3075. doi:10.1097/00001756-200009280-00008

Párdutz Á, Fejes A, Bohár Z, Tar L, Toldi J, Vécsei L (2012) Kynurenines and headache. J Neural Transm 119:285–296. doi:10.1007/s00702-011-0665-y

Paxinos G, Watson C (2007) The rat brain in stereotaxic coordinates, 6th edn. Elsevier, Amsterdam

Pereira EFR, Hilmas C, Santos MD, Alkondon M, Maelicke A, Albuquerque EX (2002) Unconventional ligands and modulators of nicotinic receptors. J Neurobiol 53:479–500. doi:10.1002/neu.10146

Quartu M, Serra MP, Ambu R, Lai ML, Del Fiacco M (2002) AMPA-type glutamate receptor subunits 2/3 in the human trigeminal sensory ganglion and subnucleus caudalis from prenatal ages to adulthood. Mech Ageing Dev 123:463–471

R Development Core Team (2002) The R Project for Statistical Computing. R Foundation for Statistical Computing

Raboisson P, Dallel R (2004) The orofacial formalin test. Neurosci Biobehav Rev 28:219–226. doi:10.1016/j.neubiorev.2003.12.003

Sahara Y, Noro N, Iida Y, Soma K, Nakamura Y (1997) Glutamate receptor subunits GluR5 and KA-2 are coexpressed in rat trigeminal ganglion neurons. J Neurosci 17:6611–6620

Sang CN, Ramadan NM, Wallihan RG, Chappell AS, Freitag FG, Smith TR, Silberstein SD, Johnson KW, Phebus LA, Bleakman D, Ornstein PL, Arnold B, Tepper SJ, Vandenhende F (2004) LY293558, a novel AMPA/GluR5 antagonist, is efficacious and well-tolerated in acute migraine. Cephalalgia 24:596–602. doi:10.1111/j.1468-2982.2004.00723.x

Schwarcz R (2004) The kynurenine pathway of tryptophan degradation as a drug target. Curr Opin Pharmacol 4:12–17. doi:10.1016/j.coph.2003.10.006

Sicuteri F, Bene E, Poggioni M, Bonazzi A (1987) Unmasking latent dysnociception in healthy subjects. Headache J Head Face Pain 27:180–185. doi:10.1111/j.1526-4610.1987.hed2704180.x

Stovner L, Hagen K, Jensen R, Katsarava Z, Lipton R, Scher A, Steiner T, Zwart J-A (2007) The global burden of headache: a documentation of headache prevalence and disability worldwide. Cephalalgia 27:193–210. doi:10.1111/j.1468-2982.2007.01288.x

Strassman AM, Vos BP (1993) Somatotopic and laminar organization of fos-like immunoreactivity in the medullary and upper cervical dorsal horn induced by noxious facial stimulation in the rat. J Comp Neurol 331:495–516. doi:10.1002/cne.903310406

Szalárdy L, Zádori D, Toldi J, Fülop F, Klivényi P, Vécsei L (2012) Manipulating kynurenic acid levels in the brain—on the edge between neuroprotection and cognitive dysfunction. Curr Top Med Chem 12:1797–1806. doi:10.2174/156802612803989264

Tallaksen-Greene SJ, Young AB, Penney JB, Beitz AJ (1992) Excitatory amino acid binding sites in the trigeminal principal sensory and spinal trigeminal nuclei of the rat. Neurosci Lett 141:79–83

Tassorelli C, Joseph SA, Nappi G (1997) Neurochemical mechanisms of nitroglycerin-induced neuronal activation in rat brain: a pharmacological investigation. Neuropharmacology 36:1417–1424

Vámos E, Párdutz Á, Varga H, Bohár Z, Tajti J, Fülöp F, Toldi J, Vécsei L (2009) l-kynurenine combined with probenecid and the novel synthetic kynurenic acid derivative attenuate nitroglycerin-induced nNOS in the rat caudal trigeminal nucleus. Neuropharmacology 57:425–429. doi:10.1016/j.neuropharm.2009.06.033

Vámos E, Fejes A, Koch J, Tajti J, Fülöp F, Toldi J, Párdutz Á, Vécsei L (2010) Kynurenate derivative attenuates the nitroglycerin-induced camKIIα and CGRP expression changes. Headache 50:834–843. doi:10.1111/j.1526-4610.2009.01574.x

Vécsei L, Szalárdy L, Fülöp F, Toldi J (2013) Kynurenines in the CNS: recent advances and new questions. Nat Rev Drug Discov 12:64–82. doi:10.1038/nrd3793

Vikelis M, Mitsikostas DD (2007) The role of glutamate and its receptors in migraine. CNS Neurol Disord Drug Targets 6:251–257

Watanabe M, Mishina M, Inoue Y (1994) Distinct gene expression of the *N*-methyl-D-aspartate receptor channel subunit in peripheral neurons of the mouse sensory ganglia and adrenal gland. Neurosci Lett 165:183–186

Weatherall MW (2015) Drug therapy in headache. Clin Med 15:273–279

Zádori D, Ilisz I, Klivényi P, Szatmári I, Fülöp F, Toldi J, Vécsei L, Péter A (2011a) Time-course of kynurenic acid concentration in mouse serum following the administration of a novel kynurenic acid analog. J Pharm Biomed Anal 55:540–543. doi:10.1016/j.jpba.2011.02.014

Zádori D, Klivényi P, Plangár I, Toldi J, Vécsei L (2011b) Endogenous neuroprotection in chronic neurodegenerative disorders: with particular regard to the kynurenines. J Cell Mol Med 15:701–717. doi:10.1111/j.1582-4934.2010.01237.x

Zádori D, Nyiri G, Szonyi A, Szatmári I, Fülöp F, Toldi J, Freund TF, Vécsei L, Klivényi P (2011c) Neuroprotective effects of a novel kynurenic acid analogue in a transgenic mouse model of Huntington's disease. J Neural Transm 118:865–875. doi:10.1007/s00702-010-0573-6

Zhang Y, Huo M, Zhou J, Xie S (2010) PKSolver: an add-in program for pharmacokinetic and pharmacodynamic data analysis in Microsoft Excel. Comput Methods Programs Biomed 99:306–314. doi:10.1016/j.cmpb.2010.01.00

III.

Pharmacology, Biochemistry and Behavior 132 (2015) 115–124

Contents lists available at ScienceDirect

Pharmacology, Biochemistry and Behavior

journal homepage: www.elsevier.com/locate/pharmbiochembeh

Central nervous system-specific alterations in the tryptophan metabolism in the 3-nitropropionic acid model of Huntington's disease

Gábor Veres [a], Máté Molnár [a], Dénes Zádori [a], Márton Szentirmai [a], Levente Szalárdy [a], Rita Török [a], Emese Fazekas [a], István Ilisz [b], László Vécsei [a,c], Péter Klivényi [a,*]

[a] Department of Neurology, Faculty of Medicine, Albert Szent-Györgyi Clinical Center, University of Szeged, Szeged, Hungary
[b] Department of Inorganic and Analytical Chemistry, University of Szeged, Szeged, Hungary
[c] MTA-SZTE Neuroscience Research Group, Szeged, Hungary

ARTICLE INFO

Article history:
Received 27 November 2014
Received in revised form 12 February 2015
Accepted 6 March 2015
Available online 13 March 2015

Keywords:
Huntington's disease
3-Nitropropionic acid
Tryptophan metabolism
HPLC
Behavioral alterations

ABSTRACT

Experiments on human samples and on genetic animal models of Huntington's disease (HD) suggest that a number of neuroactive metabolites in the kynurenine (KYN) pathway (KP) of the tryptophan (TRP) catabolism may play a role in the development of HD. Our goal in this study was to assess the concentrations of TRP, KYN, kynurenic acid and 3-hydroxykynurenine (3-OHK) in the serum and brain of 5-month-old C57Bl/6 mice in the widely used 3-nitropropionic acid (3-NP) toxin model of HD. We additionally investigated the behavioral changes through open-field, rotarod and Y-maze tests. Our findings revealed an increased TRP catabolism *via* the KP as reflected by elevated KYN/TRP ratios in the striatum, hippocampus, cerebellum and brainstem. As regards the other examined metabolites of KP, we found only a significant decrease in the 3-OHK level in the cerebellum of the 3-NP-treated mice. The open-field and rotarod tests demonstrated that treatment with 3-NP resulted in a reduced motor ability, though this had almost totally disappeared a week after the last injection, similarly as observed previously in most murine 3-NP studies. The relevance of the alterations observed in our biochemical and behavioral analyses is discussed. We propose that the identified biochemical alterations could serve as applicable therapeutic endpoints in studies of drug effects on delayed-type neurodegeneration in a relatively fast and cost-effective toxin model of HD.

1. Introduction

Huntington's disease (HD) is an autosomal dominantly inherited progressive neurodegenerative disorder which results in cognitive, psychiatric and motor disturbances. HD is caused by an expansion of the cytosine–adenine–guanine (CAG) repeat in the gene coding for the *N*-terminal region of the huntingtin protein (Htt), which leads to the formation of a polyglutamine stretch. Above 39 CAGs, there is obligatory disease development (The Huntington's Disease Collaborative Research Group, 1993). Although the exact mechanisms through which mutant Htt (mHtt) leads to the characteristic neuropathology are not fully understood, the potential roles of excitotoxicity and a neuronal mitochondrial dysfunction are among the best-established concepts (Szalardy et al., 2012; Zádori et al., 2012).

Various evidence suggest that the involvement of striatal glutamatergic excitotoxicity in the development of HD is mediated predominantly by the overactivation of *N*-methyl-D-aspartate receptors (NMDARs), and most specifically through NR2B subunit-containing NMDARs at the extrasynaptic sites (Milnerwood et al., 2010). In line with this, the expression of mHtt has been shown to sensitize the NR2B subunit-containing NMDARs (Chen et al., 1999). There is evidence indicating that such excitotoxic injury is mediated at least in part by endogenous substances, including certain metabolites of the kynurenine pathway (KP) of the tryptophan (TRP) metabolism (Fig. 1; Zádori et al., 2011).

This pathway involves a number of neuroactive compounds. Among them, quinolinic acid (QUIN) is a weak NMDAR agonist (Stone and Darlington, 2002) which demonstrated an ability to induce excitotoxic injury, which led to QUIN toxicity being utilized as an early toxin model of HD (Beal et al., 1986). This toxic effect of QUIN was revealed to be augmented by another deleterious KP metabolite, 3-hydroxykynurenine (3-OHK), which can generate oxidative stress *via* the production of reactive oxygen species (ROS) (Guidetti et al., 2000). On the other hand, kynurenic acid (KYNA) is an NMDAR antagonist at the strychnine-insensitive glycine coagonist site (Perkins and Stone, 1982) and a weak antagonist on kainate- and α-amino-3-hydroxy-5-methyl-4-isoxazolepropionic acid-sensitive ionotropic glutamate receptors (Kessler et al., 1989). Furthermore, its inhibitory potential on presynaptic α7-nicotinic acetylcholine receptors is proposed to be of

* Corresponding author at: Department of Neurology, Faculty of Medicine, Albert Szent-Györgyi Clinical Center, University of Szeged, Semmelweis u. 6, H-6725 Szeged, Hungary. Tel.: +36 62 545351; fax: +36 62 545597.
E-mail address: klivenyi.peter@med.u-szeged.hu (P. Klivényi).

http://dx.doi.org/10.1016/j.pbb.2015.03.002
0091-3057/

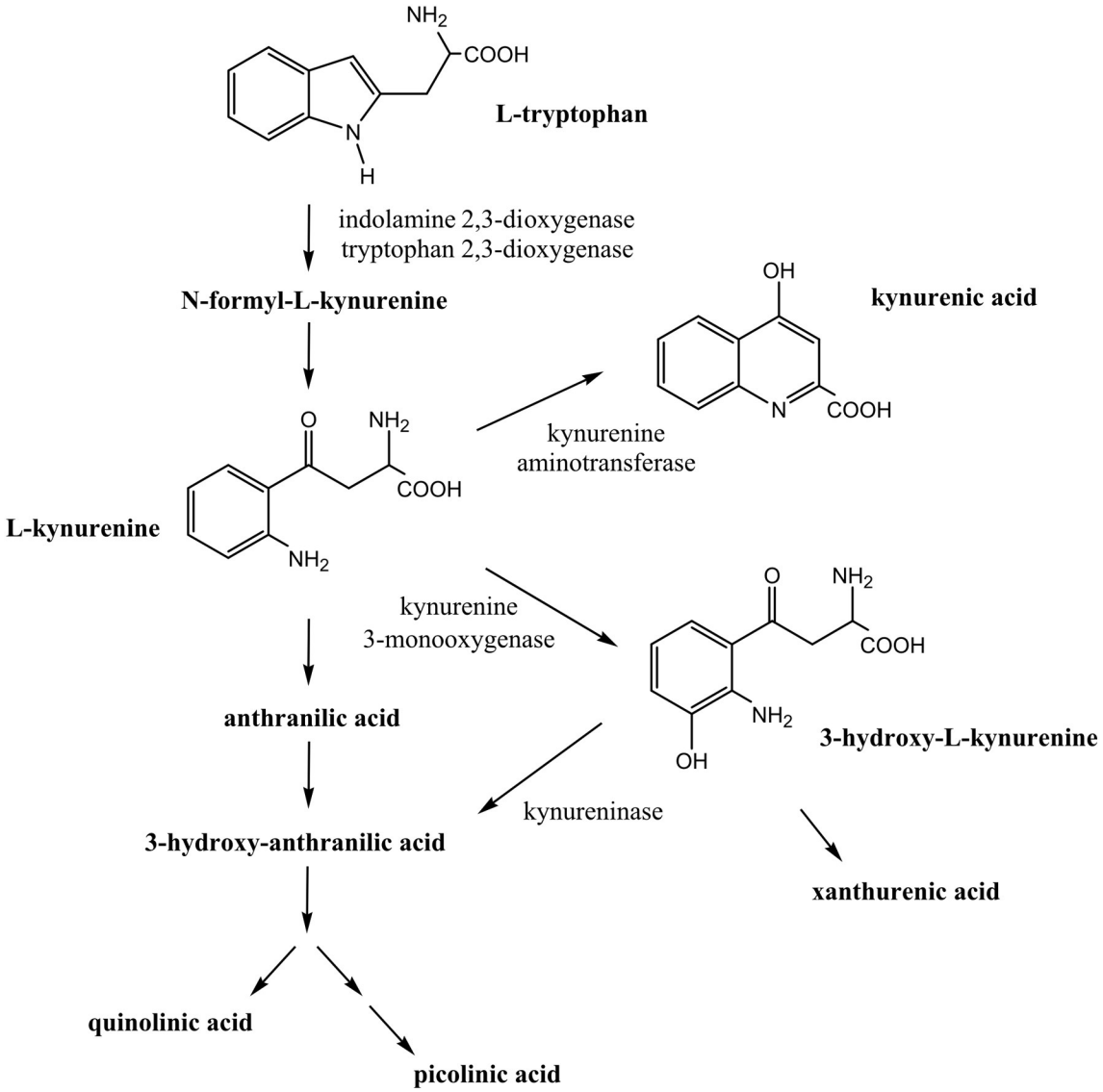

Fig. 1. Schematic depiction of the kynurenine pathway of the tryptophan metabolism.

high relevance at physiological KYNA levels, due to the suppression of presynaptic glutamate release (Hilmas et al., 2001). On this basis, KYNA was considered to be neuroprotective against NMDAR-modulated glutamatergic excitotoxicity, which has since been demonstrated by a variety of experimental evidence (Miranda et al., 1997; Sinor et al., 2000).

Besides the theoretical considerations, evidence of the presence of alterations in the KP of the TRP metabolism in tissues from HD patients and transgenic animals and in human post-mortem HD brains (Schwarcz et al., 1988; Beal et al., 1990, 1992; Heyes et al., 1992; Pearson and Reynolds, 1992; Jauch et al., 1995; Guidetti et al., 2004, 2006) is emerging. Briefly, these results indicate a relative decrease in KYNA concentrations relative to the levels of toxic neuroactive kynurenines (Zádori et al., 2011).

A decreased activity of the succinate dehydrogenase (SDH), complex II of the electron transport chain in post-mortem HD brains was one of the early findings suggestive of the role of a mitochondrial dysfunction in the development of HD (Stahl and Swanson, 1974). Furthermore, mHtt has been shown to be able to bind directly to the mitochondria, altering their normal function (Choo et al., 2004). In line with the decreased SDH activity, mitochondrial II complex inhibitors such as 3-nitropropionic acid (3-NP) or malonate have been found to be useful in the investigation of HD through their utilization in animal toxin models (Túnez et al., 2010). The 3-NP model is frequently applied as an easy and rapid way to study certain aspects of neurodegenerative processes in HD (Brouillet, 2014). Treatment with 3-NP evokes increases in the production of ROS and ·NO (La Fontaine et al., 2000) and the activation of apoptosis-related factors including caspase-3 and calpain (Duan et al., 2000; Bizat et al., 2003a), mechanisms through which 3-NP evokes striatal lesions in both rodents and primates in a rather selective manner. Several dosing regimens are applied to evoke characteristic neuropathological and behavioral alterations in rodents (Brouillet et al., 2005). Briefly, striatal neurodegeneration in rats occurs when the steady inhibition of SDH attains 50–60% (Alexi et al., 1998; Brouillet et al., 1998; Blum et al., 2002; Bizat et al., 2003b). In mice, there have been only a few studies of the dosage-related reduction in SDH activity. Lower cumulative doses (320 mg/kg) have been shown to induce an approximately 20% reduction of enzyme activity, which is not associated with marked striatal lesions (Fernagut et al., 2002a). However, higher cumulative doses (400–450 mg/kg) were widely used to induce measurable striatal lesions (Klivenyi et al., 2000, 2006). Accordingly, in a previous study we demonstrated a significant

reduction in striatal neuronal density *via* the application of unbiased semiquantitative densitometric analysis by using a subacute dosing regimen with a cumulative dose of 500 mg/kg (Török et al., 2015).

A number of publications have reported 3-NP-evoked alterations in motor and cognitive performance in rodents (Borlongan et al., 1995b; El Massioui et al., 2001; Brouillet et al., 2005; Li et al., 2009). The described alterations in motor functioning are highly reminiscent of those characteristic of human juvenile HD, such as rigidity, bradykinesia, dystonia and gait disturbances (Nance and Myers, 2001). Although it seems clear that higher cumulative doses of 3-NP cause motor and cognitive impairments, the motor dysfunctions observed undergo a considerable amelioration after the cessation of toxin administration (El Massioui et al., 2001; Fernagut et al., 2002b; Li et al., 2009). Early studies raised the possibility that the KP is altered in 3-NP models (Csillik et al., 2002; Luchowski et al., 2002), but this has not yet been further investigated.

The aims of the present study were a delayed assessment of the TRP metabolism with regard to certain metabolites of the KP following subacute 3-NP treatment, and a comparison of the time-course of the toxin-induced behavioral alterations with the data available from the literature.

2. Materials and methods

2.1. Animals and 3-NP treatment

We used 30 5-month-old male C57Bl/6 mice in this study. The animals were housed in cages under standard conditions with a 12–12-h light–dark cycle and free access to food and water. The experiments were carried out in accordance with the European Communities Council Directive (86/609/EEC) and were approved by the local animal care committee. The animals were randomly divided into two groups ($n = 16$ and $n = 14$, respectively). In the first group, 3-NP (Sigma-Aldrich, Saint Louis, MO, USA; dissolved in phosphate-buffered saline (PBS), pH adjusted to 7.4) was administered in a subacute dosing regimen as reported previously (Török et al., 2015), with twice daily intraperitoneal (i.p.) injections (50 mg/kg each) for 5 consecutive days. The second group served as the vehicle-injected control.

2.2. Behavioral assessment

2.2.1. Open-field test

Spontaneous locomotor and exploratory activities of the animals were assessed with the open-field paradigm. The first analysis was performed 3 days before the beginning of 3-NP administration to exclude any spontaneous difference between the randomly distributed animals. The second and third analyses were performed on the 3rd and the 11th day subsequent to the last day of the toxin regimen. The tests were performed at the same time of day to avoid possible changes due to diurnal rhythm. Each mouse was placed in the center of an open-field motimeter box measuring $48 * 48 * 40$ cm for 15-min tracking periods (analyzed in three 5-min periods). The movement patterns of the animals were tracked and recorded with the Conducta 1.0 system, with the use of infrared beams (Experimetria Ltd., Budapest, Hungary). The ambulation distance, the time spent in immobility and the total time spent with consecutive rearings were the parameters used to assess the motor and exploratory characteristics of the mice. The grid and the walls of the setup were thoroughly wiped with a cloth containing ethanol solution 70 v/v% after each session to prevent any bias from olfactory cues.

2.2.2. Rotarod test

The rotarod test was applied to characterize the effects of 3-NP on motor coordination. The animals were trained on the rotarod for a 3-session period for 5 min on 2 consecutive days prior to the first test day. On the first and second days of the training sessions, a constant speed of 5 and 10 rpm, respectively, was used. Following the training sessions, the first test was performed prior to the first 3-NP injection in order to exclude any inborn difference between the randomly distributed 2 groups. During the tracking sessions on the test days, an accelerating speed profile from 1 rpm to 30 rpm was set for a 5-min tracking period. The performance of each mouse was measured three times; resting periods of 30 min were allowed between consecutive tracking sessions. The latency to fall values were recorded with the TSE Rotarod Advanced system (TSE Systems International Group, Frankfurt am Main, Germany). The average latency to fall values were used for the comparative analyses. The second, third and fourth tests were performed 2 h following the second 3-NP injection and on the 1st and 10th days following the last 3-NP administration, respectively. On the day before the respective test days, a 3-session retraining at 10 rpm for 5-min with 30-min resting periods was carried out to enable the animals to recall the rotarod experience. The rods and the separating walls were thoroughly wiped with a cloth containing ethanol solution 70 v/v% after each session to prevent any bias from olfactory cues.

2.2.3. Y-maze test

An asymmetric Y-maze paradigm was applied to assess the short-term spatial memory of the mice. The Y-shaped translucent maze was placed on a black board enclosed by black walls, which prevented any view of the external environment. Unique visual cues were placed around the three arms of the maze. The test was performed on the 9th day after the end of the toxin regimen. The animals were first placed into the labyrinth and allowed to explore the common arm and only 1 of the 2 shorter arms of the maze until each mouse had spent a total of 2 min in the open short arm. After the session of acquisition, the mice were returned to their home cages for 30 min. In the trial of recall, the animals were free to enter all arms, and the tracking was stopped after a total of 2 min had been spent inside the 2 short arms. The exploratory activity of the mice was tracked and recorded with the SMART v2.5 system (Panlab, Barcelona, Spain). For evaluation, the recognition indices of the time spent and the distances traveled in the novel arm of interest were used. The recognition index was calculated *via* the following formula, where P is the examined parameter:

$$\text{recognition index} = P_{\text{novel arm}} / (P_{\text{novel arm}} + P_{\text{known arm}}).$$

The side of the novel arm was randomly distributed in each group, and the board and walls of the setup were thoroughly wiped with a cloth containing ethanol solution 70 v/v% after each session to prevent any bias from olfactory cues.

2.3. High-performance liquid chromatography (HPLC)

2.3.1. Sample preparation

The investigated reference compounds (L-TRP, L-KYN-sulfate, KYNA and 3-OHK), the substances used as internal standards (3-nitro-L-tyrosine (3-NLT) and isoproterenol (IPR)), zinc acetate dihydrate and sodium octylsulfate were purchased from Sigma-Aldrich (St. Louis, MO, USA). Acetonitrile and perchloric acid (PCA) were purchased from Scharlau (Barcelona, Spain), and acetic acid, phosphoric acid, sodium dihydrogenophosphate and disodium ethylenediaminetetraacetate were purchased from VWR International (Radnar, PA, USA).

On the 18th day of the experiment (12 days after the last 3-NP injection), the mice were deeply anesthetized with isoflurane (Forane®; Abott Laboratories Hungary Ltd., Budapest, Hungary). After thoracotomy, 0.3–0.7 ml venous blood was obtained from the right ventricle by intracardial puncture, followed by perfusion with artificial cerebrospinal fluid (composition in mM: 122 NaCl, 3 KCl, 1 Na_2SO_4, 1.25 KH_2PO_4, 10 D-glucose$*H_2O$, 1 $MgCl_2*6H_2O$, 2 $CaCl_2*2H_2O$, 6 $NaHCO_3$) for 2 min by an automatic peristaltic pump. The blood samples were left to coagulate for 30 min, and were then centrifuged for 10 min at 12,000 rpm. The supernatant sera were pipetted into polypropylene

Eppendorf tubes and stored at −80 °C until further sample handling. After perfusion, the brains were rapidly removed on ice and stored at −80 °C until analysis. Before analysis, the brain samples were weighed and then sonicated in an ice-cooled solution (250 μl) containing 2.5 w/w% PCA with 2 μM 3-NLT and 600 nM IPR as internal standards. The samples were next centrifuged at 12,000 rpm for 10 min at 4 °C, and the supernatants were collected.

Before analysis, the serum samples were thawed and, after a brief vortex 200 μl of serum sample was 'shot' onto 200 μl of precipitation solvent (containing 5 w/w% PCA with 4 μM 3-NLT and 2 μM IPR as internal standards). The samples were subsequently centrifuged at 12,000 rpm for 10 min at 4 °C, and the supernatants were collected.

2.3.2. Measurement of TRP, KYN and KYNA

The TRP, KYN and KYNA concentrations of the samples were quantified by a slight modification of the method of Hervé et al. (Hervé et al., 1996), with the use of an Agilent 1100 HPLC system (Agilent Technologies, Santa Clara, CA, USA). The system was equipped with a fluorescent and a UV detector, the fluorescent detector was set at excitation and emission wavelengths of 344 nm and 398 nm for the determination of KYNA and TRP, and the UV detector was set at 365 nm for the determination of KYN and the internal standard 3-NLT. Chromatographic separations were performed on an Onyx Monolithic C18 column, 100 mm × 4.6 mm I.D. (Phenomenex Inc., Torrance, CA, USA) after passage through a Hypersil ODS pre-column, 20 × 2.1 mm I.D., 5 μm particle size (Agilent Technologies, Santa Clara, CA, USA) with a mobile phase composition of 0.2 M zinc acetate/ACN = 95/5 (v/v%) with the pH adjusted to 6.2 with glacial acetic acid, applying isocratic elution. The flow rate and the injection volume were 1.5 ml/min and 50 μl, respectively. The peaks of the different compounds obtained during chromatographic analysis are presented in Fig. 2.

2.3.3. Measurement of 3-OHK

For determination of the concentrations of 3-OHK and its internal standard (IPR), we applied the Agilent 1100 HPLC system equipped with Model 105 electrochemical detector (Precision Instruments, Marseille, France). In brief, the working potential of the detector was set at +650 mV, using a glassy carbon electrode and an Ag/AgCl reference electrode. The mobile phase containing sodium octylsulfate (2.8 mM), sodium dihydrogenophosphate (75 mM) and disodium ethylenediaminetetraacetate (100 μM) was supplemented with acetonitrile (5 v/v%) and the pH was adjusted to 3.0 with phosphoric acid (85 w/w%). The mobile phase was delivered at a rate of 1 ml/min at 40 °C onto the reversed-phase column (HR-80 C18, 80 × 4.6 mm, 3-μm particle size; ESA Biosciences, Chelmsford, MA, USA) after passage through a pre-column (Hypersil ODS, 20 × 2.1 mm, 5-μm particle size; Agilent Technologies, Santa Clara, CA, USA). Ten-microliter aliquots were injected by the auto-sampler with the cooling module set at 4 °C. The peaks of the different compounds obtained during chromatographic analysis are presented in Fig. 2.

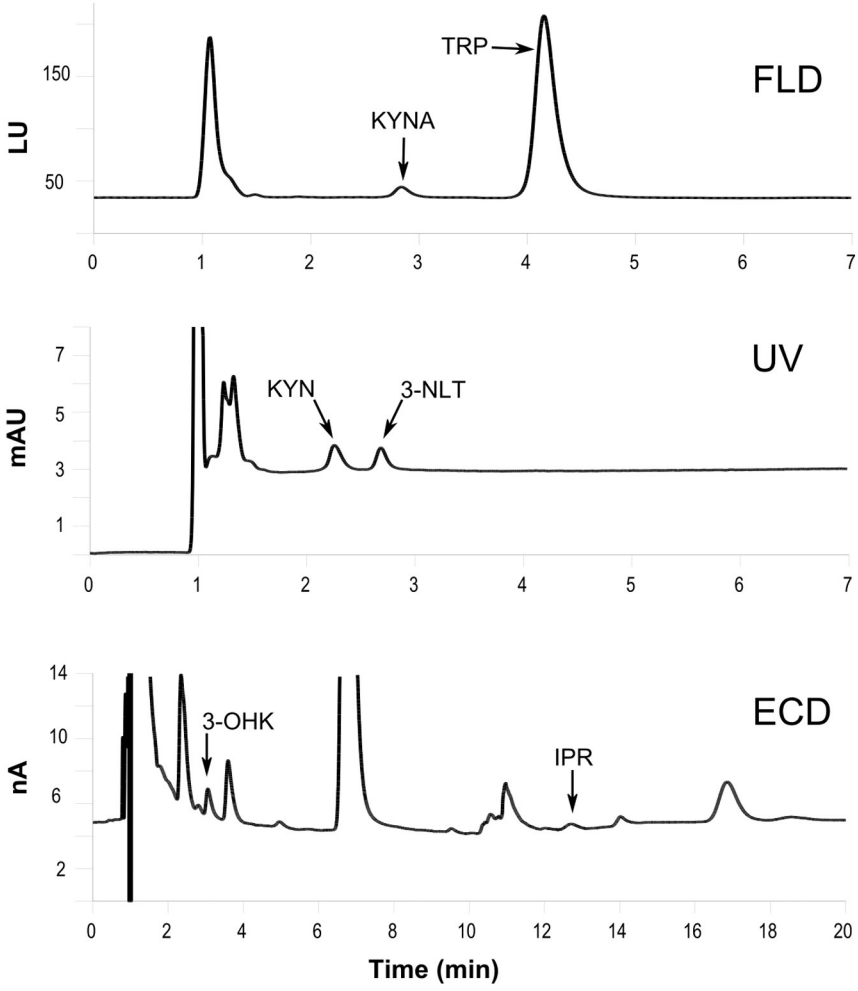

Fig. 2. Chromatograms of the analyzed compounds of the kynurenine pathway of the tryoptophan metabolism, from C57Bl/6 murine brain samples. *KYNA* kynurenic acid, *TRP* tryptophan, *KYN* kynurenine, *3-NLT* 3-nitro-L-tyrosine, *3-OHK* 3-hydroxykynurenine, *IPR* isoproterenol, *FLD* fluorescent detector, *ECD* electrochemical detector.

2.4. HPLC method validation

2.4.1. Calibration curve and linearity

Calibrants were prepared at 6 different concentration levels, from 0.1 to 50 μM, 0.05 to 5 μM, 1 to 100 nM, 10 to 200 nM, 0.5 to 7.5 μM and 25 to 600 nM for TRP, KYN, KYNA, 3-OHK and the internal standards, 3-NLT and IPR, respectively. Three parallel injections of each solution were made under the chromatographic conditions described above. The peak area responses were plotted against the corresponding concentration, and the linear regression computations were carried out by the least square method with the freely available R software (R Development Core Team, 2002). Very good linearity was observed throughout the investigated concentration ranges for TRP, KYNA, KYN, 3-OHK and the internal standards when either fluorescence, UV or electrochemical detection was applied.

2.4.2. Selectivity

The selectivity of the method was checked by comparing the chromatograms of TRP, KYN, KYNA, 3-OHK and the internal standards for blank serum and homogenized brain samples and those for spiked serum and homogenized brain samples. All compounds could be detected in their own selected chromatograms without any significant interference.

2.4.3. LOD and LLOQ

The limit of detection (LOD) and the lower limit of quantification (LLOQ) were determined *via* the signal-to-noise ratio with a threshold of 3 and 10, respectively, according to the ICH guidelines (ICH, 1995). The LOD for brain samples was 10, 40, 0.4 and 10 nM, while LLOQ was 20, 130, 1 and 30 nM for TRP, KYN, KYNA, and 3-OHK, respectively. The LOD for the serum samples was 15, 100, 1 and 10 nM, while LLOQ was 35, 275, 3.75 and 30 nM for TRP, KYN, KYNA and 3-OHK, respectively.

2.4.4. Precision

Replicate HPLC analysis showed that the relative standard deviation was ≤2.2% for the peak area response and ≤0.1% for the retention time for TRP, KYN and KYNA, whereas in the case of 3-OHK the relative standard deviation was ≤8.6% for the peak area response and ≤0.3% for the retention time.

2.4.5. Recovery

The relative recoveries were estimated by measuring spiked samples of TRP, KYN, KYNA and 3-OHK at 2 concentrations with 3 replicates of each. No significant differences were observed for the lower and higher concentrations. The recoveries for the brain samples were 86 to 91%, 98 to 100%, 82 to 92% and 69 to 74% for TRP, KYN, KYNA and 3-OHK, respectively. The recoveries for the serum samples ranged from 77 to 90%, 77 to 82%, 103 to 108% and 28 to 34% for TRP, KYN, KYNA and 3-OHK, respectively.

2.5. Statistics

All statistical analyses were performed with the use of the R software (R Development Core Team, 2002). We first checked the distribution of data populations with the Shapiro–Wilk test, and we also performed the Levene test for analysis of the homogeneity of variances. In the behavioral analyses, all the data exhibited normal distribution and equal variances were assumed, and we therefore used the independent *t*-test to compare the 2 groups. As a consequence of the multiple comparisons of the same 2 groups, the necessary corrections were carried out in *p* values according to the Bonferroni method. In the case of the HPLC analyses, due to the necessity of a large number of comparisons of data from the 2 groups obtained *via* a single measurement, two-sample *t*-tests *via* Monte-Carlo permutation (with 10,000 random permutations) were applied. We rejected the null hypothesis when the corrected *p* values were <0.05, and in such cases the differences were considered significant. Data with Gaussian or non-Gaussian distributions were plotted as means (±S.E.M.) or medians (and interquartile range), respectively.

3. Results

3.1. Behavioral assessment

Our results demonstrated a significant decrease in the latency to fall period in the 3-NP-treated animals (35.33 ± 6.97 s; $p < 0.001$, independent *t*-test) in the rotarod test 1 day after the last toxin injection in the subacute treatment regime as compared with the control group (126.34 ± 8.08 s). 10 days after the last injection, this difference had disappeared ($p = 0.16$, independent *t*-test; Fig. 3A). In the Y-maze test, there was no difference between the groups 9 days after the last injection ($p = 0.37$, independent *t*-test; Fig. 3B). In the open-field test performed 3 days after the last injection, a significant decrease was observed in the ambulation distance during the total 15-min tracking period (3-NP: 3203.2 ± 249.9 cm; control: 4874.9 ± 409.6 cm; $p = 0.003$, independent *t*-test; Fig. 3C) including that in the last 5-min period (3-NP: 950.4 ± 108.6 cm; control: 1359.5 ± 116 cm; $p = 0.028$, independent *t*-test; Fig. 3E). However, 11 days after the last 3-NP injection, the difference was significant only as regards the last 5-min period (3-NP: 985.2 ± 69.9 cm; control: 1417.1 ± 106 cm; $p = 0.001$, independent *t*-test; Fig. 3C). No difference in rearing time was detected between the groups either in the total 15-min (Fig. 3D) or in the last 5-min (Fig. 3F) tracking period.

3.2. HPLC analysis

As shown in Table 1, no difference was found in the KYNA concentration in the serum or in the investigated brain regions of the toxin-treated and control mice 12 days after the last injection, and there was no significant difference between the TRP levels of the serum samples of the toxin-treated and control mice, whereas in the case of KYN, a significant difference was detected in the cortex (2,679 ± 110 pmol/g wet weight (ww); $p = 0.017$, permutation test) relative to the control value (3,110 ± 112 pmol/g ww). However, significantly decreased TRP levels were found in the striatum (19,530 (17,700–20,440) pmol/g ww; $p = 0.0002$, permutation test), cortex (14,360 (13,540–16,300) pmol/g ww; $p = 0.003$, permutation test), hippocampus (16,550 (14,790–17,580) pmol/g ww; $p = 0.006$, permutation test), cerebellum (14,930 (14,210–16,260) pmol/g ww; $p = 0.0002$, permutation test) and brainstem (12,740 (12,280–14,100) pmol/g ww; $p = 0.0004$, permutation test) of 3-NP-treated mice as compared with the controls (27,950 (23,820–35,700); 22,860 (17,260–28,430); 26,590 (18,020–30,730); 24,810 (17,630–28,510); 20,960 (15,920–29,890) pmol/g ww, respectively). The observed decreases in TRP level were generally associated with an increased KYN/TRP ratio, an index widely used to assess the metabolic activity of KP. Indeed, a significant increase in KYN/TRP ratio was observed in the striatum (0.156 ± 0.014; $p = 0.008$, permutation test), hippocampus (0.158 ± 0.008; $p = 0.023$, permutation test), cerebellum (0.166 ± 0.01; $p = 0.008$, permutation test) and brainstem (0.166 ± 0.008; $p = 0.009$, permutation test) as compared with the control values (0.102 ± 0.011; 0.122 ± 0.011; 0.129 ± 0.007; 0.117 ± 0.013, respectively; Fig. 4); however, the difference in the cortex did not reach statistical significance. No difference in the KYN/TRP ratio was observed in the serum. Additionally, a significant decrease in 3-OHK level was observed in the cerebellum (to below the LOD; $p = 0.005$, permutation test) in the 3-NP-treated mice in comparison with the control value (66.84 (28.99–97.64) pmol/g ww), but not in the other brain regions.

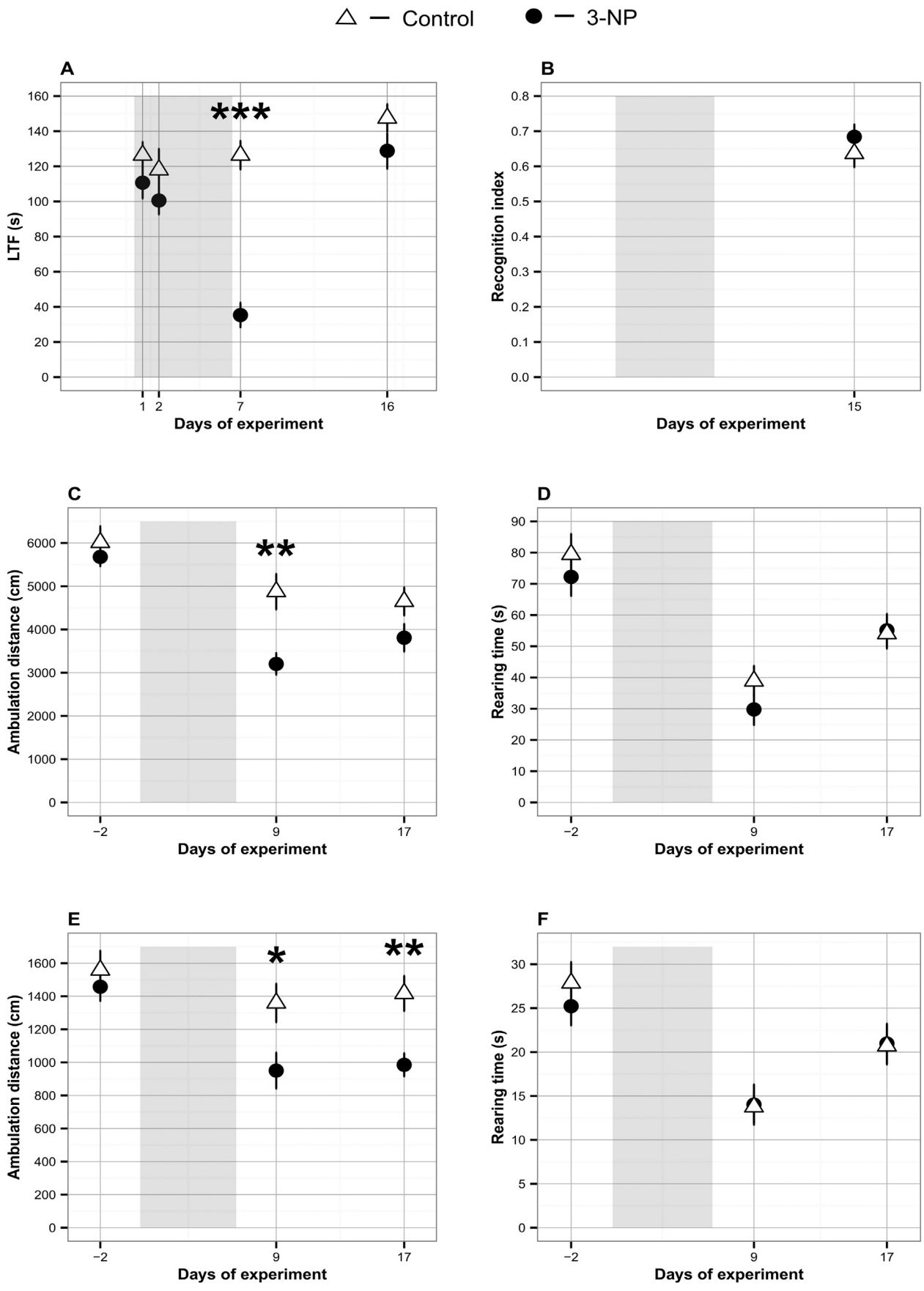
Control
3-NP
A
LTF (s)
Days of experiment
***
B
Recognition index
Days of experiment
C
Ambulation distance (cm)
Days of experiment
**
D
Rearing time (s)
Days of experiment
E
Ambulation distance (cm)
Days of experiment
*
**
F
Rearing time (s)
Days of experiment

4. Discussion

Although HD is a rare condition, it serves as a prototype of monogenically determined, but multifactorially affected neurodegenerative disorders (Kim and Fung, 2014). The study of the pathogenetic process in animal models of HD could therefore provide a valuable tool for insight into the general neurodegenerative process, yielding a possibility of finding promising targets for drug development.

From this respect, genetic rodent models are optimal tools for the study of HD in view of the possible molecular and genetic translatability to humans (Ramaswamy et al., 2007). However, animal genetic models also fail to demonstrate the pathological alterations characteristic of human HD completely. Furthermore, the relatively long duration of disease development may be a disadvantage in studies in which the therapeutic effects of potential neuroprotective agents are assessed.

Before genetic models were established, a number of toxin-based models were utilized to study the neurodegenerative processes in HD, which may still be a rapid and cost-effective way of screening the therapeutic effects of potential drug candidates prior to the costly and demanding application of genetic models. These inhibitors of the mitochondrial functions are widely used to model the mitochondrial dysfunction in HD (Browne, 2008).

SDH, the enzyme of complex II in the mitochondrial electron transport chain (Alston et al., 1977), is reversibly and irreversibly inhibited by malonate and 3-NP, respectively, toxins which have proved to furnish applicable phenotypic models of HD (Beal and Brouillet, 1993; Beal et al., 1993). 3-NP is currently the toxin most widely used to study certain neuropathological aspects of the disease.

The consecutive or continual administration of 3-NP to rodents (i.p. or subcutaneously, respectively) leads to bilateral dystonia, rigidity, gait disturbances and uncoordinated movements. At lower cumulative doses of 3-NP (<60 mg/kg), motor symptoms have been described to be manifested in mild movement disturbances, such as slowness and a subtle wobbling gait. However, some authors have also reported early-stage hyperactivity at lower cumulative doses (<40 mg/kg) (Borlongan et al., 1995a). When the cumulative dose is elevated up to 80 mg/kg, the general weakness becomes more marked and dystonia develops, the latter being particularly pronounced in the hind-limbs at this dose, and appearing soon after toxin administration (Brouillet, 2014). A further elevation of the cumulative dose (>100 mg/kg) results in more expressed weakness and rigidity (Brouillet, 2014). However, subsequent to the termination of the subacute toxin regimen in mice in the widely-applied experimental setup (as used in the current study), the detected alterations in motor functioning tend to abate and then cease (Fernagut et al., 2002a,b; Li et al., 2009). It should be noted, however, that the extended application of 3-NP in a considerably higher cumulative dose resulted in persistent locomotor deficits in one study on mice (Stefanova et al., 2003). Studies involving 3-NP intoxication in rats yielded rather inconclusive results in terms of a persistent motor dysfunction (Teunissen et al., 2001; Tasset et al., 2012).

As regards a cognitive impairment, rats treated with a cumulative dose of 190 mg/kg demonstrated a severely decreased memory function in a fear-associated memory test (a passive avoidance task) and a perceptual-learning task (an attentional set-shifting task) (El Massioui et al., 2001). However, in a simple 2-trial Y-maze paradigm, performed on the 15th day after termination of the administration of 3-NP to mice (in a cumulative dose of 320 mg/kg), the intoxicated animals did not display any 3-NP-induced memory impairment (Li et al., 2009).

The above observations in mice were confirmed by our findings, i.e. most of the behavioral changes disappeared (i.e. the latency to fall, tested by rotarod; and the ambulation distance, tested in an open-field) or could not be detected (the recognition index, tested with the Y-maze test) 11 days after the last injection. The lack of difference in cognitive performance was not influenced by any incidental difference in locomotor acitivity, because we did not observe any significant difference in the total ambulation distance within the Y-maze (not shown). It is noteworthy, however, that we observed a significant reduction in the ambulation distance parameter in the last 5 min of the open-field test in the toxin-treated animals as compared with the controls, which may reflect a slight persistent behavioral dysfunction.

As concerns to the previously observed alterations in the TRP metabolism in transgenic HD animals, the 3-OHK and KYNA levels were reported to be elevated in the striatum and cortex of a heterozygous transgenic mouse (FVB/N background, 89 CAG repeats, 12–15 months of age) model of HD (Guidetti et al., 2000). Another study involving the R6/2 mouse model of HD revealed increased kynurenine 3-monooxygenase activity in the striatum, cortex and cerebellum of 6–12-week-old animals, while the 3-hydroxyanthranilic acid oxygenase, kynurenine aminotransferase (KAT)-I and KAT-II activities (catalyzing the conversion of KYN to KYNA) in the cortex and cerebellum were unchanged. An elevated synthesis of 3-OHK was found in the striatum and a decreased kynureninase activity in the striatum and cortex of 4–12-week-old animals, but not in the cerebellum. Other investigated compounds (KYN, KYNA and QUIN) did not display any difference (Sathyasaikumar et al., 2010). In the R6/2 model, enhanced 3-OHK concentrations were observed in the striatum, cortex and cerebellum of 4–12-week-old animals, but no difference was found in younger mice (Guidetti et al., 2006). In the Hdh^{Q92} and Hdh^{Q111} models, 5–17-month-old animals demonstrated increased levels of 3-OHK in the striatum, cortex and cerebellum, and of QUIN in the striatum and cortex, whereas there were no differences in younger animals (Guidetti et al., 2006). In the YAC128 model, the 3-OHK concentrations were increased in the striatum, cortex and cerebellum of 5–12-month-old mice, while the QUIN levels were elevated only in the striatum and cortex of 8–12-month-old animals (Guidetti et al., 2006). In the same YAC128 mouse model, the striatal expression of indoleamine 2,3-dioxygenase (IDO)-1 (probably the most important enzyme participating in the TRP catabolism in the brain), was found to be up-regulated, whereas IDO-2 and tryptophan 2,3-dioxygenase did not undergo any significant change. As concerns metabolite concentrations, the levels of TRP and 3-OHK proved to be decreased in the striatum of 3-month-old animals. However, no difference in TRP level was found in 12-month-old mice, while 3-OHK and KYN were significantly elevated in the striatum. The KYNA and QUIN concentrations did not change in either group (Mazarei et al., 2013). Studies on the hippocampus did not indicate significant difference in any examined model or age group (Guidetti et al., 2006).

In contrast with genetic models, there are no available published data on the effects of 3-NP toxicity on the concentrations of TRP and KP metabolites under *in vivo* conditions in mice. One of the two studies of the effects of the chronic treatment of rats with 3-NP demonstrated a significant decrease in the amount of KAT-I-immunoreactive cells, predominantly in the striatum (Csillik et al., 2002). The other study on *ex vivo* rat cortical slices, showed that 3-NP dose-dependently inhibited the production of KYNA and led to decreased KAT-I and KAT-II activities in the cortical tissue homogenates (Luchowski et al., 2002). No murine studies have been conducted previously to assess the effects of *in vivo* applied 3-NP on the KP metabolism at the metabolite level *per se*, and there have been no studies of KP alterations due to 3-NP intoxication in the serum, which would allow conclusions as to the possible effects

Fig. 3. The effects of 3-NP treatment on different behavioral parameters in C57Bl/6 mice. Shortly after the last 3-NP injection, the latency to fall was significantly decreased in the rotarod test (A), but this difference had disappeared 9 days later. The Y-maze test, performed 9 days after the last 3-NP injection, did not reveal any difference between the groups (B). In the open-field paradigm 3 days after the last 3-NP injection, the ambulation distance was significantly decreased in the total 15-min examination period (C) and in the last 5-min period (E). However, 11 days after the last 3-NP injection, the difference was significant only in the last 5 min. No difference in rearing time was detected (D, F). The gray area indicates the 3-NP treatment period.3-NP mice: n = 16, control mice: n = 14; data are means ± S.E.M.; *3-NP* 3-nitropropionic acid, *LTF* latency to fall, $^{*}p < 0.05$, $^{**}p < 0.01$, and $^{***}p < 0.001$.

Table 1
The concentrations of some metabolites of the KP in different brain regions and serum of control and 3-NP treated mice.

	TRP		KYN		KYNA		3-OHK	
	Ctrl	3-NP	Ctrl	3-NP	Ctrl	3-NP	Ctrl	3-NP
Serum (μM)	102.8 (89.8–115.4)	88.6 (83.2–94.5)	1.39 ± 0.09	1.12 ± 0.12	0.19 (0.17–0.21)	0.10 (0.09–0.18)	<LOD	<LOD
Striatum (pmol/g ww)	27950 (23820–35700)	19530*** (17700–20440)	2922 ± 288	3001 ± 309	5.73 (<LOD–21.91)	<LOD	<LOD	<LOD
Cortex (pmol/g ww)	22860 (17260–28430)	14360** (13540–16300)	3110 ± 112	2679* ± 110	5.07 (<LOD–7.72)	6.67 (3.04–7.08)	<LOD	<LOD
Hippocampus (pmol/g ww)	26590 (18020–30730)	16550** (14790–17580)	2914 ± 176	2723 ± 208	<LOD (<LOD–7.66)	<LOD (<LOD–7.68)	<LOD	<LOD
Cerebellum (pmol/g ww)	24810 (17630–28510)	14930*** (14210–16260)	3060 ± 238	2521 ± 182	<LOD (<LOD–4.18)	<LOD (<LOD–7.45)	66.84 (28.99–97.64)	<LOD**
Brainstem (pmol/g ww)	20960 (15920–29890)	12740*** (12280–14100)	2389 ± 118	2169 ± 111	<LOD	<LOD	<LOD (<LOD–25.50)	<LOD

The concentration of TRP and some of its metabolites were measured from five different brain regions and serum of C57Bl/6 mice with HPLC. TRP levels were significantly decreased in all brain regions of 3-NP treated mice. In the cortex and cerebellum of toxin treated mice there was also a significant depletion in KYN and 3-OHK concentration, respectively. KYN results are expressed as mean ± S.E.M.; the other substances are shown as median (interquartile range). *KP* kynurenine pathway, *TRP* tryptophan, *KYN* kynurenine, *KYNA* kynurenic acid, *3-OHK* 3-hydroxykynurenine, *3-NP* 3-nitropropionic acid, *ctrl* control, *LOD* limit of detection, and *ww* wet weight.
* $p < 0.05$.
** $p < 0.01$.
*** $p < 0.001$.

of systemic KP alterations within the CNS. We have now quantitatively assessed the levels of 4 KP metabolites in the striatum, cortex, hippocampus, cerebellum and brainstem of mice, with a relatively high number of animals per group (n = 14–16).

Our findings indicated a decreased TRP level in association with an increased KYN/TRP ratio in most of the examined brain regions of C57Bl/6 mice treated with 3-NP, and also a reduced concentration of 3-OHK in the cerebellum. It is noteworthy that we did not detect any significant difference in serum samples, which suggests that the observed alterations are specific for the examined brain regions and are not affected by a systemic change and/or an altered permeability of the blood–brain barrier. Our results on 5-month-old 3-NP-treated animals resemble those from studies of 3-month-old transgenic YAC128 animals (Mazarei et al., 2013), which is known to be one of the best animal strains for the modeling of the alterations in human HD (Slow, 2003; Pouladi et al., 2013). The increase observed in the KYN/TRP ratio is comparable with the previous finding of increased IDO-1 activity in the brain (but not the serum) of YAC128 animals, an alteration reflecting that observed in several neurodegenerative diseases and their animal models (Vécsei et al., 2013), and suggested to contribute to the neurodegenerative process. The similarity of the findings of the KP alterations in this 3-NP model with those observed previously in genetic models (and especially the YAC128 model) leads us to presume that the KP alterations observed in transgenic animals might be secondary to a mitochondrial dysfunction as present in the pathogenesis of HD, and that 3-NP toxicity may comprise a useful and cheap tool with which to screen the efficacy of potential drug candidates before the application of more demanding genetic models.

The rationale of our study was to find a valuable biomarker for therapeutic studies in the widely applied subacute 3-NP model of HD with previously demonstrated neurodegenerative characteristics, at a time point when merely minor behavioral alterations persist. Accordingly, we have confirmed that the behavioral alterations evoked by 3-NP toxicity are mostly intermittent, similarly as observed previously by others, which suggests that these alterations might be only functional and do not reflect the long-term effects of delayed-type neurodegeneration. On the other hand, at this delayed time point, we detected a marked persistent increases in the KYN/TRP ratio in the striatum, hippocampus, cerebellum and brainstem and a slight reduction in the level of 3-OHK in the cerebellum. Such alterations have not been reported earlier in 3-NP studies and are similar to those seen in young genetic animal models (especially in 3-month-old YAC128 transgenic mice). In the era of advanced genetic models of HD, our findings demonstrate the continued relevance and applicability of toxin models, which may provide

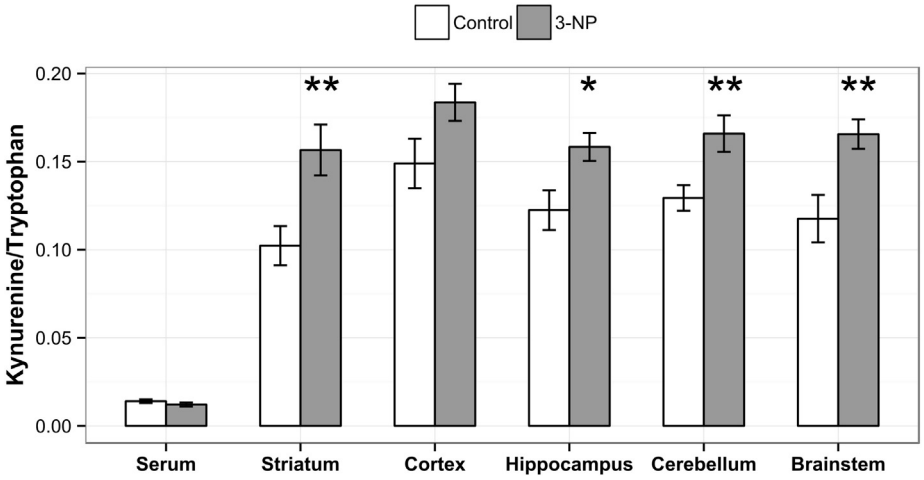

Fig. 4. The effects of 3-NP treatment on the KYN/TRP ratio in the serum and different brain regions of C57Bl/6 mice. The KYN/TRP ratio was significantly elevated in the striatum, hippocampus, cerebellum and brainstem of the 3-NP-treated mice. The increase in the cortex did not reach the level of statistical significance. No alteration was observed in the serum. Data are means ± S.E.M.; *3-NP* 3-nitropropionic acid, *KYN* kynurenine, *TRP* tryptophan, *$p < 0.05$, and **$p < 0.01$.

cost-effective and rapid ways of screening potential drug candidates to treat this currently intractable disease.

Acknowledgments

This research was supported by TÁMOP-4.2.2.A-11/1/KONV-2012-0052, MTA-SZTE Neuroscience Research Group and Hungarian Brain Research Program – Grant No. KTIA_NAP_13-A_III/9, and in the frame of TÁMOP 4.2.4. A/1-11-1-2012-0001 "National Excellence Program – elaborating and operating an inland student and researcher personal support system". The project was subsidized by the European Union and co-financed by the European Social Fund.

References

Alexi T, Hughes PE, Knüsel B, Tobin AJ. Metabolic compromise with systemic 3-nitropropionic acid produces striatal apoptosis in Sprague–Dawley rats but not in BALB/c ByJ mice. Exp Neurol 1998;153:74–93.

Alston T, Mela L, Bright HJ. 3-Nitropropionate, the toxic substance of *Indigofera*, is a suicide inactivator of succinate dehydrogenase. Proc Natl Acad Sci U S A 1977;74:3767–71.

Beal M, Brouillet E. Neurochemical and histologic characterization of striatal excitotoxic lesions produced by the mitochondrial toxin 3-nitropropionic acid. J Neurosci 1993;13(10):4181–92.

Beal MF, Kowall NW, Ellison DW, Mazurek MF, Swartz KJ, Martin JB. Replication of the neurochemical characteristics of Huntington's disease by quinolinic acid. Nature 1986;321:168–71.

Beal MF, Matson WR, Swartz KJ, Gamache PH, Bird ED. Kynurenine pathway measurements in Huntington's disease striatum: evidence for reduced formation of kynurenic acid. J Neurochem 1990;55:1327–39.

Beal MF, Matson W, Storey E. Kynurenic acid concentrations are reduced in Huntington's disease cerebral cortex. J Neurol Sci 1992;108:80–7.

Beal MF, Brouillet E, Jenkins B, Henshaw R, Rosen B, Hyman BT. Age-dependent striatal excitotoxic lesions produced by the endogenous mitochondrial inhibitor malonate. J Neurochem 1993;61:1147–50.

Bizat N, Hermel J, Jacquard C, Cre C, Escartin C, Hantraye P, et al. Calpain is a major cell death effector in selective striatal degeneration induced in vivo by 3-nitropropionate: implications for Huntington's disease. J Neurosci 2003a;23:5020–30.

Bizat N, Hermel JM, Humbert S, Jacquard C, Créminon C, Escartin C, et al. In vivo calpain/caspase cross-talk during 3-nitropropionic acid-induced striatal degeneration: implication of a calpain-mediated cleavage of active caspase-3. J Biol Chem 2003b;278:43245–53.

Blum D, Gall D, Galas MC, d'Alcantara P, Bantubungi K, Schiffmann SN. The adenosine A1 receptor agonist adenosine amine congener exerts a neuroprotective effect against the development of striatal lesions and motor impairments in the 3-nitropropionic acid model of neurotoxicity. J Neurosci 2002;22:9122–33.

Borlongan CV, Koutouzis TK, Freeman TB, Cahill DW, Sanberg PR. Behavioral pathology induced by repeated systemic injections of 3-nitropropionic acid mimics the motoric symptoms of Huntington's disease. Brain Res 1995a;697:254–7.

Borlongan CV, Koutouzis TK, Randall TS, Freeman TB, Cahill DW, Sanberg PR. Systemic 3-nitropropionic acid: behavioral deficits and striatal damage in adult rats. Brain Res Bull 1995b;36:549–56.

Brouillet E. The 3-NP model of striatal neurodegeneration. Curr Protoc Neurosci 2014;67:9.48.1–9.48.14.

Brouillet E, Guyot MC, Mittoux V, Altairac S, Condé F, Palfi S, et al. Partial inhibition of brain succinate dehydrogenase by 3-nitropropionic acid is sufficient to initiate striatal degeneration in rat. J Neurochem 1998;70:794–805.

Brouillet E, Jacquard C, Bizat N, Blum D. 3-Nitropropionic acid: a mitochondrial toxin to uncover physiopathological mechanisms underlying striatal degeneration in Huntington's disease. J Neurochem 2005;95:1521–40.

Browne SE. Mitochondria and Huntington's disease pathogenesis: insight from genetic and chemical models. Ann N Y Acad Sci 2008;1147:358–82.

Chen N, Luo T, Wellington C, Metzler M, McCutcheon K, Hayden MR, et al. Subtype-specific enhancement of NMDA receptor currents by mutant huntingtin. J Neurochem 1999;72:1890–8.

Choo YS, Johnson GVW, MacDonald M, Detloff PJ, Lesort M. Mutant huntingtin directly increases susceptibility of mitochondria to the calcium-induced permeability transition and cytochrome c release. Hum Mol Genet 2004;13:1407–20.

Csillik A, Knyihár E, Okuno E, Krisztin-Péva B, Csillik B, Vécsei L. Effect of 3-nitropropionic acid on kynurenine aminotransferase in the rat brain. Exp Neurol 2002;177:233–41.

Duan W, Guo Z, Mattson MP. Participation of par-4 in the degeneration of striatal neurons induced by metabolic compromise with 3-nitropropionic acid. Exp Neurol 2000;165:1–11.

El Massioui N, Ouary S, Chéruel F, Hantraye P, Brouillet E. Perseverative behavior underlying attentional set-shifting deficits in rats chronically treated with the neurotoxin 3-nitropropionic acid. Exp Neurol 2001;172:172–81.

Fernagut PO, Diguet E, Jaber M, Bioulac B, Tison F. Dopamine transporter knock-out mice are hypersensitive to 3-nitropropionic acid-induced striatal damage. Eur J Neurosci 2002a;15:2053–6.

Fernagut PO, Diguet E, Stefanova N, Biran M, Wenning GK, Canioni P, et al. Subacute systemic 3-nitropropionic acid intoxication induces a distinct motor disorder in adult C57Bl/6 mice: behavioural and histopathological characterisation. Neuroscience 2002b;114:1005–17.

Guidetti P, Hemachandra Reddy P, Tagle DA, Schwarcz R. Early kynurenergic impairment in Huntington's disease and in a transgenic animal model. Neurosci Lett 2000;283:233–5.

Guidetti P, Luthi-Carter RE, Augood SJ, Schwarcz R. Neostriatal and cortical quinolinate levels are increased in early grade Huntington's disease. Neurobiol Dis 2004;17:455–61.

Guidetti P, Bates GP, Graham RK, Hayden MR, Leavitt BR, MacDonald ME, et al. Elevated brain 3-hydroxykynurenine and quinolinate levels in Huntington disease mice. Neurobiol Dis 2006;23:190–7.

Hervé C, Beyne P, Jamault H, Delacoux E. Determination of tryptophan and its kynurenine pathway metabolites in human serum by high-performance liquid chromatography with simultaneous ultraviolet and fluorimetric detection. J Chromatogr B Biomed Appl 1996;675:157–61.

Heyes MP, Saito K, Crowley JS, Davis LE, Demitrack MA, Der M, et al. Quinolinic acid and kynurenine pathway metabolism in inflammatory and non-inflammatory neurological disease. Brain 1992;115:1249–73.

Hilmas C, Pereira EF, Alkondon M, Rassoulpour a, Schwarcz R, Albuquerque EX. The brain metabolite kynurenic acid inhibits alpha7 nicotinic receptor activity and increases non-alpha7 nicotinic receptor expression: physiopathological implications. J Neurosci 2001;21:7463–73.

ICH. ICH harmonised tripartite guideline, validation of analytical procedures. Fed Regist 1995;60:11260.

Jauch D, Urbańska E, Guidetti P. Dysfunction of brain kynurenic acid metabolism in Huntington's disease: focus on kynurenine aminotransferases. J Neurol Sci 1995;130:39–47.

Kessler M, Terramani T, Lynch G, Baudry M. A glycine site associated with N-methyl-D-aspartic acid receptors: characterization and identification of a new class of antagonists. J Neurochem 1989;52:1319–28.

Kim SD, Fung VSC. An update on Huntington's disease: from the gene to the clinic. Curr Opin Neurol 2014;27:477–83.

Klivenyi P, Andreassen OA, Ferrante RJ, Dedeoglu A, Mueller G, Lancelot E, et al. Mice deficient in cellular glutathione peroxidase show increased vulnerability to malonate, 3-nitropropionic acid, and 1-methyl-4-phenyl-1,2,5,6-tetrahydropyridine. 2000;20:1–7.

Klivenyi P, Siwek D, Gardian G, Yang L, Starkov A, Cleren C, et al. Mice lacking alpha-synuclein are resistant to mitochondrial toxins. Neurobiol Dis 2006;21:541–8.

La Fontaine MA, Geddes JW, Banks A, Allan Butterfield D. Effect of exogenous and endogenous antioxidants on 3-nitropropionic acid-induced in vivo oxidative stress and striatal lesions: insights into Huntington's disease. J Neurochem 2000;75:1709–15.

Li XM, Zhu BG, Ni JB, Cao CY, Zhang JP, Zhao XD, et al. No spatial memory deficit exists in Kunming mice that recently recovered from motor defects following 3-nitropropionic acid intoxication. Neurosci Bull 2009;25:87–93.

Luchowski P, Luchowska E, Turski WA, Urbanska EM. 1-Methyl-4-phenylpyridinium and 3-nitropropionic acid diminish cortical synthesis of kynurenic acid via interference with kynurenine aminotransferases in rats. Neurosci Lett 2002;330:49–52.

Mazarei G, Budac DP, Lu G, Adomat H, Tomlinson Guns ES, Möller T, et al. Age-dependent alterations of the kynurenine pathway in the YAC128 mouse model of Huntington disease. J Neurochem 2013;127:852–67.

Milnerwood AJ, Gladding CM, Pouladi M, Kaufman AM, Hines RM, Boyd JD, et al. Early increase in extrasynaptic NMDA receptor signaling and expression contributes to phenotype onset in Huntington's disease mice. Neuron 2010;65:178–90.

Miranda A, Boegman R, Beninger R, Jhamandas K. Protection against quinolinic acid-mediated excitotoxicity in nigrostriatal dopaminergic neurons by endogenous kynurenic acid. Neuroscience 1997;78:967–75.

Nance MA, Myers RH. Juvenile onset Huntington's disease — clinical and research perspectives. Ment Retard Dev Disabil Res Rev 2001;7:153–7.

Pearson S, Reynolds G. Increased brain concentrations of a neurotoxin, 3-hydroxykynurenine, in Huntington's disease. Neurosci Lett 1992;144:199–201.

Perkins MN, Stone TW. An iontophoretic investigation of the actions of convulsant kynurenines and their interaction with the endogenous excitant quinolinic acid. Brain Res 1982;247:184–7.

Pouladi M, Morton J, Hayden MR. Choosing an animal model for the study of Huntington's disease. Nat Rev Neurosci 2013;14:708–21.

R Development Core Team. The R project for statistical computing. In: RDC Team, editor. Text R Foundation for Statistical, Computing; 2002. p. 1–9.

Ramaswamy S, McBride JL, Kordower JH. Animal models of Huntington's disease. ILAR J 2007;48:356–73.

Sathyasaikumar KV, Stachowski EK, Amori L, Guidetti P, Muchowski PJ, Schwarcz R. Dysfunctional kynurenine pathway metabolism in the R6/2 mouse model of Huntington's disease. J Neurochem 2010;113:1416–25.

Schwarcz R, Okuno E, White RJ, Bird ED, Whetsell WO. 3-Hydroxyanthranilate oxygenase activity is increased in the brains of Huntington disease victims. Proc Natl Acad Sci U S A 1988;85:4079–81.

Sinor JD, Du S, Venneti S, Blitzblau RC, Leszkiewicz DN, Rosenberg P, et al. NMDA and glutamate evoke excitotoxicity at distinct cellular locations in rat cortical neurons in vitro. J Neurosci 2000;20:8831–7.

Slow EJ. Selective striatal neuronal loss in a YAC128 mouse model of Huntington disease. Hum Mol Genet 2003;12:1555–67.

Stahl WL, Swanson PD. Biochemical abnormalities in Huntington's chorea brains. Neurology 1974;24:813–9.

Stefanova N, Puschban Z, Fernagut PO, Brouillet E, Tison F, Reindl M, et al. Neuropathological and behavioral changes induced by various treatment paradigms with MPTP and 3-nitropropionic acid in mice: towards a model of striatonigral degeneration (multiple system atrophy). Acta Neuropathol 2003;106:157–66.

Stone TW, Darlington LG. Endogenous kynurenines as targets for drug discovery and development. Nat Rev Drug Discov 2002;1:609–20.
Szalardy L, Klivenyi P, Zadori D, Fulop F, Toldi J, Vecsei L. Mitochondrial disturbances, tryptophan metabolites and neurodegeneration: medicinal chemistry aspects. Curr Med Chem 2012;19:1899–920.
Tasset I, Medina FJ, Jimena I, Agüera E, Gascón F, Feijóo M, et al. Neuroprotective effects of extremely low-frequency electromagnetic fields on a Huntington's disease rat model: effects on neurotrophic factors and neuronal density. Neuroscience 2012;209:54–63.
Teunissen CE, Steinbusch HW, Angevaren M, Appels M, de Bruijn C, Prickaerts J, et al. Behavioural correlates of striatal glial fibrillary acidic protein in the 3-nitropropionic acid rat model: disturbed walking pattern and spatial orientation. Neuroscience 2001;105:153–67.
The Huntington's Disease Collaborative Research Group. A novel gene containing a trinucleotide that is expanded and unstable on Huntington' s disease chromosomes. Cell 1993;72:971–83.
Török R, Kónya JA, Zádori D, Veres G, Szalárdy L, Vécsei L, et al. mRNA expression levels of PGC-1α in a transgenic and a toxin model of Huntington's disease. Cell Mol Neurobiol 2015. http://dx.doi.org/10.1007/s10571-014-0124-z. [in press].
Túnez I, Tasset I, Pérez-De La Cruz V, Santamaría A. 3-Nitropropionic acid as a tool to study the mechanisms involved in Huntington's disease: past, present and future. Molecules 2010;15:878–916.
Vécsei L, Szalárdy L, Fülöp F, Toldi J. Kynurenines in the CNS: recent advances and new questions. Nat Rev Drug Discov 2013;12:64–82.
Zádori D, Klivényi P, Plangár I, Toldi J, Vécsei L. Endogenous neuroprotection in chronic neurodegenerative disorders: with particular regard to the kynurenines. J Cell Mol Med 2011;15:701–17.
Zádori D, Klivényi P, Szalárdy L, Fülöp F, Toldi J, Vécsei L. Mitochondrial disturbances, excitotoxicity, neuroinflammation and kynurenines: novel therapeutic strategies for neurodegenerative disorders. J Neurol Sci 2012;322:187–91.

IV.

Brain Research 1660 (2017) 20–26

Contents lists available at ScienceDirect

Brain Research

journal homepage: www.elsevier.com/locate/bres

Research report

Effect of MPTP on mRNA expression of PGC-1α in mouse brain

Rita Torok [a], Andras Salamon [a], Evelin Sumegi [a], Denes Zadori [a], Gabor Veres [b], Mate Fort Molnar [a], Laszlo Vecsei [a,b], Peter Klivenyi [a,*]

[a] Department of Neurology, University of Szeged, Semmelweis u. 6, H-6725 Szeged, Hungary
[b] MTA-SZTE Neuroscience Research Group of the Hungarian Academy of Sciences and University of Szeged, Semmelweis u. 6, H-6725 Szeged, Hungary

ARTICLE INFO

Article history:
Received 28 October 2016
Received in revised form 5 January 2017
Accepted 30 January 2017
Available online 2 February 2017

Keywords:
FL-PGC-1α
NT-PGC-1α
CNS-PGC-1α
MPTP
Preconditioning
Dopamine

ABSTRACT

The peroxisome proliferator-activated receptor-γ (PPARγ) coactivator 1α (PGC-1α) is a key regulator of mitochondrial biogenesis, respiration and adaptive thermogenesis. Besides the full-length protein (FL-PGC-1α), several other functionally active PGC-1α isoforms were identified as a result of alternative splicing (e.g., N-truncated PGC-1α; NT-PGC-1α) or alternative promoter usage (e.g., central nervous system-specific PGC-1α isoforms; CNS-PGC-1α). Achieving neuroprotection via CNS-targeted pharmacological stimulation is limited due to poor penetration of the blood brain barrier (BBB) by the proposed pharmaceutical agents, so preconditioning emerged as another option. The current study aimed to examine of how the expression levels of FL-, NT-, CNS- and reference PGC-1α isoforms change in different brain regions following various 1-methyl-4-phenyl-1,2,3,6-tetrahydropyridine (MPTP) treatment regimens, including chronic low-dose treatment for preconditioning. Ninety minutes following the acute treatment regimen, the expression levels of FL-, NT- and CNS-PGC-1α isoforms increased significantly in the striatum, cortex and cerebellum. However, this elevation diminished 7 days following the last MPTP injection in the acute treatment regimen. The chronic low-dose administration of MPTP, which did not cause significant toxic effects in light of the relatively unaltered dopamine levels, did not result in any significant change of PGC-1α expression. The elevation of PGC-1α levels following acute treatment may demonstrate a short-term compensatory mechanism against mitochondrial damage induced by the complex I inhibitor MPTP. However, drug-induced preconditioning by chronic low-dose MPTP seems not to induce protective responses via the PGC-1α system.

1. Introduction

Parkinson's disease (PD) is a progressive neurodegenerative disorder characterized by the loss of dopaminergic neurons, and the presence of Lewy bodies in the substantia nigra (SN) pars compacta (Forno, 1996). Although the precise pathomechanism of PD is not fully understood, several molecular mechanisms of neuronal death were described in the pathogenesis, including mitochondrial dysfunction, energy deficit and oxidative stress (Bose and Beal, 2016). It is postulated that life-long cumulative low-dose exposure to mitochondrial toxins may contribute to the pathogenesis of certain neurodegenerative disorders (Harris and Blain, 2004). The delineation of 1-methyl-4-phenyl-1,2,3,6-tetrahydropyridine (MPTP) induced Parkinsonian symptoms yielded one of the first pieces of evidence that mitochondrial dysfunction is involved in PD pathogenesis (Forno et al., 1993). Accordingly, systemic MPTP administration has been widely used to study disease mechanisms in various *in vivo* animal studies (Javitch et al., 1985).

Besides environmental factors, several causative or susceptibility genes have been identified in PD, many of them having direct implications in mitochondrial dysfunction (Kalinderi et al., 2016). Peroxisome proliferator-activated receptor-gamma (PPARγ) coactivator-1 alpha (PGC-1α) is one of them, which may play a role in PD pathogenesis. PGC-1α is a multifunctional transcriptional coactivator of nuclear respiratory factors 1 and 2 (NRF-1, -2), estrogen-related receptors (ERRs) and PPARs amongst others, and hereby regulates mitochondrial function and biogenesis (Knutti and Kralli, 2001).

Analysis of human brain samples indicated that PD is associated with the increased methylation of PGC-1α promoter and the reduced expression of PGC-1α itself (Su et al., 2015) and its downstream-regulated genes in the SN of PD patients (Zheng et al., 2010). Furthermore, possible associations of PGC-1α poly-

* Corresponding author.
E-mail address: klivenyi.peter@med.u-szeged.hu (P. Klivenyi).

http://dx.doi.org/10.1016/j.brainres.2017.01.032
0006-8993/

morphisms with PD risk, age of onset and longevity were described as well (Clark et al., 2011). Reduced expression of PGC-1α leads to enhanced α-synuclein oligomerization, too (Ebrahim et al., 2010), and accordingly, overexpression of PGC-1α produced neuroprotection against α-synuclein- and rotenone-induced neurotoxicity (Zheng et al., 2010).

Several PGC-1α isoforms were identified as a result of alternative splicing and alternative promoter usage (Martinez-Redondo et al., 2015). The proximal promoter of PGC-1α has been reported as an important key regulator in several neurodegenerative diseases, including PD (Su et al., 2015). With regard to alternative splicing, besides the full-length protein (FL-PGC-1α), the N-truncated PGC-1α (NT-PGC-1α) isoform was discovered, which is a shorter, but active isoform of PGC-1α (Zhang et al., 2009). Recent studies identified further different tissue-specific isoforms of PGC-1α, including central nervous system-specific isoforms (CNS-PGC-1α (Ruas et al., 2012; Soyal et al., 2012)). The novel CNS-specific isoforms originated from a new promoter located 587 kb upstream of exon 2 (Choi et al., 2013; Soyal et al., 2012). A recent study demonstrated that both PGC-1α reference gene and CNS-PGC-1α are downregulated in human PD brain and in experimental models with α-synuclein oligomerization, and that the pharmacological activation or genetic overexpression of PGC-1α reference gene reduced α-synuclein oligomerization and toxicity (Eschbach et al., 2015). In contrast, the loss of PGC-1α enhances the vulnerability of SN pars compacta dopaminergic neurons to α-synuclein toxicity (Ciron et al., 2015). These data suggest that PGC-1α downregulation and α-synuclein oligomerization form a vicious circle (Eschbach et al., 2015). Similarly to PD, certain mutations in amyotrophic lateral sclerosis inhibit the expression of CNS-specific isoforms, indicating this as a common finding in neurodegeneration (Bayer et al., 2017).

St-Pierre et al. described that PGC-1α-deficient mice are more sensitive to MPTP toxicity compared to the controls (St-Pierre et al., 2006). Interestingly, the sub-chronic administration of MPTP to mice resulted in the significant elevation of PGC-1α expression in the striatum after 24 h that was normalized following 72 h (Swanson et al., 2013). This may represent an adaptive mechanism to neurotoxicity. Accordingly, the protective effect of PGC-1α was demonstrated previously as well; pioglitazone- and resveratrol-induced activation of PGC-1α was protective against MPTP toxicity (Breidert et al., 2002; Dehmer et al., 2004). However, there is a seeming controversy with regard to the effect of genetically-induced overexpression of PGC-1α on MPTP neurotoxicity. On the one hand, the transgenic overexpression of PGC-1α was proven to be protective against MPTP (Mudo et al., 2012), on the other hand, the adenovirus vector-mediated overexpression of PGC-1α resulted in dopamine depletion in the SN (Ciron et al., 2012) and consequently enhanced susceptibility to MPTP (Clark et al., 2012). Clarification of this issue needs further studies.

Evidence suggests a beneficial role of PGC-1α stimulation in neurodegenerative disorders. However, CNS-targeted pharmacological stimulation is limited due to the poor penetration of the blood brain barrier (BBB) by the above-mentioned compounds, so preconditioning emerged as another option to achieve neuroprotection. It was previously demonstrated that the acute administration of the selective complex II inhibitor 3-nitropropionic acid (3-NP) increased the expression of both FL- and NT-PGC-1α isoforms in the striatum of C57Bl/6 mice (Torok et al., 2015). As the available data are limited with regard to the alteration of tissue-specific PGC-1α expression in the brain following MPTP administration, this study aimed to examine the expression levels of several PGC-1α isoforms in different brain regions following various MPTP treatment regimens. The hypothesis that low doses of MPTP may produce compensatory, protective alterations in the PGC-1α system was tested as well.

2. Results

2.1. Gene expression analysis

Ninety minutes following the last MPTP injection of the acute treatment of MPTP, the FL-PGC-1α and NT-PGC-1α expression significantly increased in the striatum (FL-PGC-1α: ctrl: 0.97 (0.92–1.04), MPTP: 1.47 (1.21–1.83), $p = 0.0048$; NT-PGC-1α: ctrl: 0.44 (0.40–0.49), MPTP: 0.70 (0.56–0.78), $p = 0.019$), cortex (FL-PGC-1α: ctrl: 0.96 (0.91–1.06), MPTP: 1.23 (1.15–1.43), $p = 0.009$; NT-PGC-1α: ctrl: 0.46 (0.43–0.48), MPTP: 0.69 (0.59–0.71), $p = 0.0012$) and cerebellum (FL-PGC-1α: ctrl: 1.50 (1.27–1.90), MPTP: 2.40 (2.07–2.76), $p = 0.013$; NT-PGC-1α: ctrl: 0.67 (0.48–0.86), MPTP: 1.21 (1.14–1.44), $p = 0.009$) (Fig. 1A, B). Furthermore, MPTP-induced increases in CNS-PGC-1α expression were also significantly larger in all investigated brain regions compared to the controls (striatum: ctrl: 1.03 (0.88–1.11), MPTP: 1.38 (1.34–1.78), $p = 0.0069$; cortex: ctrl: 0.91 (0.80–0.98), MPTP: 1.41 (1.24–1.42), $p = 0.0048$; cerebellum: ctrl: 1.51 (1.20–1.98), MPTP: 2.77 (2.34–3.17), $p = 0.019$) (Fig. 1C). However, there was not any difference between the Ref-PGC-1α levels in the striatum (ctrl: 0.11 (0.10–0.12), MPTP: 0.11 (0.95–0.12)), cortex (ctrl: 0.11 (0.11–0.12), MPTP: 0.09 (0.08–0.10)) and cerebellum (ctrl: 0.21 (0.20–0.29), MPTP: 0.28 (0.24–0.29)) of MPTP-treated and control mice (Fig. 1D).

One week following the last injection in the acute treatment regimen, there was not any significant change either in the FL-, NT-, CNS-, or in the Ref-PGC-1α levels between the control and the MPTP-treated animals in any brain area (Fig. 2A–D).

Furthermore, the low-dose 12-day MPTP-treatment did not influence the expression levels of FL-PGC-1α, NT-PGC-1α, CNS-PGC-1α and Ref-PGC-1α in any brain region (Fig. 3A–D).

2.2. HPLC measurement

Dopamine (DA), 3,4-dihydroxyphenylacetic acid (DOPAC) and homovanillic acid (HVA) values in the respective control groups of the 3 treatment regimens were compared to each other, and there were no significant differences. Therefore the values in these control groups were pooled for further comparisons with the MPTP-treated groups. MPTP administration caused significant reductions in striatal DA (ctrl: 8.08 ± 0.50, MPTP: 4.36 ± 0.92, $p = 0.0005$), DOPAC (ctrl: 2.57 ± 0.21, MPTP: 0.44 ± 0.08, $p = 3.78 * 10^{-8}$) and HVA (ctrl: 2.18 ± 0.12, MPTP 0.67 ± 0.11, $p = 5.12 * 10^{-10}$) levels compared to control values 90 min following its last administration in the acute treatment regimen (acute-1 day; Fig. 4). Moreover, a significant reduction in metabolite levels was also observed one week after the last injection in the acute treatment regimen (acute-7 days; Fig. 4) in the DA (ctrl: 8.08 ± 0.50, MPTP: 1.34 ± 0.43, $p = 4.86 * 10^{-8}$), DOPAC (ctrl: 2.57 ± 0.21, MPTP: 0.76 ± 0.15, $p = 7 * 10^{-6}$) and HVA (ctrl: 2.18 ± 0.12, MPTP: 0.81 ± 0.13, $p = 5.08 * 10^{-8}$) values in the striatum of the MPTP-treated mice compared to the control animals. However, chronic MPTP treatment resulted in significant reductions of only striatal HVA (ctrl: 2.18 ± 0.12, MPTP 1.40 ± 0.08, $p = 0.0005$) levels, striatal DA (ctrl: 8.08 ± 0.50, MPTP: 6.83 ± 0.48) and DOPAC (ctrl: 2.57 ± 0.21; MPTP 1.99 ± 0.23) levels were not decreased significantly (Fig. 4). Seven days following the acute treatment regimen DA levels significantly decreased compared to those data from samples obtained 90 min following the last MPTP injection in the acute treatment regimen ($p = 0.039$).

3. Discussion

PGC-1α is essential in normal mitochondrial function and its deficiency may contribute to neurodegeneration, while its stimula-

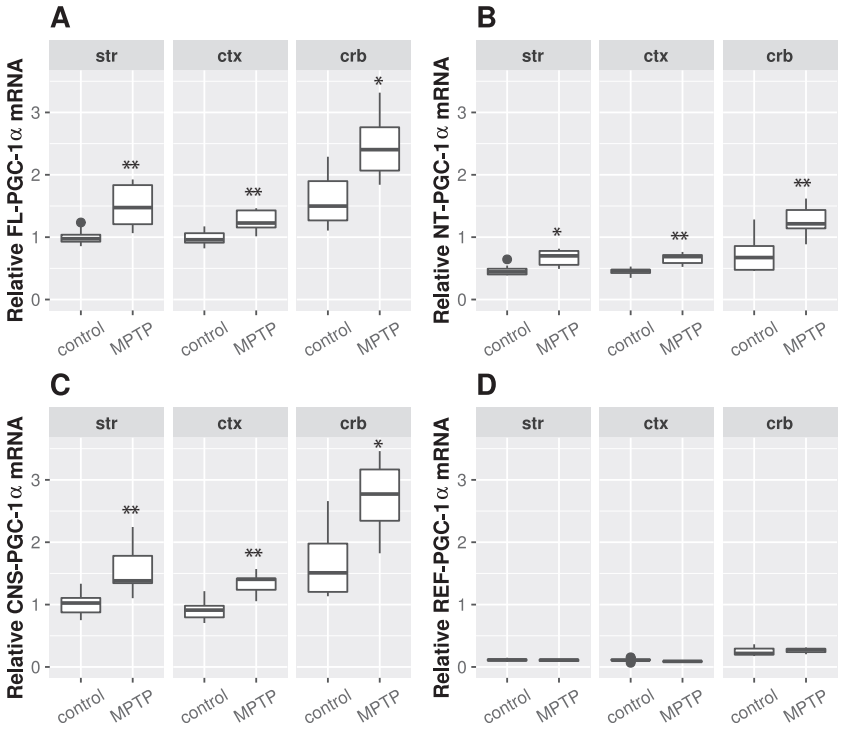

Fig. 1. The relative mRNA expression of PGC-1α isoforms in the striatum, cortex and the cerebellum of mice 90 min after acute MPTP intoxication. The FL-PGC-1α, NT-PGC-1α and CNS-PGC-1α levels were significantly increased in the striatum, cortex and the cerebellum of MPTP-treated mice. (A, B, C respectively). The Ref-PGC-1α expression did not change in any brain areas of MPTP-treated mice compared to the controls (D). Values are plotted as medians and interquartile range; $^{*}p < 0.05$, $^{**}p < 0.01$; *MPTP* MPTP-treated; *str* striatum, *ctx* cortex, *crb* cerebellum.

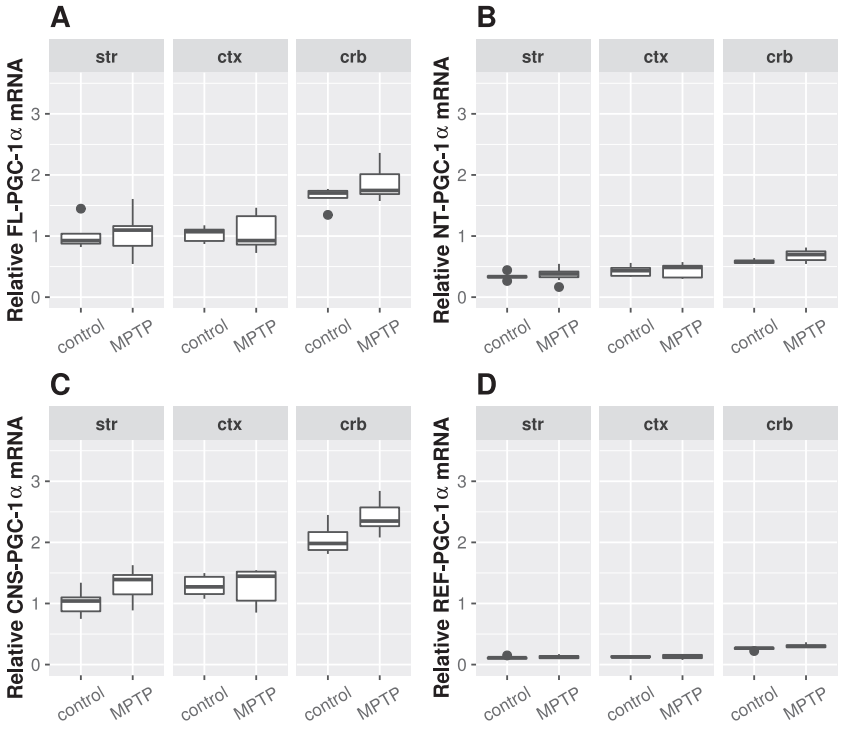

Fig. 2. The relative mRNA expression of PGC-1α isoforms in the striatum, cortex and the cerebellum of mice 7 days after acute MPTP intoxication. The expression levels of the PGC-1α isoforms did not change in any brain areas of MPTP-treated mice (A–D). Values are plotted as medians and interquartile range; *MPTP* MPTP-treated; *str* striatum, *ctx* cortex, *crb* cerebellum.

tion was demonstrated to be neuroprotective in certain models (Breidert et al., 2002; Dehmer et al., 2004; Eschbach et al., 2015; Mudo et al., 2012). Accordingly, the pharmacological induction of PGC-1α expression may be considered as a neuroprotective approach, but currently this possibility seems to be limited in light of the reduced BBB penetration of the potential pharmaceutical agents.

The aim of the current study was a thorough assessment of the expression of PGC-1α isoforms in various brain regions following different MPTP administration regimens, including a

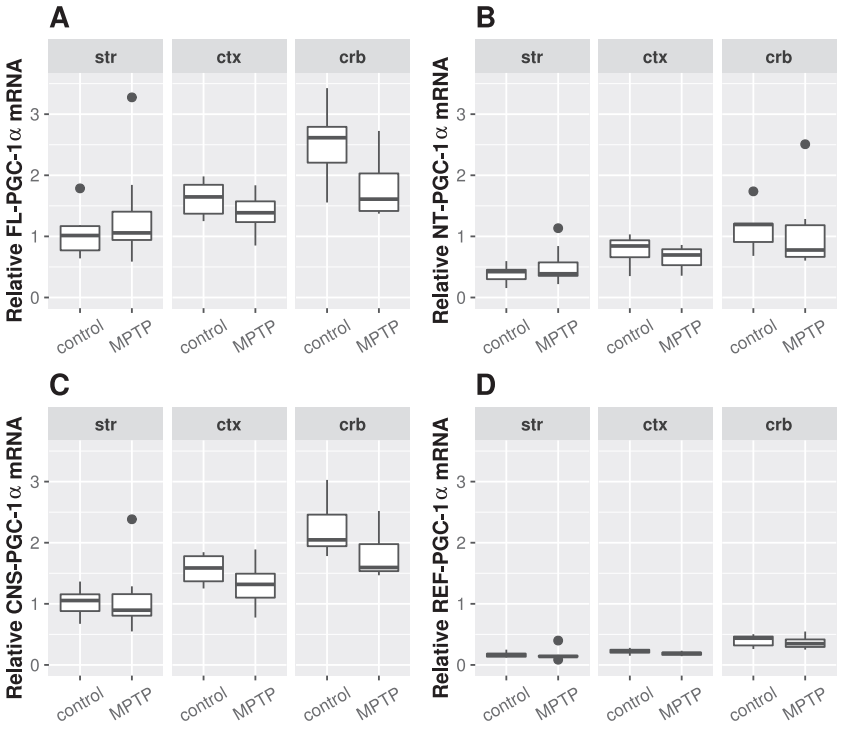

Fig. 3. The relative mRNA expression of PGC-1α isoforms in the striatum, cortex and the cerebellum of mice following a 12-day treatment with low-dose MPTP. The expression levels of the PGC-1α isoforms did not change in any brain areas of MPTP-treated mice (A–D). Values are plotted as medians and interquartile range; *MPTP* MPTP-treated; *str* striatum, *ctx* cortex, *crb* cerebellum.

low-dose chronic one, possibly mimicking drug-induced preconditioning.

Ninety minutes following the last MPTP injection of the high-dose acute treatment regimen of MPTP (75 mg/kg/day total dose) the expression level of FL-, NT- and CNS- PGC-1α isoforms increased significantly in the striatum, cortex and cerebellum. However, this elevation was diminished 7 days following the last MPTP injection in the acute treatment regimen. Torok et al. (Torok et al., 2015) demonstrated that the acute (90 min following a single dose injection of 100 mg/kg dose), but not the subacute (50 mg/kg twice daily for 5 days) 3-NP treatment regimen induced the overexpression of FL- and NT- PGC-1α isoforms mainly in the striatum (3-NP is a rather selective striatal neurotoxin (Brouillet et al., 2005)) similar to the results of the current study. Those findings were explained by a proposed reduced neuronal adaptive capability of the striatum following the neurotoxic insult. The above-mentioned results of the current study may also be explained by the propagation of the neurotoxic process following 7 days of the acute treatment regimen given the extent of decrease in striatal DA levels. The elevation of PGC-1α expression, especially that of the CNS-specific isoform, may indicate a short-term compensatory protective mechanism against mitochondrial dysfunction induced by the complex I inhibitor MPTP. It is hard to interpret the increased expression of PGC-1α in the cerebellum, which is not primarily affected in MPTP toxicity. However, several lines of evidence indicate that MPTP neurotoxicity is not highly selective to dopaminergic neurons; in specific circumstances systemic MPTP administration resulted in Purkinje cell loss (Takada et al., 1993). The involvement of the cerebellum in disease mechanisms of different neurodegenerative disorders such as amyotrophic lateral sclerosis, Huntington's disease (HD) and PD is frequently seen (Rees et al., 2014; Tan et al., 2016; Wu and Hallett, 2013). Furthermore, increasing evidence suggest that PGC-1α expression is associated with degenerative changes in the CNS, including cerebellum (Torok et al., 2015). It was hypothesized that the elevation of PGC-1α in the cerebellum is a compensatory mechanism against the energy deficit which may be an important factor underlying the relative resistance of cerebellar neurons against neurodegenerative processes in HD and in PD.

The drug-induced preconditioning by applying low-dose neurotoxic agents may stimulate neuroprotective mechanisms, resulting in the amelioration of neurodegenerative process. This approach has already been demonstrated to be beneficial in case of 3-NP: the low-dose of toxin treatment increased tolerance to ischemia and hypoxia in rats and gerbils (Horiguchi et al., 2003; Riepe et al., 1997; Wiegand et al., 1999). Although the exact mechanism is not fully understood, the overexpression of free radical scavenging enzymes may be involved: acute 3-NP treatment activated superoxide dismutase (SOD) and catalase (CAT) in several brain areas (Binienda et al., 1998). Similarly, an increase in SOD activity in the glial cells of the striatum and SN was observed following MPTP treatment (Kurosaki et al., 2004). The preconditioning by MPTP is not intended to suggest a future direct therapeutic approach, but rather aimed at finding key players which may help to alleviate the pathological alterations. The situation may be similar to ischemic preconditioning where the outcome in myocardial infarction may depend substantially on which medications were applied with an influence on preconditioning (Tomai et al., 1999). This may be especially important in light of the fact that environmental toxins could play a role in the pathogenies of idiopathic PD. The chronic low-dose administration of MPTP in the current study neither resulted in significant DA depletion (i.e. neurotoxic effect at biochemical level), nor in any significant change in PGC-1α expression. These data suggest that drug-induced preconditioning by MPTP may not evoke apparent responses in the PGC-1α system.

In conclusion the current study demonstrated that acute severe mitochondrial dysfunction initiated protection via elevating the expression of brain specific isoforms of the mitochondrial master regulator PGC-1α. However, low-dose chronic administration of

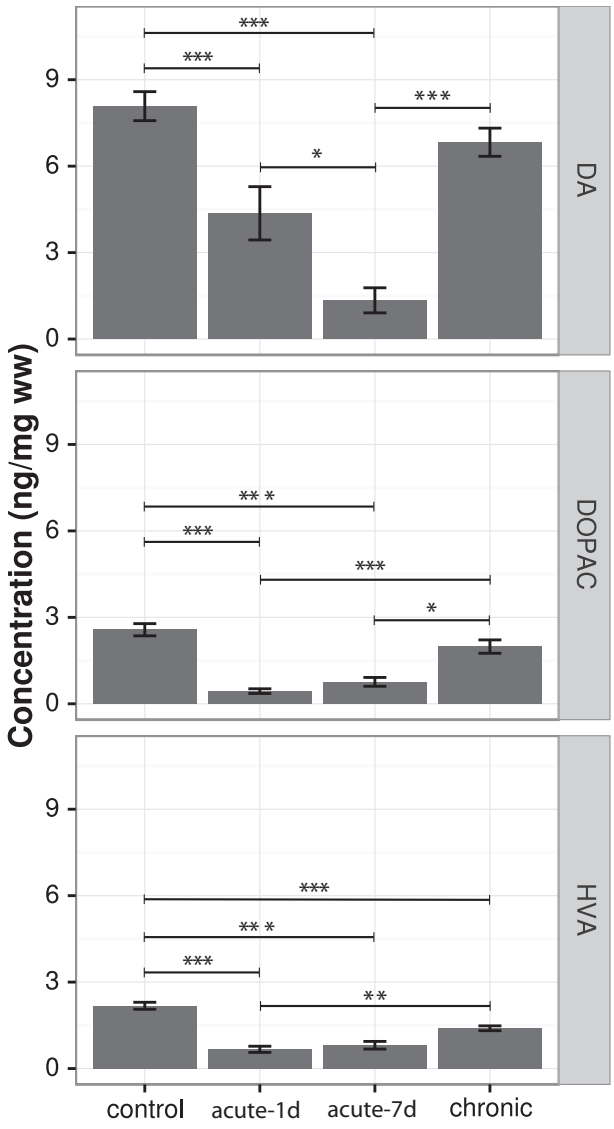

Fig. 4. Striatal dopamine, DOPAC and HVA concentrations of MPTP-treated mice in 3 different treatment regimens. Ninety minutes (acute-1d) and 7 days (acute-7d) after acute MPTP intoxication, DA, DOPAC and HVA levels significantly decreased in the striatum compared to the controls. The chronic (12 day) low-dose MPTP treatment did not influence the striatal level of DA and DOPAC, only HVA levels were significantly decreased. Values are plotted as means ± S.E.M; $^{***}p < 0.001$; *DA* dopamine, *DOPAC* 3,4-dihydroxyphenylacetic acid, *HVA* homovanillic acid.

mitochondrial toxin MPTP did not induce those protective mechanisms with the involvement of PGC-1α.

4. Experimental procedures

4.1. Animals

12-Week-old C57Bl/6J male mice were used in this study. The animal strain was originally obtained from Jackson Labs (Jackson Laboratories, Bar Harbor, ME, USA).

The animals were housed in cages and maintained under standard laboratory conditions with 12–12 h light–dark cycle and free access to food and water. The experiments were carried out in accordance with the European Communities Council Directive (86/609/EEC) and were approved by the local animal care committee.

4.2. Treatment and sample handling

MPTP was dissolved in phosphate-buffered saline (PBS; pH adjusted to 7.4) and was administered intraperitoneally (i.p.). Animals were randomly divided into six groups (n = 7–8 in each group). The first and second group received i.p. injection of 15 mg/kg body weight MPTP 5 times at 2 h intervals. The animals in the first group were deeply anesthetized with isoflurane (Forane; Abott Laboratories Hungary Ltd., Budapest, Hungary) and the brains were dissected ninety minutes following the last MPTP injection (acute treatment – acute (day 1) assessment), while animals in the second group were deeply anesthetized with isoflurane and the brains were dissected one week later (acute treatment – subacute (day 7) assessment). The mice in the third group were injected i.p. with 15 mg/kg body weight MPTP once a day for 12 days (low-dose chronic treatment). Ninety minutes following the last injection the animals were euthanized via isoflurane overdose as well. The fourth, fifth and sixth groups served as the respective control groups, and were injected with 0.1 M PBS according to the above-detailed treatment regimen. During the dissection process the brains were rapidly removed on ice and immediately halved at the midline. Following that, both hemispheres were further cut to obtain the striatum, cortex and cerebellum. Thereafter, these samples were stored at −80°C until the RT-PCR and HPLC analysis.

4.3. RT-PCR analysis

The left striatum, cortex and cerebellum were homogenized and Trizol reagent was used to extract RNA according to the manufacturer's protocol. The RNA was quantified spectrophotometrically, and the integrity of RNA was confirmed by gel electrophoresis using 1% agarose gel. 1 μg of total RNA was reverse-transcribed applying random hexamer primers and reverse transcriptase according to the RevertAid First Strand cDNA Synthesis Kit protocol (Thermo Fisher Scientific Inc., Marietta, OH, USA). cDNAs were kept at −20°C until further use.

Real-time PCR reactions were carried out in a 20 μl final volume.

The following, previously published primers were used: for FL-PGC-1α, 5′-TGCCATTGTTAAGACCGAG-3′ (forward) and 5′-TTGGG GTCATTTGGTGAC-3′ (reverse); for NT-PGC-1α, 5′-GGTCACTGGAA GATATGGC-3′ (reverse); for CNS-PGC-1α and Ref-PGC-1α, 5′-AAT TGGAGCCCCATGGATGAAGG-3′ and 5′-TGAGTCTGTATGGAGTGA CATCGAGTG-3′ (both forward), and 5′-TCAAATGAGGG CAATCCGTC-3′ (reverse), respectively (Chang et al., 2012; Soyal et al., 2012). qRT-PCR reaction conditions were 95°C for 2 min, followed by 40 cycles of 95°C for 10 s, and 60°C for 30 s. Target gene expression was normalized to the endogenous control gene 18S rRNA (Applied Biosystems, Carlsbad, CA, USA). The relative expression was determined using the $2^{-\Delta\Delta Ct}$ method (Livak and Schmittgen, 2001).

4.4. Dopamine measurement

DA and its metabolites, DOPAC and HVA were measured by reversed-phase chromatography from the right striatum of the MPTP-treated and the control animals, using an Agilent 1100 high-performance liquid chromatography (HPLC) system (Agilent Technologies, Santa Clara, CA, USA) combined with a Model 105 electrochemical detector (Precision Instruments, Marseille, France) under isocratic conditions. The striata were weighed and then homogenized in an ice-cold solution (750 μl) containing perchloric acid (70% wt/wt), sodium metabisulfite (0.1 M), disodium ethylenediaminetetraacetate (0.1 M), distilled water and 0.25 mM isoproterenol for 30 s. The homogenate was centrifuged at

12,000*g* for 10 min at 4°C. The supernatant was stored at −20°C until the analysis. The supernatants were measured with an Agilent 1100 high-performance liquid chromatography (HPLC) system (Agilent Technologies, Santa Clara, CA, USA) combined with a Model 105 electrochemical detector (Precision Instruments, Marseille, France) under isocratic conditions. In brief, the working potential of the detector was set at +750 mV, using a glassy carbon electrode and a Ag/AgCl reference electrode. The mobile phase containing sodium dihydrogenphosphate (75 mM), sodium octylsulfate (2.8 mM) and disodium ethylenediaminetetraacetate (50 μM) was supplemented with acetonitrile (10% v/v) and the pH was adjusted to 3 with phosphoric acid (85% w/w). The mobile phase was delivered at a rate of 1 ml/min at 40°C onto the reversed-phase column (HR-80 C18, 80 × 4.6 mm, 3 μm particle size; ESA Biosciences, Chelmsford, MA, USA) after passage through a pre-column (SecurityGuard, 4 × 3.0 mm I.D., 5 μm particle size, Phenomenex Inc., Torrance, CA, USA)). 10 μl aliquots were injected by the autosampler with the cooling module set at 4°C. With regard to method validation, the following parameters are reported briefly. The LOD and LLOQ for the investigated compounds in the brain samples were 2 ng/ml and 10 ng/ml, respectively. With regard to precision, the relative standard deviation was ⩽ 3.25% for the peak area responses and ⩽ 0.05% for the retention times. The recoveries ranged from 109 to 110%, 108 to 109% and 99 to 102% for DA, DOPAC and HVA, respectively.

4.5. Statistics

All statistical analyses were performed with the use of the R software (R Development Core Team). The distribution of data populations was checked with the Shapiro–Wilk test, and Levene test was also performed for the analysis of the homogeneity of variances. In case of gene expression analysis, due to the necessity of a large number of comparisons of data, two-sample *t*-tests *via* Monte-Carlo permutation (with 10,000 random permutations) were applied for RT-PCR results. In case of HPLC analysis, all the data exhibited normal distribution and equal variances were assumed, and therefore ANOVA was used with Bonferroni post hoc comparison. The null hypothesis was rejected when the corrected p values were < 0.05, and in such cases the differences were considered significant. FL- and NT-PGC-1α levels of gene expression of all brain areas were calculated relative to the levels of FL-PGC-1α gene expression in the striatum, whereas the CNS- and Ref-PGC-1α expression levels of all brain areas were calculated relative to the level of CNS-PGC-1α expression in the striatum. Data with Gaussian or non-Gaussian distributions were plotted as means (± S.E.M.) or medians (and interquartile range), respectively.

Funding sources

The study was supported by the Hungarian Brain Research Program – Grant No. KTIA_13_NAP-A-II/18 and MTA-SZTE Neuroscience Research Group. Denes Zadori was supported by the Janos Bolyai Research Scholarship of the Hungarian Academy of Sciences.

Conflict of interest

The authors declare there is no conflict of interest.

References

Bayer, H., Lang, K., Buck, E., Higelin, J., Barteczko, L., Pasquarelli, N., Sprissler, J., Lucas, T., Holzmann, K., Demestre, M., Lindenberg, K.S., Danzer, K.M., Boeckers, T., Ludolph, A.C., Dupuis, L., Weydt, P., Witting, A., 2017. ALS-causing mutations differentially affect PGC-1alpha expression and function in the brain vs. peripheral tissues. Neurobiol. Dis. 97, 36–45.

Binienda, Z., Simmons, C., Hussain, S., Slikker Jr., W., Ali, S.F., 1998. Effect of acute exposure to 3-nitropropionic acid on activities of endogenous antioxidants in the rat brain. Neurosci. Lett. 251, 173–176.

Bose, A., Beal, M.F., 2016. Mitochondrial dysfunction in Parkinson's disease. J. Neurochem. 139 (Suppl 1), 216–231.

Breidert, T., Callebert, J., Heneka, M.T., Landreth, G., Launay, J.M., Hirsch, E.C., 2002. Protective action of the peroxisome proliferator-activated receptor-gamma agonist pioglitazone in a mouse model of Parkinson's disease. J. Neurochem. 82, 615–624.

Brouillet, E., Jacquard, C., Bizat, N., Blum, D., 2005. 3-Nitropropionic acid: a mitochondrial toxin to uncover physiopathological mechanisms underlying striatal degeneration in Huntington's disease. J. Neurochem. 95, 1521–1540.

Chang, J.S., Fernand, V., Zhang, Y., Shin, J., Jun, H.J., Joshi, Y., Gettys, T.W., 2012. NT-PGC-1alpha protein is sufficient to link beta3-adrenergic receptor activation to transcriptional and physiological components of adaptive thermogenesis. J. Biol. Chem. 287, 9100–9111.

Choi, J., Batchu, V.V., Schubert, M., Castellani, R.J., Russell, J.W., 2013. A novel PGC-1alpha isoform in brain localizes to mitochondria and associates with PINK1 and VDAC. Biochem. Biophys. Res. Commun. 435, 671–677.

Ciron, C., Lengacher, S., Dusonchet, J., Aebischer, P., Schneider, B.L., 2012. Sustained expression of PGC-1alpha in the rat nigrostriatal system selectively impairs dopaminergic function. Hum. Mol. Genet. 21, 1861–1876.

Ciron, C., Zheng, L., Bobela, W., Knott, G.W., Leone, T.C., Kelly, D.P., Schneider, B.L., 2015. PGC-1alpha activity in nigral dopamine neurons determines vulnerability to alpha-synuclein. Acta Neuropathol. Commun. 3, 16.

Clark, J., Reddy, S., Zheng, K., Betensky, R.A., Simon, D.K., 2011. Association of PGC-1alpha polymorphisms with age of onset and risk of Parkinson's disease. BMC Med. Genet. 12, 69.

Clark, J., Silvaggi, J.M., Kiselak, T., Zheng, K., Clore, E.L., Dai, Y., Bass, C.E., Simon, D.K., 2012. Pgc-1alpha overexpression downregulates Pitx3 and increases susceptibility to MPTP toxicity associated with decreased Bdnf. PLoS ONE 7, e48925.

Dehmer, T., Heneka, M.T., Sastre, M., Dichgans, J., Schulz, J.B., 2004. Protection by pioglitazone in the MPTP model of Parkinson's disease correlates with I kappa B alpha induction and block of NF kappa B and iNOS activation. J. Neurochem. 88, 494–501.

Ebrahim, A.S., Ko, L.W., Yen, S.H., 2010. Reduced expression of peroxisome-proliferator activated receptor gamma coactivator-1alpha enhances alpha-synuclein oligomerization and down regulates AKT/GSK3beta signaling pathway in human neuronal cells that inducibly express alpha-synuclein. Neurosci. Lett. 473, 120–125.

Eschbach, J., von Einem, B., Muller, K., Bayer, H., Scheffold, A., Morrison, B.E., Rudolph, K.L., Thal, D.R., Witting, A., Weydt, P., Otto, M., Fauler, M., Liss, B., McLean, P.J., Spada, A.R., Ludolph, A.C., Weishaupt, J.H., Danzer, K.M., 2015. Mutual exacerbation of peroxisome proliferator-activated receptor gamma coactivator 1alpha deregulation and alpha-synuclein oligomerization. Ann. Neurol. 77, 15–32.

Forno, L.S., DeLanney, L.E., Irwin, I., Langston, J.W., 1993. Similarities and differences between MPTP-induced parkinsonsim and Parkinson's disease. Neuropathologic considerations. Adv. Neurol. 60, 600–608.

Forno, L.S., 1996. Neuropathology of Parkinson's disease. J. Neuropathol. Exp. Neurol. 55, 259–272.

Harris, J.B., Blain, P.G., 2004. Neurotoxicology: what the neurologist needs to know. J. Neurol. Neurosurg. Psychiatry 75 (Suppl 3), iii29–iii34.

Horiguchi, T., Kis, B., Rajapakse, N., Shimizu, K., Busija, D.W., 2003. Opening of mitochondrial ATP-sensitive potassium channels is a trigger of 3-nitropropionic acid-induced tolerance to transient focal cerebral ischemia in rats. Stroke 34, 1015–1020.

Javitch, J.A., D'Amato, R.J., Strittmatter, S.M., Snyder, S.H., 1985. Parkinsonism-inducing neurotoxin, N-methyl-4-phenyl-1,2,3,6 -tetrahydropyridine: uptake of the metabolite N-methyl-4-phenylpyridine by dopamine neurons explains selective toxicity. Proc. Natl. Acad. Sci. U.S.A. 82, 2173–2177.

Kalinderi, K., Bostantjopoulou, S., Fidani, L., 2016. The genetic background of Parkinson's disease: current progress and future prospects. Acta Neurol. Scand. 134, 314–326.

Knutti, D., Kralli, A., 2001. PGC-1, a versatile coactivator. Trends Endocrinol. Metab. 12, 360–365.

Kurosaki, R., Muramatsu, Y., Kato, H., Araki, T., 2004. Biochemical, behavioral and immunohistochemical alterations in MPTP-treated mouse model of Parkinson's disease. Pharmacol. Biochem. Behav. 78, 143–153.

Livak, K.J., Schmittgen, T.D., 2001. Analysis of relative gene expression data using real-time quantitative PCR and the 2(-Delta Delta C(T)) Method. Methods 25, 402–408.

Martinez-Redondo, V., Pettersson, A.T., Ruas, J.L., 2015. The hitchhiker's guide to PGC-1alpha isoform structure and biological functions. Diabetologia 58, 1969–1977.

Mudo, G., Makela, J., Di Liberto, V., Tselykh, T.V., Olivieri, M., Piepponen, P., Eriksson, O., Malkia, A., Bonomo, A., Kairisalo, M., Aguirre, J.A., Korhonen, L., Belluardo, N., Lindholm, D., 2012. Transgenic expression and activation of PGC-1alpha protect dopaminergic neurons in the MPTP mouse model of Parkinson's disease. Cell. Mol. Life Sci. 69, 1153–1165.

Rees, E.M., Farmer, R., Cole, J.H., Haider, S., Durr, A., Landwehrmeyer, B., Scahill, R.I., Tabrizi, S.J., Hobbs, N.Z., 2014. Cerebellar abnormalities in Huntington's disease: a role in motor and psychiatric impairment? Mov. Disord. 29, 1648–1654.

Riepe, M.W., Esclaire, F., Kasischke, K., Schreiber, S., Nakase, H., Kempski, O., Ludolph, A.C., Dirnagl, U., Hugon, J., 1997. Increased hypoxic tolerance by chemical inhibition of oxidative phosphorylation: "chemical preconditioning". J. Cereb. Blood Flow Metab. 17, 257–264.

Ruas, J.L., White, J.P., Rao, R.R., Kleiner, S., Brannan, K.T., Harrison, B.C., Greene, N.P., Wu, J., Estall, J.L., Irving, B.A., Lanza, I.R., Rasbach, K.A., Okutsu, M., Nair, K.S., Yan, Z., Leinwand, L.A., Spiegelman, B.M., 2012. A PGC-1alpha isoform induced by resistance training regulates skeletal muscle hypertrophy. Cell 151, 1319–1331.

Soyal, S.M., Felder, T.K., Auer, S., Hahne, P., Oberkofler, H., Witting, A., Paulmichl, M., Landwehrmeyer, G.B., Weydt, P., Patsch, W.European Huntington Disease Network, 2012. A greatly extended PPARGC1A genomic locus encodes several new brain-specific isoforms and influences Huntington disease age of onset. Hum. Mol. Genet. 21, 3461–3473.

St-Pierre, J., Drori, S., Uldry, M., Silvaggi, J.M., Rhee, J., Jager, S., Handschin, C., Zheng, K., Lin, J., Yang, W., Simon, D.K., Bachoo, R., Spiegelman, B.M., 2006. Suppression of reactive oxygen species and neurodegeneration by the PGC-1 transcriptional coactivators. Cell 127, 397–408.

Su, X., Chu, Y., Kordower, J.H., Li, B., Cao, H., Huang, L., Nishida, M., Song, L., Wang, D., Federoff, H.J., 2015. PGC-1alpha promoter methylation in Parkinson's disease. PLoS ONE 10, e0134087.

Swanson, C.R., Du, E., Johnson, D.A., Johnson, J.A., Emborg, M.E., 2013. Neuroprotective properties of a novel non-thiazoledinedione partial PPAR-gamma agonist against MPTP. PPAR Res. 2013, 582809.

Takada, M., Sugimoto, T., Hattori, T., 1993. MPTP neurotoxicity to cerebellar Purkinje cells in mice. Neurosci. Lett. 150, 49–52.

Tan, R.H., Kril, J.J., McGinley, C., Hassani, M., Masuda-Suzukake, M., Hasegawa, M., Mito, R., Kiernan, M.C., Halliday, G.M., 2016. Cerebellar neuronal loss in amyotrophic lateral sclerosis cases with ATXN2 intermediate repeat expansions. Ann. Neurol. 79, 295–305.

Tomai, F., Crea, F., Chiariello, L., Gioffre, P.A., 1999. Ischemic preconditioning in humans: models, mediators, and clinical relevance. Circulation 100, 559–563.

Torok, R., Konya, J.A., Zadori, D., Veres, G., Szalardy, L., Vecsei, L., Klivenyi, P., 2015. MRNA expression levels of PGC-1alpha in a transgenic and a toxin model of Huntington's disease. Cell. Mol. Neurobiol. 35, 293–301.

Wiegand, F., Liao, W., Busch, C., Castell, S., Knapp, F., Lindauer, U., Megow, D., Meisel, A., Redetzky, A., Ruscher, K., Trendelenburg, G., Victorov, I., Riepe, M., Diener, H. C., Dirnagl, U., 1999. Respiratory chain inhibition induces tolerance to focal cerebral ischemia. J. Cereb. Blood Flow Metab. 19, 1229–1237.

Wu, T., Hallett, M., 2013. The cerebellum in Parkinson's disease. Brain 136, 696–709.

Zhang, Y., Huypens, P., Adamson, A.W., Chang, J.S., Henagan, T.M., Boudreau, A., Lenard, N.R., Burk, D., Klein, J., Perwitz, N., Shin, J., Fasshauer, M., Kralli, A., Gettys, T.W., 2009. Alternative mRNA splicing produces a novel biologically active short isoform of PGC-1alpha. J. Biol. Chem. 284, 32813–32826.

Zheng, B., Liao, Z., Locascio, J.J., Lesniak, K.A., Roderick, S.S., Watt, M.L., Eklund, A.C., Zhang-James, Y., Kim, P.D., Hauser, M.A., Grunblatt, E., Moran, L.B., Mandel, S.A., Riederer, P., Miller, R.M., Federoff, H.J., Wullner, U., Papapetropoulos, S., Youdim, M.B., Cantuti-Castelvetri, I., Young, A.B., Vance, J.M., Davis, R.L., Hedreen, J.C., Adler, C.H., Beach, T.G., Graeber, M.B., Middleton, F.A., Rochet, J.C., Scherzer, C.R. Global PD Gene Expression (GPEX) Consortium, 2010. PGC-1alpha, a potential therapeutic target for early intervention in Parkinson's disease. Sci. Transl. Med. 2, 52ra73.

V.

Received: 31 October 2016 | Revised: 20 January 2017 | Accepted: 6 February 2017

DOI 10.1002/bmc.3953

WILEY Biomedical Chromatography

RESEARCH ARTICLE

The establishment of tocopherol reference intervals for Hungarian adult population using a validated HPLC method

Gábor Veres[1,2] | László Szpisjak[1] | Attila Bajtai[1] | Andrea Siska[3] | Péter Klivényi[1] | István Ilisz[4] | Imre Földesi[3] | László Vécsei[1,2] | Dénes Zádori[1]

[1] Department of Neurology, Faculty of Medicine, Albert Szent-Györgyi Clinical Center, University of Szeged, Szeged, Hungary

[2] MTA-SZTE Neuroscience Research Group, Szeged, Hungary

[3] Department of Laboratory Medicine, Faculty of Medicine, Albert Szent-Györgyi Clinical Center, University of Szeged, Szeged, Hungary

[4] Department of Inorganic and Analytical Chemistry, Faculty of Science and Informatics, University of Szeged, Szeged, Hungary

Correspondence
Dénes Zádori, Department of Neurology, Faculty of Medicine, Albert Szent-Györgyi Clinical Center, University of Szeged, Semmelweis u. 6, H-6725 Szeged, Hungary.
Email: zadori.denes@med.u-szeged.hu

Funding information
János Bolyai Research Scholarship of the Hungarian Academy of Sciences; Hungarian Brain Research Program, Grant/Award Number: KTIA_13_NAP-A_II/18.

Abstract

Evidence suggests that decreased α-tocopherol (the most biologically active substance in the vitamin E group) level can cause neurological symptoms, most likely ataxia. The aim of the current study was to first provide reference intervals for serum tocopherols in the adult Hungarian population with appropriate sample size, recruiting healthy control subjects and neurological patients suffering from conditions without symptoms of ataxia, myopathy or cognitive deficiency. A validated HPLC method applying a diode array detector and rac-tocol as internal standard was utilized for that purpose. Furthermore, serum cholesterol levels were determined as well for data normalization. The calculated 2.5–97.5% reference intervals for α-, β/γ- and δ-tocopherols were 24.62–54.67, 0.81–3.69 and 0.29–1.07 μM, respectively, whereas the tocopherol/cholesterol ratios were 5.11–11.27, 0.14–0.72 and 0.06–0.22 μmol/mmol, respectively. The establishment of these reference intervals may improve the diagnostic accuracy of tocopherol measurements in certain neurological conditions with decreased tocopherol levels. Moreover, the current study draws special attention to the possible pitfalls in the complex process of the determination of reference intervals as well, including the selection of study population, the application of internal standard and method validation and the calculation of tocopherol/cholesterol ratios.

KEYWORDS

cholesterol, HPLC, human samples, reference interval, tocopherol

1 | INTRODUCTION

Most of the deleterious effects of pathological processes in the human organism are mediated by the formation of reactive species (RS; Szalárdy, Zádori, Klivényi, Toldi, & Vécsei, 2015). The synthesis and toxic effects of RS are ameliorated by a complex system of antioxidant machinery, including enzymatic (e.g. superoxide dismutase, catalase and glutathione peroxidase; Sies, 1997) and nonenzymatic mechanisms (Figure 1).

The latter group consists of numerous chemical compounds, such as vitamin E, vitamin C, coenzyme Q10, β-carotene, glutathione and flavonoids with proved antioxidant properties (Sies, 1993). In addition to the capability of these agents to react with RS, their sufficient tissue concentrations and their suitability for regeneration are desirable properties as well for efficient antioxidant protection (Rose & Bode, 1993).

Abbreviations used: α-TTP, α-tocopherol transport protein; ACN, acetonitrile; BHT, butylated hydroxy toluene; OND, other neurological disease; RI, reference interval; RS, reactive species; THF, tetrahydofurane

The vitamin E group includes four tocotrienols and four tocopherols as lipid soluble antioxidants. Their molecular structure comprises a chromanol ring with an aliphatic side chain, unsaturated for tocotrienols and saturated for tocopherols. Depending on the number and position of methyl groups on the chromanol ring, α-, β-, γ- and δ-tocotrienols and tocopherols can be distinguished (Hacquebard & Carpentier, 2005). The bioavailability of tocotrienols is inefficient and physiological serum concentrations are low (O'Byrne et al., 2000), suggesting that under normal circumstances their role as antioxidants is negligible. However, increasing α-tocotrienol concentration by its external supplementation can ameliorate the symptoms caused by α-tocopherol deficiency (Sen, Khanna, & Roy, 2007). α-Tocopherol has the highest concentration and biological activity from the vitamin E group, while the other tocopherols have a less expressed role in antioxidant protection (Hacquebard & Carpentier, 2005). Tocopherols are taken up by the enterocytes from the intestines and they are incorporated into the secreted chylomicrons and transported to the liver (Cooper, 1997). In the liver, the cytosolic α-tocopherol transport protein (α-TTP)

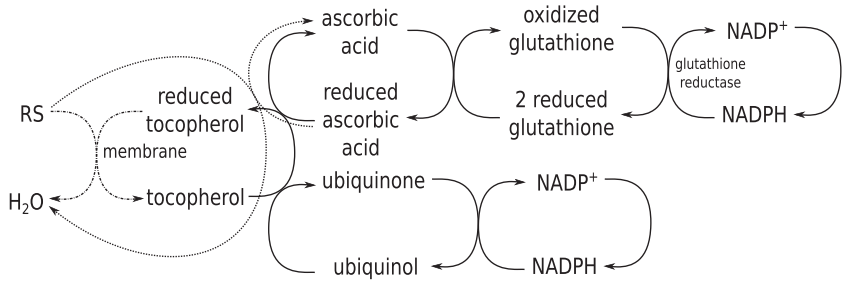

FIGURE 1 The schematic depiction of nonenzymatic mechanisms in antioxidant protection. NADPH, reduced nicotinamide adenine dinucleotide phosphate; RS, reactive species

recognizes and binds α-tocopherol with good selectivity, and the majority of the other forms of tocopherols are rapidly excreted in the bile. α-TTP is responsible for the secretion of α-tocopherol into plasma and very-low-density lipoprotein particles (Arita, Nomura, Arai, & Inoue, 1997). Very-low-density lipoprotein is catabolized on the periphery by lipoprotein lipase, localized at the endothelium, and the formed high-density lipoprotein and low-density lipoprotein particles become responsible for the distribution of α-tocopherol to extrahepatic tissues (Mardones & Rigotti, 2004). With regard to the other forms of vitamin E, there is no discrimination between them and α-tocopherol during absorption from the intestines; however, in the liver there is a preferential secretion of α-tocopherol into the blood, as well as a preferential metabolism of the other forms (Traber, 2013). Accordingly, cholesterol levels and metabolism may considerably influence the bioavailability of tocopherols (Schmölz, Birringer, Lorkowski, & Wallert, 2016).

The major causes of severe tocopherol deficiency are malabsorption disorders with decreased intestinal lipid uptake (e.g. cholestasis, cystic fibrosis, short bowel syndrome), abetalipoproteinemia and ataxia with vitamin E deficiency where the underlying pathological alteration is the decreased activity of α-TTP caused by mutations in the TTPA gene (Morley et al., 2004).

Decreased vitamin-E levels are associated with several neurological symptoms, such as cerebellar ataxia, peripheral neuropathy and myopathy (Muller, 2010; Ueda et al., 2009), as the nervous system is particularly sensitive to oxidative damage resulting from reduced antioxidant capacity (Zádori, Klivényi, Plangár, Toldi, & Vécsei, 2011; Zádori et al., 2012). Accordingly, in addition to the above-mentioned disorders with their characteristic symptoms, some other neuropsychiatric conditions, such as Alzheimer's disease (Lopes da Silva et al., 2014) and the exacerbation of multiple sclerosis (Karg et al., 1999) can also be accompanied by significantly reduced serum or plasma tocopherol levels. Therefore, the measurement of serum tocopherol levels is advised to be part of the differential diagnostic process in certain neuropsychiatric conditions. The establishment of unbiased reference values for the targeted population is essential for that purpose.

The aim of the current study was to develop an unbiased method for tocopherol (α-, β/γ- and δ-tocopherol) measurements in human serum samples and to hereby establish reference intervals (RI) via the participation of 120 individuals for the adult Hungarian population based on the pooling of the values of control subjects without any chronic disease and neurological patients suffering from conditions without symptoms of ataxia, myopathy or cognitive deficiency (the so-called control group of other neurological diseases; OND).

2 | MATERIALS AND METHODS

2.1 | Materials

The investigated reference compounds {α-, γ-, δ-tocopherol; (2*R*)-2,5,7,8-tetramethyl-2-[(4*R*,8*R*)-(4,8,12-trimethyltridecyl)]-6-chromanol, (2*R*)-2,7,8-trimethyl-2-[(4*R*,8*R*)-4,8,12-trimethyltridecyl]-6-chromanol, (2*R*)-2,8-dimethyl-2-[(4*R*,8*R*)-4,8,12-trimethyltridecyl]-6-chromanol, respectively}, ammonium acetate, ascorbic acid {(5*R*)-[(1*S*)-1,2-dihydroxyethyl]-3,4-dihydroxyfuran-2(5H)-one}, butylated hydroxy toluene (BHT), dioxane and methanol were purchased from Sigma-Aldrich (Saint Louis, MO, USA), rac-tocol [2-methyl-2-(4,8,12-trimethyltridecyl)-6-chromanol, as internal standard] was purchased from Matreya LLC. (Pleasant Gap, PA, USA), and acetonitrile (ACN), absolute ethanol, *n*-hexane and tetrahydofurane (THF) were purchased from VWR International (Radnar, PA, USA).

2.2 | Enrollment criteria and sample preparation

The study sample population comprised 30 male (age range 21–71 years, mean age 49.50 year) and 30 female volunteer individuals (age range 25–76 years, mean age 50.03 year) without any major chronic illness and 30 male (age range 18–73 years, mean age 49.43 year) and 30 female (age range 24–78 years, mean age 49.60 year) patients with OND (main diagnoses for males were the following: ischemic stroke, 8; Parkinson's disease, 5; epilepsy, 5; lumbar disk disorder, 3; and other, 9; main diagnoses for females were the following: multiple sclerosis in remission, 8; ischemic stroke, 6; epilepsy, 5; and other, 11) where the presence of ataxia, myopathy or cognitive dysfunction were excluding criteria. The distribution of the age of the subjects was Gaussian in all groups ($p > 0.05$, Anderson–Darling test) and the variances were equal ($p = 0.98$, Levene test). There was no significant difference between the groups ($F = 0.01$, $p = 0.99$, one-way ANOVA). The recent regular intake of antihyperlipidemic agents or any kind of drugs or food supplements containing antioxidants were exclusion criteria as well in all groups. All participating individuals were of Hungarian origin and were enrolled in the Department of Neurology at the University of Szeged. The study was approved by the Ethics Committee of the Faculty of Medicine, University of Szeged (19/2014). All study participants gave their written informed consent, in accordance with the Declaration of Helsinki.

Blood was collected by venipuncture into gold-top vacutainers following fasting for 12 h. The blood was immediately centrifuged at 3500 rpm for 10 min. A 200 μL aliquot of the supernatant serum was shot into a solution containing 200 μL ascorbic acid (0.085 M) and

400 µL BHT (1.14 mM) and the resulting solution was stored at −80°C until measurement, while the remaining serum was aliquoted and stored at −80°C as well.

Before high-performance liquid chromatography (HPLC) measurement, 600 µL *n*-hexane containing 1.14 mM BHT and rac-tocol as internal standard was added to the freshly thawed serum samples treated with antioxidants (800 µL). This mixture was mixed for 1 min, then centrifuged at 3500 rpm for 5 min at 4°C. The hexane layer was transferred to a test vial and evaporated under nitrogene flow. The residue was reconstituted with 75 µL ACN and 50 µL EtOH–dioxane (1:1). The resulting solution was transferred into a 200 µL glass insert placed into an amber-colored vial for measurement.

2.3 | Serum cholesterol and triglyceride measurement

Total cholesterol and triglyceride levels were determined by commercially available kits from Diasys (Diagnostics Systems GmbH, Holzheim, Germany) on Roche Modular P800 analyser (Roche, Rotkreuz, Switzerland).

2.4 | Chromatographic conditions

The concentrations of α-, β/γ-, δ-tocopherol were quantified with an Agilent 1200 HPLC system (Agilent Technologies, Santa Clara, CA, USA) equipped with an UV/VIS diode array detector applying the modified method of Hess, Keller, Oberlin, Bonfanti, and Schuep (1991). Chromatographic separations were performed on an Alltech Prevail C_{18} column, 150 × 4.6 mm i.d., 5 µm particle size (Alltech Associates Inc., Deerfield, IL, USA) after passage through a SecurityGuard precolumn, 4 × 3.0 mm i.d., 5 µm particle size (Phenomenex Inc., Torrance, CA, USA) with a mobile phase composition of ACN–THF–MeOH–1% *w/v* ammonium acetate–distilled water (684:220:68:28:28) applying isocratic elution. The flow rate and the injection volume were 2.1 mL/min and 50 µL, respectively. The detector was set at 292 (α-tocopherol) and 297 (β/γ-, δ-tocopherol, rac-tocol) nm.

Separating β- and γ-tocopherol is challenging because they only differ in the position of a methyl group. With the use of a C_{18} column these two compounds have almost the same retention times (Saha, Walia, Kundu, & Pathak, 2013). The β- and γ-tocopherols can only be separated with the application of special columns and methods (Gornas et al., 2014; Grebenstein & Frank, 2012), the application of which may be challenging for routine clinical practice. Accordingly, only γ-tocopherol was applied as a standard compound for the establishment of the calibration curve in this study, and the concentration at the corresponding retention time includes both substances and is reported as β/γ-tocopherol.

2.5 | HPLC method validation for serum samples

2.5.1 | Calibration curve and linearity

Calibrants were prepared in six different concentration levels and spiked serum samples were used with concentration ranges of 0–40, 0–6, 0–6 and 0–24 µM for α-, β/γ-, δ-tocopherol and rac-tocol, respectively. The peak area responses were plotted against the corresponding concentration, and linear regression computations were carried out by the least square method with the freely available R software (R Development Core Team, 2002). Very good linearity ($R^2 \geq 0.99$) was observed throughout the concentration ranges for α-, β/γ-, δ-tocopherol and rac-tocol.

2.5.2 | Selectivity

The selectivity of the method was checked by comparing the chromatograms of α-, β/γ-, δ-tocopherol and rac-tocol for a blank serum sample and those for a spiked sample. All compounds could be detected in their own selected chromatograms without any significant interference, as can be seen in Figure 2.

2.5.3 | Precision

For the determination of within-run precision five samples for four concentration levels were applied (i.e., 20 replicates altogether). This study was repeated two more times with at least one week intervals to obtain between-run precision. With regard to within-run precision the coefficients of variation of the measured concentrations were 4.53, 3.72 and 5.11% for α-, β/γ- and δ-tocopherols, respectively, whereas in case of between-run precision, they were 3.59, 5.93 and 4.76% for α-, β/γ- and δ-tocopherol, respectively.

2.5.4 | Recovery

The relative recoveries were estimated by measuring spiked samples of α-, β/γ- and δ-tocopherol at two different concentrations with three replicates of each. No significant differences were observed for the lower and higher concentrations. The recoveries for the serum samples ranged from 86 to 105%, from 95 to 108% and from 116 to 124% for α-, β/γ- and δ-tocopherol, respectively.

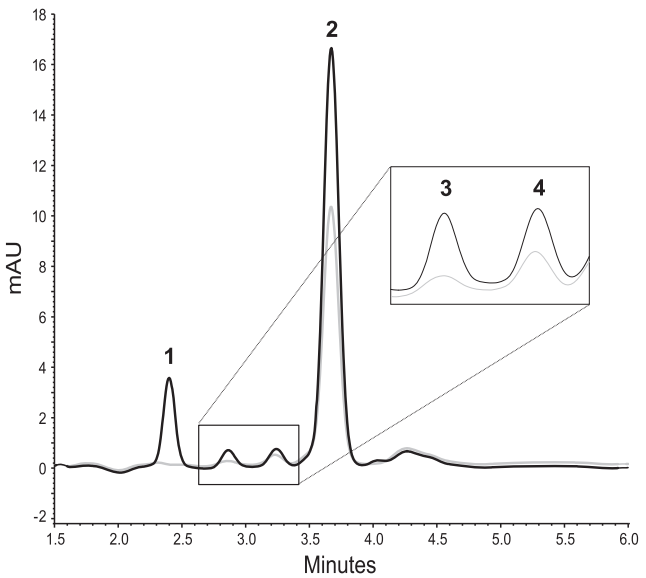

FIGURE 2 The representative chromatograms of tocopherol measurement. The gray line represents a blank serum sample which was spiked with a mixture containing rac-tocol (1), α-tocopherol (2), γ-tocopherol (4) and δ-tocopherol (3) (black line). The peak spiked with γ-tocopherol may contain β-tocopherol from the blank serum as well

2.6 | Statistics

All statistical calculations were performed with the use of the freely available R software (R Development Core Team, 2002) according to the International Federation of Clinical Chemistry and Laboratory Medicine and Clinical and Laboratory Standards Institute guidelines (Horowitz, 2016). Based on these guidelines, the minimum required number of individuals for the determination of RI with the bootstrap method is at least 100. First we checked the distribution of our data with the Anderson–Darling test and we also performed the Levene test for analysis of the homogeneity of variances. If the distribution proved to be Gaussian and the variances were equal, one-way ANOVA was applied to compare the groups, otherwise the Kruskal–Wallis test was utilized. To obtain the necessary quantiles and their confidence intervals for the determination of the reference intervals, the bootstrap method (1000 iterations) was applied. The correlation between the concentration of the measured compounds and the age of individuals in the sample population was examined with the nonparametric Spearman's test. We rejected the null hypothesis when the corrected *p*-values were ≤0.05, and in such cases the differences were considered significant. Data with Gaussian or non-Gaussian distributions were plotted as means (±SD) or medians (and interquartile range), respectively.

3 | RESULTS

The group-wise comparisons failed to detect any significant difference between groups regarding the concentrations of α-tocopherol ($p = 0.48$, $\chi^2 = 2.46$; Kruskal–Wallis test), β/γ-tocopherol ($p = 0.47$, $\chi^2 = 2.53$; Kruskal–Wallis test) or δ-tocopherol ($p = 0.82$, $\chi^2 = 0.94$; Kruskal–Wallis test; Table 1).

Accordingly, in order to establish RI with appropriate subject numbers, the values for each measured compounds were pooled and the minimum required sample size ($n = 120$) was achieved. For the determination of lower (2.5%) and upper (97.5%) RI with the corresponding confidence intervals and standard errors, the bootstrap method was applied and the results are demonstrated in Table 2.

To obtain cholesterol-corrected tocopherol values as well, serum cholesterol concentrations were determined for each subject [median and interquartile range 4.99 mM (4.31–5.54)] and the tocopherol/cholesterol ratios were calculated. The bootstrap method was applied again for the lipid corrected values (Table 3). To assess the incidental effect of age on measured serum lipid levels, the Spearman test was performed. The cholesterol levels positively correlated with the age of subjects ($p < 0.001$, Spearman's $\rho = 0.34$; Figure 3).

In the case of uncorrected α- and β/γ-tocopherol concentrations, this correlation with age is present as well (α-tocopherol: $p = 0.002$, Spearman's $\rho = 0.28$, Figure 4A; β/γ-tocopherol: $p = 0.001$, Spearman's $\rho = 0.29$, Figure 4C) whereas δ-tocopherol levels did not correlate with age ($p = 0.98$, Spearman's $\rho = 0.003$, Figure 4E). When tocopherol levels were normalized to cholesterol levels, all the correlations with age were eliminated (α-tocopherol: $p = 0.99$, Spearman's $\rho = -0.0007$, Figure 4B; β/γ-tocopherol: $p = 0.14$, Spearman's $\rho = 0.14$, Figure 4D; δ-tocopherol: $p = 0.051$, Spearman's $\rho = -0.18$, Figure 4F).

TABLE 1 Serum tocopherol concentrations of subjects belonging to the control and OND groups

	Controls (women)	Controls (men)	OND patients (women)	OND patients (men)	Group comparisons (*p*)
α-Tocopherol (μM)	38.08 (33.70–44.10)	35.38 (31.35–45.83)	34.26 (29.40–41.60)	33.93 (30.54–41.08)	0.48 ($\chi^2 = 2.46$)
β/γ-Tocopherol (μM)	1.83 (1.32–2.23)	1.68 (1.39–2.52)	1.57 (1.33–1.82)	1.75 (1.52–2.21)	0.47 ($\chi^2 = 2.53$)
δ-Tocopherol (μM)	0.63 (0.52–0.86)	0.62 (0.53–0.78)	0.62 (0.55–0.82)	0.65 (0.57–0.75)	0.82 ($\chi^2 = 0.94$)

Group-wise comparisons (Kruskal–Wallis test) of the four groups failed to detect any significant difference between serum tocopherol levels. Data are presented as median and interquartile range. OND, Other neurological disease.

TABLE 2 The calculated uncorrected lower (2.5%) and upper (97.5%) reference intervals for tocopherols for the assessed Hungarian population ($n = 120$)

	2.5%	SE	CI (95%)	97.5%	SE	CI (95%)
α-Tocopherol (μM)	24.62	0.76	23.24–26.26	54.67	4.09	46.88–61.84
β/γ-Tocopherol (μM)	0.81	0.13	0.60–1.11	3.69	0.45	2.71–4.55
δ-Tocopherol (μM)	0.29	0.03	0.22–0.32	1.07	0.13	0.80–1.29

SE, Standard error; CI, confidence interval.

TABLE 3 The calculated cholesterol corrected lower (2.5%) and upper (97.5%) reference intervals for tocopherols for the assessed Hungarian population ($n = 120$)

	2.5%	SE	CI (95%)	97.5%	SE	CI (95%)
α-Tocopherol (μmol/mmol)	5.11	0.14	4.79–5.36	11.27	0.69	9.91–12.82
β/γ-Tocopherol (μmol/mmol)	0.14	0.02	0.10–0.19	0.72	0.07	0.60–0.88
δ-Tocopherol (μmol/mmol)	0.06	0.01	0.05–0.07	0.22	0.03	0.16–0.27

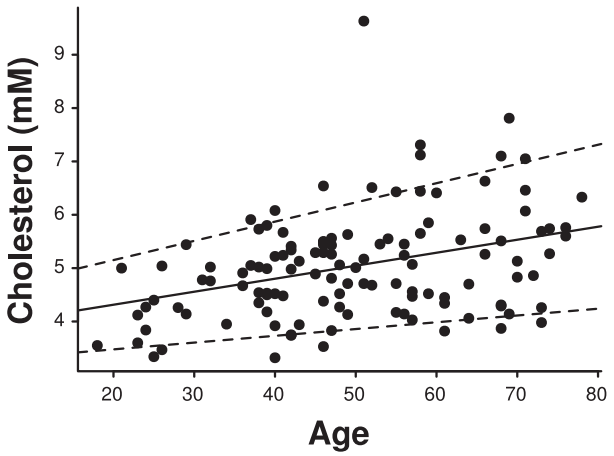

FIGURE 3 Serum cholesterol concentrations in function of age. There is a positive correlation between cholesterol levels and age ($p < 0.001$, Spearman's $\rho = 0.34$)

4 | DISCUSSION

The determination of exact serum tocopherol concentrations may be substantial for the diagnosis and therapeutic monitoring of certain conditions usually accompanied by neurological symptoms, such as ataxia, myopathy or cognitive deficiency (La Fata, Weber, & Mohajeri, 2014; Muller, 2010). Although the symptoms of genetically determined disorders with tocopherol deficiency usually manifest during childhood (Raizman et al., 2014), malabsorption disorders and late-onset genetically determined metabolic conditions preferentially appear in adulthood, indicating the need for tocopherol measurement in adult population as well (Ueda et al., 2009). However, these concentrations alone hold little diagnostic value, for proper evaluation physicians need a well-established RI, which can considerably vary between populations (Table S1 in the Supporting Information). The underlying cause of this variation may be multifactorial, mainly including nonstandardized patient selection criteria and some methodological issues. The

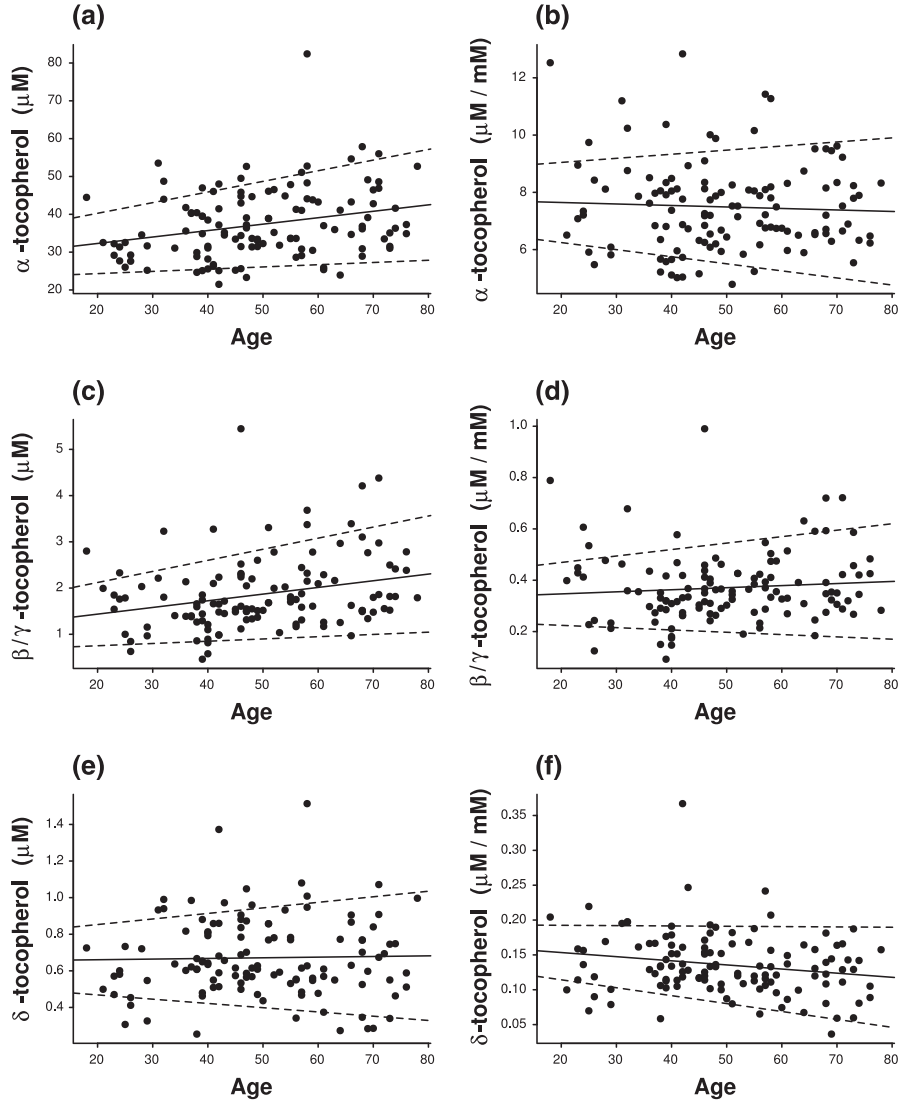

FIGURE 4 Serum tocopherol concentrations and tocopherol/cholesterol ratios plotted against the age of participants. The level of α-tocopherol positively correlates with age ($p = 0.002$, Spearman's $\rho = 0.28$; A), similarly to β/γ-tocopherol ($p = 0.001$, Spearman's $\rho = 0.29$; C), whereas δ-tocopherol levels do not correlate with age ($p = 0.98$, Spearman's $\rho = 0.003$; E). The cholesterol corrected values of α-tocopherol ($p = 0.99$, Spearman's $\rho = -0.0007$; B) and β/γ-tocopherol ($p = 0.14$, Spearman's $\rho = 0.14$; D) do not further significantly correlate with age, and the correlation of δ-tocopherol levels with age also remained nonsignificant ($p = 0.051$, Spearman's $\rho = -0.18$; F)

aim of the current study was to establish RIs for the Hungarian population and to compare the method of patient selection and the analytical procedure with those of previously published studies.

The investigated population in this study is homogeneously distributed with regard to age and covers a considerably wide age range for the adult population. The selection of a homogeneous study population may have a special importance, because age distribution can considerably influence reference values in light of the fact that the levels of certain tocopherols significantly increase with age (Figure 4; Rifkind & Segal, 1983). Accordingly when the investigated reference population includes young individuals, the results may be skewed to lower levels (Ford, Schleicher, Mokdad, Ajani, & Liu, 2006; Paliakov et al., 2009; Quesada, Mata-Granados, & Luque De Castro, 2004; Zhao, Monahan, McNulty, Gibney, & Gibney, 2014). Moving on to another qualitative aspect of the composition of the study population, in addition to the involvement of subjects without any chronic illness, the group of assessed individuals also comprised patients with different neurological disorders where tocopherol levels were not previously reported to be abnormal (the establishment of the so-called control group of OND). This study setup may ensure the absence of significant alterations of tocopherol levels in neurological cases lacking the symptoms of ataxia, myopathy and cognitive deficiency, which may be important for future screening studies. Following thorough statistical assessment resulting in the lack of significant differences, these subgroups become suitable for pooling, i.e. the number of individuals in the reference population can be increased easily to the desired level. Several previous studies lack this study setup including well-detailed description of the health condition of reference individuals, possibly introducing a bias into the reference values (Table S1; Paliakov et al., 2009; Quesada et al., 2004). In the current study design, special attention was paid to dietary factors and to the intake of special medicines (e.g. statins) and food supplements as well, because these may considerably alter the levels of the assessed compounds (Colquhoun et al., 2005). The lack of this kind of standardization introduces another bias into the establishment of RIs (Table S1; Winbauer, Pingree, & Nuttall, 1999; Yuan et al., 2014).

With regard to the analytical procedure of the determination of tocopherol concentrations from biological matrices, several difficulties can emerge as well. While the use of serum or heparinized plasma for measurement does not affect α-tocopherol level (Table S1), the application of oxalate, citrate or ethylenediaminetetraacetic acid significantly reduces its concentration (Nierenberg & Lester, 1985). The most problematic step in the measurement process may be the sample preparation, which includes liquid–liquid extraction into *n*-hexane, evaporation under nitrogen flow and reconstitution in organic solvents. The emerging problems during these steps and during sample injection can considerably contribute to the overall error of the measurement. Internal standards in known quantity can be utilized to compensate for the bias between the measured and true concentrations. In the current study, rac-tocol was applied as internal standard, but several other compounds can be utilized (Table S1).

Another important matter may be the validation of the applied analytical procedure, which can provide valuable information about the robustness of the measurement and the validity of the reported values. For scientific publications at least a partial method validation is required (ICH, 1995). Without method validation the reliability of the presented data is questionable. Approximately 80% of the previous studies presenting human tocopherol concentrations applied a validation procedure (Table S1).

Tocopherol levels are often reported as tocopherol–cholesterol ratios based on the fact that there is a close relationship between the concentrations of tocopherols and lipids in the blood (Thurnham, Davies, Crump, Situnayake, & Davis, 1986). However, under special circumstances lipid-corrected tocopherol levels can be misleading, because it was reported that malnutrition and infectious diseases in children can lower the levels of circulating cholesterol and its lipoprotein carriers, which alteration can mask decreased tocopherol levels if only corrected values are reported (Das, Thurnham, & Das, 1996; Sauerwein et al., 1997; Squali Houssaïni et al., 2001). Contrarily, when obese children were investigated, their α-tocopherol levels were normal while their tocopherol–cholesterol ratios were significantly lower compared with the control group (Strauss, 1999). With regard to adults, in light of the fact that lipid status can vary with aging (Figure 3; Rifkind & Segal, 1983), the application of lipid-corrected values may be necessary for the characterization of vitamin E status (Horwitt, Harvey, Dahm, & Searcy, 1972; Thurnham et al., 1986). Nevertheless, the report of serum tocopherol concentrations with lipid ratios may be practical for the proper evaluation of tocopherol status. However, only one-third of the papers reported both of them (Table S1 in the Supporting Information).

In conclusion, the current study presents RIs for the first time for serum tocopherol concentrations and their corresponding cholesterol corrected values with regard to the adult Hungarian population. These results can facilitate the diagnostic process for certain neurological conditions, such as ataxia with vitamin E deficiency. Moreover, this paper draws attention to the importance of thorough design associated with the establishment of these RIs and the possible pitfalls in tocopherol measurements.

ACKNOWLEDGEMENTS

The authors are grateful to Péter Monostori and Eszter Karg (Department of Pediatrics, University of Szeged, Szeged, Hungary) for their valuable advice during method development. Furthermore, we would like to thank Adrienn Szabó-Laboda (Department of Neurology, Faculty of Medicine, Albert Szent-Györgyi Clinical Center, University of Szeged) and Edina Cseh (Department of Neurology, Faculty of Medicine, Albert Szent-Györgyi Clinical Center, University of Szeged and Babeş-Bolyai University, Faculty of Chemistry and Chemical Engineering, Cluj-Napoca) for their assistance during the measurements. This research was supported by the Hungarian Brain Research Program – grant no. KTIA_13_NAP-A_II/18. Dr Dénes Zádori was supported by the János Bolyai Research Scholarship of the Hungarian Academy of Sciences.

DISCLOSURE OF INTEREST

The authors report no conflict of interest.

REFERENCES

Arita, M., Nomura, K., Arai, H., & Inoue, K. (1997). Alpha-tocopherol transfer protein stimulates the secretion of alpha-tocopherol from a cultured liver cell line through a brefeldin A-insensitive pathway. *Proceedings of the National Academy of Sciences of the United States of America*, *94*, 12437–12441.

Colquhoun, D. M., Jackson, R., Walters, M., Hicks, B. J., Goldsmith, J., Young, P., … Kostner, K. M. (2005). Effects of simvastatin on blood lipids, vitamin E, coenzyme Q 10 levels and left ventricular function in humans. *European Journal of Clinical Investigation*, *35*, 251–258.

Cooper, A. D. (1997). Hepatic uptake of chylomicron remnants. *Journal of Lipid Research*, *38*, 2173–2192.

Das, B. S., Thurnham, D. I., & Das, D. B. (1996). Plasma alpha-tocopherol, retinol, and carotenoids in children with falciparum malaria. *The American Journal of Clinical Nutrition*, *64*, 94–100.

Ford, E. S., Schleicher, R. L., Mokdad, A. H., Ajani, U. A., & Liu, S. (2006). Distribution of serum concentrations of alpha-tocopherol and gamma-tocopherol in the US population. *The American Journal of Clinical Nutrition*, *84*, 375–383.

Gornas, P., Siger, A., Czubinski, J., Dwiecki, K., Seglina, D., & Nogala-Kalucka, M. (2014). An alternative RP-HPLC method for the separation and determination of tocopherol and tocotrienol homologues as butter authenticity markers: A comparative study between two European countries. *European Journal of Lipid Science and Technology*, *116*, 895–903.

Grebenstein, N., & Frank, J. (2012). Rapid baseline-separation of all eight tocopherols and tocotrienols by reversed-phase liquid-chromatography with a solid-core pentafluorophenyl column and their sensitive quantification in plasma and liver. *Journal of Chromatography A*, *1243*, 39–46.

Hacquebard, M., & Carpentier, Y. A. (2005). Vitamin E: Absorption, plasma transport and cell uptake. *Current Opinion in Clinical Nutrition and Metabolic Care*, *8*, 133–138.

Hess, D., Keller, H. E., Oberlin, B., Bonfanti, R., & Schuep, W. (1991). Simultaneous determination of retinol, tocopherols, carotenes and lycopene in plasma by means of high performance liquid chromatography on reversed phase. *International Journal for Vitamin and Nutrition Research*, *61*, 232–238.

Horowitz, G. L. (2016). Establishment and use of reference values. In *Tietz Textbook of Clinical Chemistry and Molecular Diagnostics* (5th ed.)). Oxford: Elsevier chapter 5.

Horwitt, M. K., Harvey, C. C., Dahm, C. H., & Searcy, M. T. (1972). Relationship between tocopherol and serum lipid levels for determination of nutritional adequacy. *Annals of the New York Academy of Sciences*, *203*, 223–236.

ICH (1995). ICH Harmonized tripartite guideline, validation of analytical procedures. *Federal Register*, *60*, 11260.

Karg, E., Klivényi, P., Németh, I., Bencsik, K., Pintér, S., & Vécsei, L. (1999). Nonenzymatic antioxidants of blood in multiple sclerosis. *Journal of Neurology*, *246*, 533–539.

La Fata, G., Weber, P., & Mohajeri, M. H. (2014). Effects of vitamin E on cognitive performance during ageing and in Alzheimer's disease. *Nutrients*, *6*, 5453–5472.

Lopes da Silva, S., Vellas, B., Elemans, S., Luchsinger, J., Kamphuis, P., Yaffe, K., … Stijnen, T. (2014). Plasma nutrient status of patients with Alzheimer's disease: Systematic review and meta-analysis. *Alzheimer's and Dementia*, *10*, 485–502.

Mardones, P., & Rigotti, A. (2004). Cellular mechanisms of vitamin E uptake: Relevance in alpha-tocopherol metabolism and potential implications for disease. *Journal of Nutritional Biochemistry*, *15*, 252–260.

Morley, S., Panagabko, C., Shineman, D., Mani, B., Stocker, A., Atkinson, J., & Manor, D. (2004). Molecular determinants of heritable vitamin E deficiency. *Biochemistry*, *43*, 4143–4149.

Muller, D. P. R. (2010). Vitamin E and neurological function. *Molecular Nutrition and Food Research*, *54*, 710–718.

Nierenberg, D. W., & Lester, D. C. (1985). Determination of vitamins A and E in serum and plasma using a simplified clarification method and high-performance liquid chromatography. *Journal of Chromatography*, *345*, 275–284.

O'Byrne, D., Grundy, S., Packer, L., Devaraj, S., Baldenius, K., Hoppe, P. P., … Traber, M. G. (2000). Studies of LDL oxidation following alpha-, gamma-, or delta-tocotrienyl acetate supplementation of hypercholesterolemic humans. *Free Radical Biology and Medicine*, *29*, 834–845.

Paliakov, E. M., Crow, B. S., Bishop, M. J., Norton, D., George, J., & Bralley, J. A. (2009). Rapid quantitative determination of fat-soluble vitamins and coenzyme Q-10 in human serum by reversed phase ultra-high pressure liquid chromatography with UV detection. *Journal of Chromatography B: Analytical Technologies in the Biomedical and Life Sciences*, *877*, 89–94.

Quesada, J. M., Mata-Granados, J. M., & Luque De Castro, M. D. (2004). Automated method for the determination of fat-soluble vitamins in serum. *Journal of Steroid Biochemistry and Molecular Biology*, *89–90*, 473–477.

R Development Core Team. The R Project for Statistical Computing. Text 1–9. R Foundation for Statistical Computing, 2002. Available from: http://www.r-project.org/

Raizman, J. E., Cohen, A. H., Teodoro-Morrison, T., Wan, B., Khun-Chen, M., Wilkenson, C., … Adeli, K. (2014). Pediatric reference value distributions for vitamins a and E in the CALIPER cohort and establishment of age-stratified reference intervals. *Clinical Biochemistry*, *47*, 812–815.

Rifkind, B. M., & Segal, P. (1983). Lipid research clinics program reference values for hyperlipidemia and hypolipidemia. *JAMA*, *250*, 1869–1872.

Rose, R. C., & Bode, A. M. (1993). Biology of free radical scavengers: An evaluation of ascorbate. *FASEB Journal: Official Publication of the Federation of American Societies for Experimental Biology*, *7*, 1135–1142.

Saha, S., Walia, S., Kundu, A., & Pathak, N. (2013). Effect of mobile phase on resolution of the isomers and homologues of tocopherols on a triacontyl stationary phase. *Analytical and Bioanalytical Chemistry*, *405*, 9285–9295.

Sauerwein, R. W., Mulder, J. A., Mulder, L., Lowe, B., Peshu, N., Demacker, P. N., … Marsh, K. (1997). Inflammatory mediators in children with protein-energy malnutrition. *The American Journal of Clinical Nutrition*, *65*, 1534–1539.

Schmölz, L., Birringer, M., Lorkowski, S., & Wallert, M. (2016). Complexity of vitamin E metabolism. *World Journal of Biological Chemistry*, *7*, 14–43.

Sen, C. K., Khanna, S., & Roy, S. (2007). Tocotrienols in health and disease: The other half of the natural vitamin E family. *Molecular Aspects of Medicine*, *28*, 692–728.

Sies, H. (1993). Strategies of antioxidant defense. *European Journal of Biochemistry*, *215*, 213–219.

Sies, H. (1997). Oxidative stress: Oxidants and antioxidants. *Experimental Physiology*, *82*, 291–295.

Squali Houssaïni, F. Z., Foulon, T., Payen, N., Iraqi, M. R., Arnaud, J., & Groslambert, P. (2001). Plasma fatty acid status in Moroccan children: Increased lipid peroxidation and impaired polyunsaturated fatty acid metabolism in protein-calorie malnutrition. *Biomedicine and Pharmacotherapy*, *55*, 155–152.

Strauss, R. S. (1999). Comparison of serum concentrations of α-tocopherol and β-carotene in a cross-sectional sample of obese and nonobese children (NHANES III). *The Journal of Pediatrics*, *134*, 160–165.

Szalárdy, L., Zádori, D., Klivényi, P., Toldi, J., & Vécsei, L. (2015). Electron transport disturbances and neurodegeneration: From Albert Szent-Györgyi's concept (Szeged) till novel approaches to boost mitochondrial bioenergetics. *Oxidative Medicine and Cellular Longevity*, 498401.

Thurnham, D. I., Davies, J. A., Crump, B. J., Situnayake, R. D., & Davis, M. (1986). The use of different lipids to express serum tocopherol: Lipid ratios for the measurement of vitamin E status. *Annals of Clinical Biochemistry*, *23*, 514–520.

Traber, M. G. (2013). Mechanisms for the prevention of vitamin E excess. *Journal of Lipid Research*, *54*, 2295–2306.

Ueda, N., Suzuki, Y., Rino, Y., Takahashi, T., Imada, T., Takanashi, Y., & Kuroiwa, Y. (2009). Correlation between neurological dysfunction with vitamin E deficiency and gastrectomy. *Journal of the Neurological Sciences*, *287*, 216–220.

Winbauer, A. N., Pingree, S. S., & Nuttall, K. L. (1999). Evaluating serum alpha-tocopherol (vitamin E) in terms of a lipid ratio. *Annals of Clinical and Laboratory Science*, *29*, 185–191.

Yuan, C., Burgyan, M., Bunch, D. R., Reineks, E., Jackson, R., Steinle, R., & Wang, S. (2014). Fast, simple, and sensitive high-performance liquid chromatography method for measuring vitamins a and E in human blood plasma. *Journal of Separation Science*, *37*, 2293–2299.

Zádori, D., Klivényi, P., Plangár, I., Toldi, J., & Vécsei, L. (2011). Endogenous neuroprotection in chronic neurodegenerative disorders: With particular regard to the kynurenines. *Journal of Cellular and Molecular Medicine*, *15*, 701–717.

Zádori, D., Klivényi, P., Szalárdy, L., Fülöp, F., Toldi, J., & Vécsei, L. (2012). Mitochondrial disturbances, excitotoxicity, neuroinflammation and kynurenines: Novel therapeutic strategies for neurodegenerative disorders. *Journal of the Neurological Sciences*, *322*, 187–191.

Zhao, Y., Monahan, F. J., McNulty, B. A., Gibney, M. J., & Gibney, E. R. (2014). Effect of vitamin E intake from food and supplement sources on plasma α- and γ-tocopherol concentrations in a healthy Irish adult population. *The British Journal of Nutrition*, *112*, 1575–1585.

SUPPORTING INFORMATION

Additional Supporting Information may be found online in the supporting information tab for this article.

How to cite this article: Veres G, Szpisjak L, Bajtai A, et al. The establishment of tocopherol reference intervals for Hungarian adult population using a validated HPLC method. *Biomedical Chromatography*. 2017;e3953. https://doi.org/10.1002/bmc.3953